

Contents

Responses to comments from reviewer #1	1
Responses to comments from reviewer #2	13
Marked-up manuscript.....	37

Responses to comments from reviewer #1

This manuscript analyzed 3 months continuous measurement of particle size distribution from 1.2 nm to 10000 nm during winter 2018 in Beijing. This kind of observation, that cover almost the full range of particle size and include both charged and neutral clusters/particles, is rather limited in China. New particle formation and haze days were discussed separately, and found a clear correlation between the cluster and nucleation modes during NPF days. In addition, the work found that all modes in the sub-micron size range were correlated with NO_x, indicate traffic emission can contribute to all particle sizes. In general, the manuscript did provide useful information and knowledge, but some more in-depth analysis is encouraged. The manuscript is in general well written and documented. The topic fits well in the scope of ACP. I recommend this manuscript can be published after some revisions.

We would like to thank the referee for the suggestions and careful editorial comments. Our replies (text in blue) to the comments (text in black) item by item and modification in our manuscript (text in red) as per suggestions of the referee are presented as below:

Comments:

More discussions on the charged ions/clusters from NAIS are encouraged. Can the ion induced nucleation be observed? Is it important?

We thank the reviewer for their suggestions. We did observe ion induced nucleation during our observation however we think that it constitutes only a minor fraction in comparison to neutral nucleation mechanism. Both cluster ion number concentration and the formation rate of 1.5 nm ions constituted a small fraction of total clusters number concentration and total formation rate of 1.5 nm clusters.

The following discussion and figures (Figure R1-1, Figure R1-2, Figure R1-3 and Figure R1-4) were added to the manuscript:

2.4.1 Calculation of the growth rate

The growth rates of cluster and nucleation mode particles were calculated from positive ion data and particle data from Neutral Cluster and Air Ion Spectrometer (NAIS), respectively, by using the appearance time method introduced by Lehtipalo et al. (2014). In this method, the particle number concentration of particles of size dp is recorded as a function of time, and the appearance time of particles of size dp is determined as the time when their number concentration reaches 50% of its maximum value during new particle formation (NPF) events.

The growth rates (GR) were calculated according to:

$$GR = \frac{dp_2 - dp_1}{t_2 - t_1} \quad (1)$$

where t_2 and t_1 are the appearance times of particles with sizes of dp_2 and dp_1 respectively. Figure R1-4 shows an example of how this method was used.

2.4.2 Calculation of the coagulation sink

The coagulation sink (CoagS) was calculated according to the equation (2) introduced by Kulmala et al. (2012):

$$CoagS_{dp} = \int K(dp, d'p)n(d'p)dd'p \cong \sum_{d'p=dp}^{d'p=max} K(dp, d'p)N_{d'p} \quad (2)$$

where $K(dp, d'p)$ is the coagulation coefficient of particles with sizes of dp and $d'p$, $N_{d'p}$ is the particle number concentration with size of $d'p$.

2.4.3 Calculation of the formation rate

The formation rate of 1.5-nm particles ($J_{1.5}$) was calculated using particle number concentrations measured with a Particle Sizer Magnifier (PSM). The formation rate of 1.5-nm ions ($J_{1.5}^{\pm}$) was calculated using positive and negative ions data from the Neutral Cluster and Air Ion Spectrometer (NAIS) as well as PSM data. The upper limit used was 3 nm. The values of $J_{1.5}$ and $J_{1.5}^{\pm}$ were calculated following the methods introduced by Kulmala et al. (2012) with equation (3) and equation (4), respectively:

$$J_{dp} = \frac{dN_{dp}}{dt} + CoagS_{dp} \cdot N_{dp} + \frac{GR}{\Delta dp} \cdot N_{dp} \quad (3)$$

where $CoagS_{dp}$ is coagulation sink in the size range of $[dp, dp + \Delta dp]$ and GR is the growth rate.

$$J_{dp}^{\pm} = \frac{dN_{dp}^{\pm}}{dt} + CoagS_{dp} \cdot N_{dp}^{\pm} + \frac{GR}{\Delta dp} \cdot N_{dp}^{\pm} + \alpha \cdot N_{dp}^{\pm} \cdot N_{<dp}^{\mp} - \chi N_{dp} \cdot N_{<dp}^{\pm} \quad (4)$$

The fourth and fifth terms on the right hand side of equation (4) represent ion-ion recombination and charging of neutral particles by smaller ions, respectively, α is the ion-ion recombination coefficient and χ is the ion-aerosol attachment coefficient.

3.5 Atmospheric ions and ion induced nucleation in Beijing

In order to estimate the contribution of ions to the total cluster mode particle number concentration and the importance of ion induced nucleation in Beijing, we studied ion number concentrations in the size range of 0.8-7 nm by dividing them into 3 sub-size bins: constant pool (0.8-1.5 nm), charged clusters (1.5-3 nm) and larger ions (3-7 nm). As shown in Figure R1-1, number concentrations of positive ions were higher than those negative ions in all the size bins on both NPF event days and haze days. We will only discuss positive ions here.

The median number concentration of positive ions in the constant pool on NPF event days was only 100 cm^{-3} in Beijing, much less than that in boreal forest (600 cm^{-3} ; Mazon et al., 2016). Also, the median number concentration of positive charged clusters was 20 cm^{-3} on the NPF event days, and the ratio to the total cluster mode particle number concentration was 0.001 to 0.004 during the NPF time window (Figure R1-2). This ratio is comparable to that observed in San Pietro Capofiume (0.004), in which the anthropogenic pollution level was also high, but clearly lower than that observed in another megacity in China, Nanjing, (0.02) (Kontkanen et

al., 2017). Considerably higher ratios were observed in clean environments, for example during winter in the boreal forest at Hyytiälä, Finland (0.7; Kontkanen et al., 2017). The median number concentration of larger ions (3- 7 nm) on the NPF event days was 30 cm^{-3} , a little bit higher than the charged cluster mode particle number concentration, indicating that not all of the larger ions originate from the growth of charged clusters, but rather from charging of neutral particles by smaller ions. On the haze days, charged ion number concentrations were much lower than those on the NPF days which could be attributed to the higher condensation sink.

The diurnal pattern of the ratio of number concentration between charged and total cluster mode particles was the highest during the night with a maximum of 0.008, and had a trough during daytime with a minimum of 0.001 on the NPF event days. Such diurnal pattern is similar to earlier observations in Nanjing, San Pietro Capofiume and Hyytiälä (Kontkanen et al., 2017). This ratio reached its minimum around noon, because the total cluster mode particle number concentration reached its maximum around that time due to NPF. The ratio had a small peak at around 9:00, similar to earlier observations in Centreville and Po Valley (Kontkanen et al., 2016; Kontkanen et al., 2017). The possible reason is that charged clusters were activated earlier in the morning than neutral clusters. The ratio increased from the midnight until about 4:00, similar to the number concentration of charged clusters.

As shown in Figure R1-3, the diurnal median of the ratio between the formation rate of positive ions of 1.5 nm ($J_{1.5}^+$) and the total clusters of 1.5 nm ($J_{1.5}$) varied from 0.0009 to 0.006. This result is comparable to observations in Shanghai, where the positive ion induced nucleation contributed only 0.05% to the total formation rate of 1.7-nm particles ($J_{1.7}$) (Yao et al., 2018).

There are some overlap for the particle size distribution between NAIS and PSD. It would be good that the authors can provide some information about the inter comparison between these two techniques.

Indeed, we added the discussion on instrument comparison and related figures (Figure R1-5 and Figure R1-6) to the manuscript (line 186) as per suggestion of the referee.

The Particle Size Distribution system (PSD) and Neutral Cluster and Air Ion Spectrometer (NAIS) had an overlapping particle size distribution over the mobility diameter range of 3-42 nm. As shown in Figure R1-5, total particle number concentrations from the NAIS and PSD system correlated well with each other on both NPF event days (R^2 was 0.92) and haze days (R^2 was 0.90) in the overlapping size range. The slopes between the total particle number concentration from the PSD system and that from the NAIS were 0.90 and 0.85 on the NPF event days and haze days, respectively. The particle number size distribution in the overlapping size range of the NAIS and PSD system matched well on both NPF event days and haze days as shown in Figure R1-6.

I would suggest to provide 1 plot to show the traffic emission derived increase of cluster and nucleation mode particles, and maybe the correlation plot between cluster mode particles and NO_x during the non-NPF days.

We thank the referee for the suggestions. We added Figure R1-7 to the manuscript. Correspondingly, we updated our discussion in lines 252- 259 as below:

In Figure R1-7, we show the median diurnal pattern of particle number size distribution on the NPF event days and haze days separately. On the NPF event days, we observed cluster formation from diameters smaller than 3 nm. The growth of newly-formed particles lasted for several hours, resulting in a consecutive increase of the particle number concentrations in all the four modes. During traffic rush hours in the morning and evening, we observed an increase of particle number concentrations in the size range of cluster mode to around 100 nm.

On the haze days, we still observed an increase of particle number concentration in the size range of cluster mode to Aitken mode during rush hours. Traditionally, NPF events occur during the time window between sunrise and sunset by photochemical reactions (Kerminen et al., 2018). The binary or ternary nucleation between sulfuric acid and water, ammonia or amines are usually thought of as sources of atmospheric cluster mode particles, especially in heavily polluted environments (Kulmala et al., 2013; Kulmala et al., 2014; Yao et al., 2018; Chu et al., 2019). The burst of cluster mode particle number concentration outside the traditional NPF time window, especially during the rush hours in the afternoon, suggests a very different source of cluster mode particles from traditional nucleation, e.g. nucleation from gases emitted by traffic (Rönkkö et al., 2017).

As shown in Figure 6, on the NPF event days, the cluster mode particle number concentration started to increase at the time of sunrise and peaked around noon with a wide single peak, showing the typical behavior related to NPF events (Kulmala et al., 2012). Comparatively, on the haze days, the cluster mode particle number concentration showed a double peak pattern similar to the diurnal cycle of NO_x (Figure 5). This observation is consistent with our discussion above that traffic emission possibly contributed to cluster mode particles. By comparing cluster mode particle number concentrations between the haze days and NPF event days, we estimated that traffic-related cluster mode particles could contribute up to 40-50 % of the total cluster mode particle number concentration on the NPF event days.

It is a bit unusual that there were no overlap between NPF and haze days. There were quite many studies that observed NPF with considerable high concentrations of $\text{PM}_{2.5}$. What will happen if classify the haze days by the concentration of $\text{PM}_{2.5}$, i.e. $100 \mu\text{g}/\text{m}^3$?

We thank the referee for the suggestions. We observed NPF events and haze events on the same days, but not at the same time. We classified haze days not only according to the visibility and relative humidity but also according to the time period haze events lasted. Days were classified as haze days when haze lasted for at least 12 consecutive hours. According to this classification, we did not observe any overlap between NPF event days and haze days.

As per suggestion to the referee, we classified haze days by the concentration of $\text{PM}_{2.5}$, i.e. $100 \mu\text{g}/\text{m}^3$. We show time series of particle number size distribution and $\text{PM}_{2.5}$ concentration during our observations in Figure R1-8. In Figure R1-8, the NPF events can be identified with the 'banana shapes'. We did not observe any NPF events happening at the same time when $\text{PM}_{2.5}$ concentration was higher than $100 \mu\text{g}/\text{m}^3$.

Table 2, change the color-marked numbers to, i.e. bold or italic.

We modified Table 2 as per suggestion to the referee.

Figs. 7-9, where were the data points of “others”?

The data points of ‘others’ are those that do not belong to the classification of NPF or haze days. They are usually polluted days during which we do not observe any NPF, but cannot be classified as haze days due to low PM loading resulting in not so bad visibility. To make the plots clearer, we only present NPF and haze days here.

Fig. 9, there showed pretty good correlation between Aitken mode particles and accumulation mode particles during NPF days. What’s the possible reason?

On the NPF event days, Aitken and accumulation mode particle number concentrations correlated positively with each other, as well as with the SO₂ and NO_x concentration. This suggests that on the NPF event days, Aitken and accumulation mode particles were both formed during regional transportation as secondary particles and were emitted by traffic as primary particles.

To make the discussion on correlation between each of the modes, we updated the discussion at section 3.4 and separate Table 3 into Table R1a and Table R1b according NPF event days and haze days, in addition we changed Figure 9 into Figure R1-9 as following:

3.4 Correlation between different particle modes

Table R1a and Table R1b as well as Figure R1-9 show the correlation between particle number concentrations in different modes. On the NPF event days, cluster and nucleation mode particle number concentrations correlated positively with each other due to their common dominant source, NPF. Both cluster and nucleation mode particle number concentrations correlated negatively with the Aitken and accumulation mode particle number concentrations because, as discussed earlier, high concentrations of large particles tend to suppress NPF and subsequent growth of newly-formed particles.

On the NPF event days, Aitken and accumulation mode particle number concentrations correlated positively with each other, as well as with the SO₂ and NO_x concentration. This suggests that on the NPF event days, Aitken and accumulation mode particles both formed during regional transportation as secondary particles and were emitted by traffic as primary particles.

On the haze days, cluster and nucleation mode particle number concentrations correlated positively with each other, and with the Aitken mode particle number concentration. This is suggestive of a similar dominating sources for these particle, most likely traffic emissions. Similar to the NPF event days, cluster and nucleation mode particle number concentrations correlated negatively with the accumulation mode particle number concentration, even though this correlation was rather weak (Table R1b).

The Aitken mode particle number concentration had a negative correlation with the accumulation mode particle number concentration on the haze days.

Figures and Tables

Table R1a: Correlation coefficients between particle number concentration of every mode on NPF event days. The time window was 08:00 - 14:00. High correlation coefficients ($|R|>0.5$) are marked with bold and italic.

	Cluster	Nucleation	Aitken	Accumulation
Cluster	1			
Nucleation	0.76 ^a	1		
Aitken	-0.46 ^a	-0.33 ^b	1	
Accumulation	-0.66 ^a	-0.66 ^c	0.7 ^c	1

^a included 516 data points (the time resolution was 12 minutes), ^b included 1251 data points (the time resolution was 5 min), ^c included 1331 data points (the time resolution was 5 min).

Table R1b: Correlation coefficients between particle number concentration of every mode on haze days. The time window was 08:00 - 14:00. High correlation coefficients ($|R|>0.5$) are marked with bold and italic.

	Cluster	Nucleation	Aitken	Accumulation
Cluster	1			
Nucleation	0.74 ^a	1		
Aitken	0.41 ^a	0.48 ^b	1	
Accumulation	-0.22 ^a	-0.33 ^c	-0.5 ^c	1

^a included 342 data points (the time resolution was 12 minutes), ^b included 824 data points (the time resolution was 5 min), ^c included 845 data points (the time resolution was 5 min).

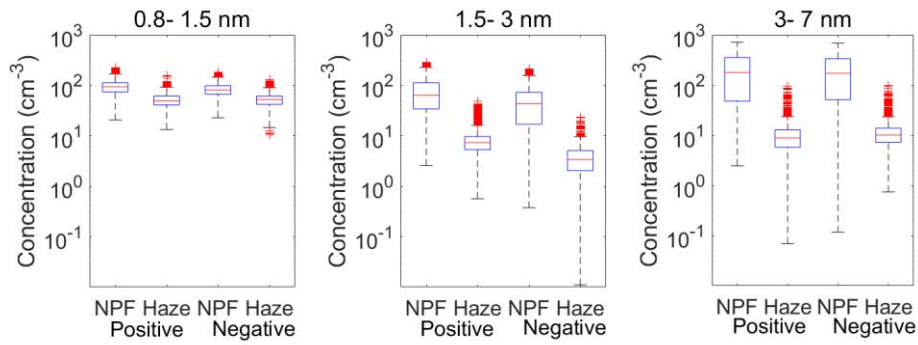


Figure R1-1: Positive and negative ion number concentrations in the size bins of 0.8- 1.5nm, 1.5-3 nm and 3-7 nm on NPF event days and haze days separately. The whiskers include 99.3% of data of every group. Data out of $1.5 \times$ interquartile range are posited outside the whiskers and considered as outliers. The lines in the boxes represent the median value, the lower of the boxes represent 25% of the number concentration, and the upper of the boxes represent 75% of the number concentration. Data marked with red pluses represent outliers.

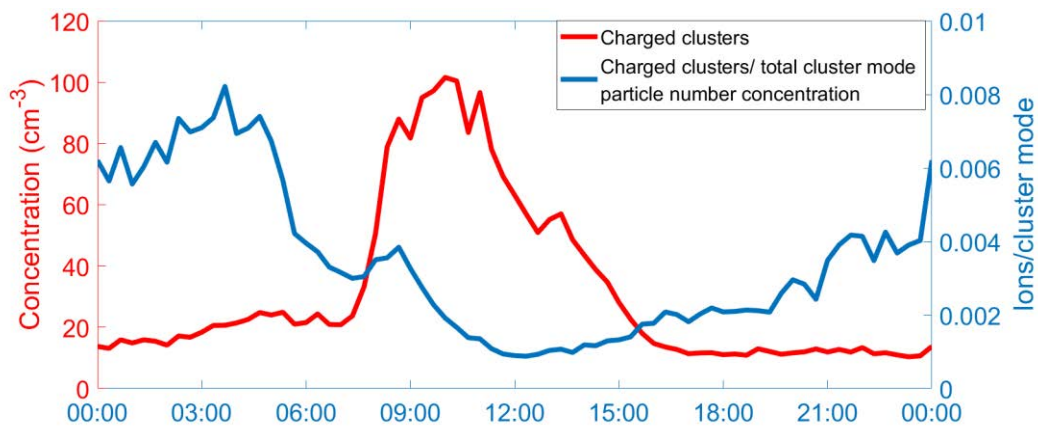


Figure R1-2: Diurnal pattern of charged clusters (1.5-3 nm) number concentration (red line) and ratio of charged clusters to total cluster mode (1.5-3 nm) particle number concentration on the NPF event days (blue line). The time resolution of the used data was 12 min.

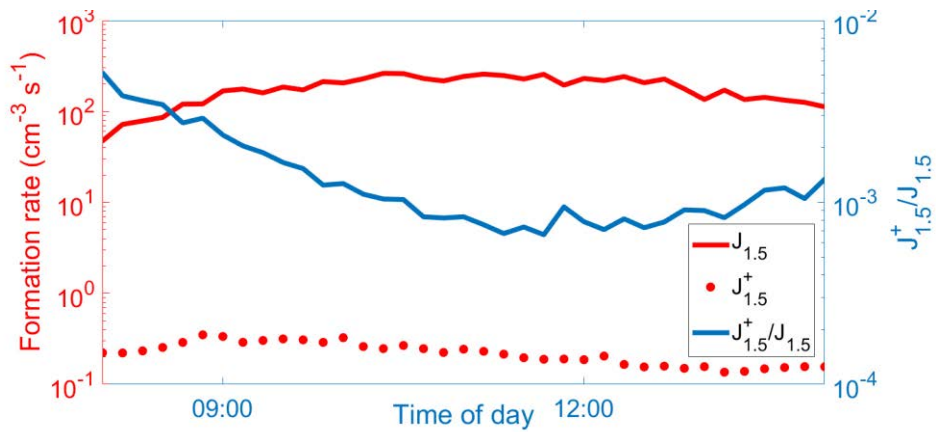


Figure R1-3: Diurnal pattern of formation rate of positive charged clusters of 1.5 nm (red dots) and neutral clusters of 1.5 nm (red line) and the ratio between them (blue line) on the NPF event days during the NPF time window we chose. The time resolution of the used data was 12 min.

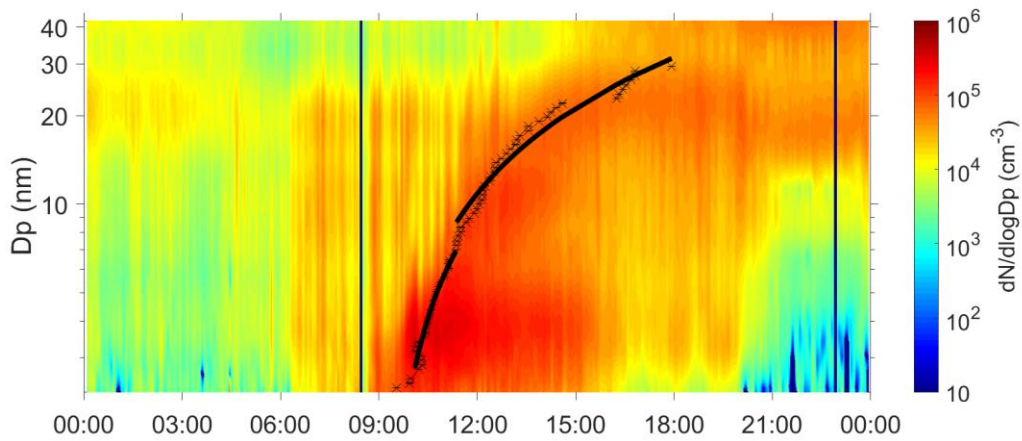


Figure R1-4: An example of how the appearance time method was used to calculate growth rate. The appearance time was recorded as a function of particle diameter as the black stars in the figure. The black lines are the fitted growth periods. The growth rates were calculated by calculating the slopes of the black lines.

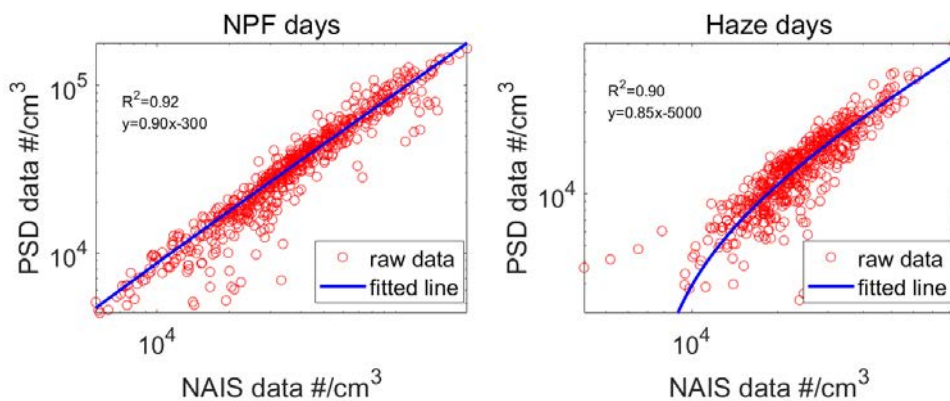


Figure R1-5: Total particle number concentration in size range of 3-42 nm from NAIS and PSD system. There are 1271 data points on the plots of NPF days and 887 data points on the plots of haze days. The time resolution was 5 minutes.

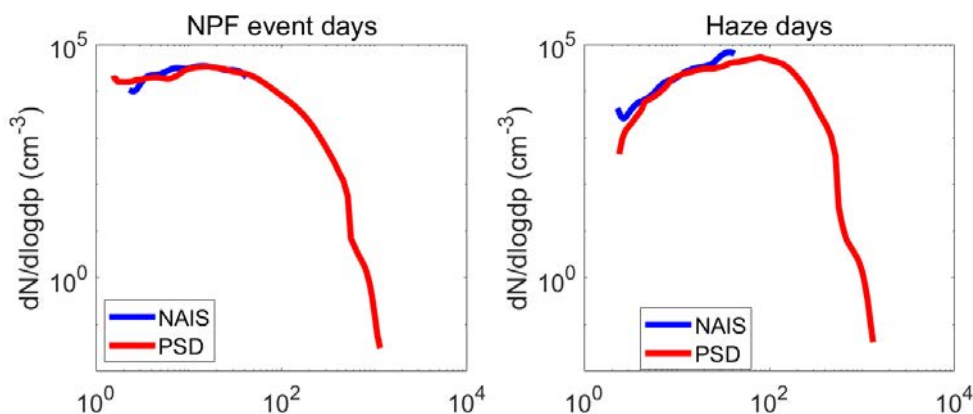


Figure R1-6: Median particle number size distribution of data from NAIS (blue line) and PSD system (red line) on NPF event days (left panel) and haze days (right panel) during our observation. The time resolution we used here for every point was 1h.

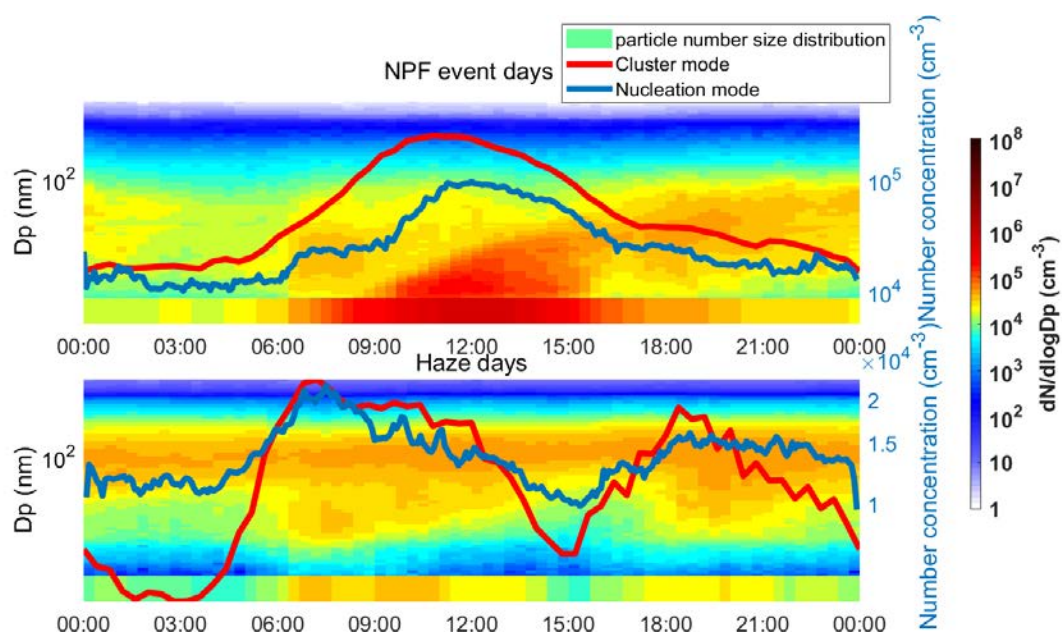


Figure R1-7: Median diurnal patterns of the particle number size distribution over the size range of 1.5-1000 nm and number concentrations of cluster mode (red lines) and nucleation mode (blue lines) particles on the NPF event days (upper panel) and haze days (lower panel). The time resolution for every data point of particle number size distribution and cluster mode particle number concentration was 12 minutes. The time resolution of every data point of nucleation mode particle number concentration was 5 minutes.

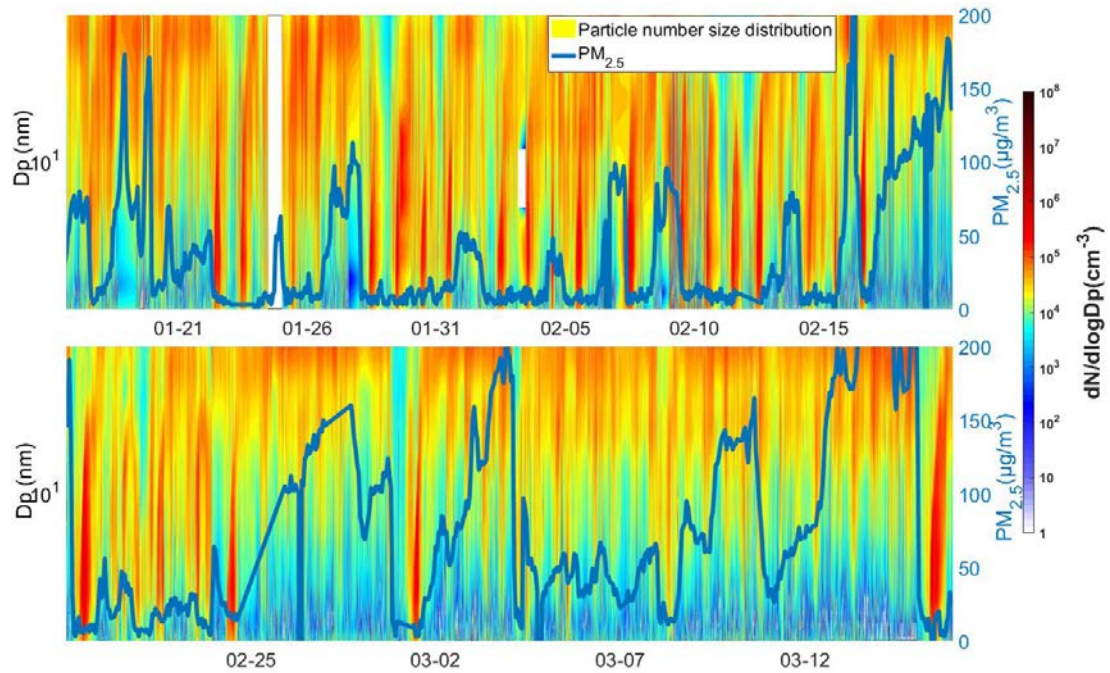


Figure R1-8: Time series of particle number size distribution and $PM_{2.5}$ concentration (blue line) during our observation period.

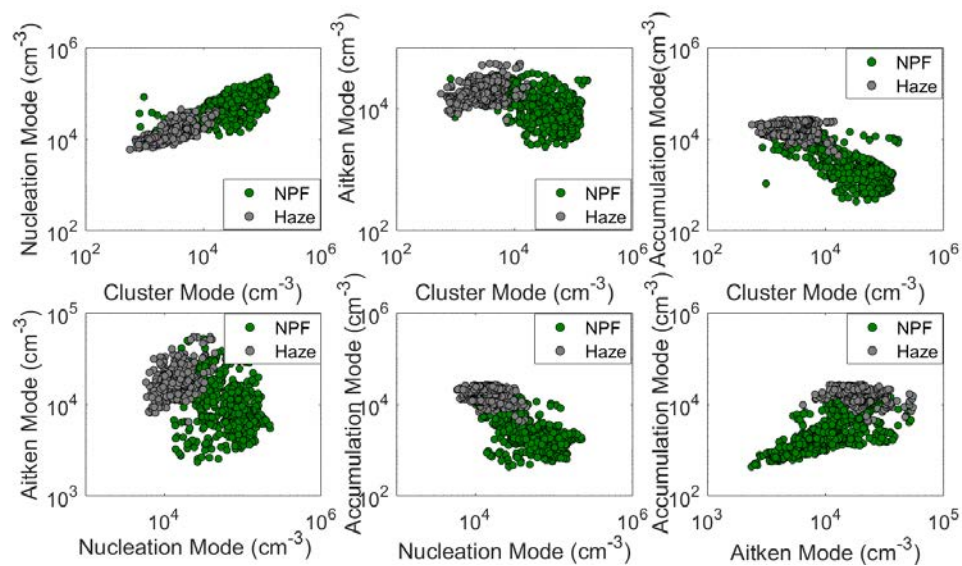


Figure R1-9: Correlation between every mode each other on NPF event days (green dots) and haze days (grey dots). The time resolution of data in the plots of correlation between cluster mode and other modes was 12 min and the time resolution of other data points was 5 min.

References

- Chu, B. W., Kerminen, V. M., Bianchi, F., Yan, C., Petäjä, T., and Kulmala, M.: Atmospheric new particle formation in China, *Atmos Chem Phys*, 19, 115-138, <https://doi.org/10.5194/acp-19-115-2019>, 2019.
- Kerminen, V. M., Chen, X. M., Vakkari, V., Petäjä, T., Kulmala, M., and Bianchi, F.: Atmospheric new particle formation and growth: review of field observations, *Environ Res Lett*, 13, <https://doi.org/10.1088/1748-9326/aadf3c>, 2018.
- Kontkanen, J., Järvinen, E., Manninen, H. E., Lehtipalo, K., Kangasluoma, J., Decesari, S., Gobbi, G. P., Laaksonen, A., Petäjä, T., and Kulmala, M.: High concentrations of sub-3nm clusters and frequent new particle formation observed in the Po Valley, Italy, during the PEGASOS 2012 campaign, *Atmos Chem Phys*, 16, 17, <https://doi.org/10.5194/acp-16-1919-2016>, 2016.
- Kontkanen, J., Lehtipalo, K., Ahonen, L., Kangasluoma, J., Manninen, H. E., Hakala, J., Rose, C., Sellegri, K., Xiao, S., Wang, L., Qi, X. M., Nie, W., Ding, A. J., Yu, H., Lee, S., Kerminen, V. M., Petaja, T., and Kulmala, M.: Measurements of sub-3nm particles using a particle size magnifier in different environments: from clean mountain top to polluted megacities, *Atmos Chem Phys*, 17, 2163-2187, 2017.
- Kulmala, M., Petäjä, T., Nieminen, T., Sipilä, M., Manninen, H. E., Lehtipalo, K., Dal Maso, M., Aalto, P. P., Junninen, H., Paasonen, P., Riipinen, I., Lehtinen, K. E. J., Laaksonen, A., and Kerminen, V. M.: Measurement of the nucleation of atmospheric aerosol particles, *Nat Protoc*, 7, 1651-1667, <https://doi.org/10.1038/nprot.2012.091>, 2012.
- Kulmala, M., Kontkanen, J., Junninen, H., Lehtipalo, K., Manninen, H. E., Nieminen, T., Petäjä, T., Sipilä, M., Schobesberger, S., Rantala, P., Franchin, A., Jokinen, T., Järvinen, E., Äijälä, M., Kangasluoma, J., Hakala, J., Aalto, P. P., Paasonen, P., Mikkilä, J., Vanhanen, J., Aalto, J., Hakola, H., Makkonen, U., Ruuskanen, T., Mauldin, R. L., Duplissy, J., Vehkamäki, H., Bäck, J., Kortelainen, A., Riipinen, I., Kurtén, T., Johnston, M. V., Smith, J. N., Ehn, M., Mentel, T. F., Lehtinen, K. E. J., Laaksonen, A., Kerminen, V. M., and Worsnop, D. R.: Direct Observations of Atmospheric Aerosol Nucleation, *Science*, 339, 943-946, <https://doi.org/10.1126/science.1227385>, 2013.
- Kulmala, M., Petaja, T., Ehn, M., Thornton, J., Sipila, M., Worsnop, D. R., and Kerminen, V. M.: Chemistry of Atmospheric Nucleation: On the Recent Advances on Precursor Characterization and Atmospheric Cluster Composition in Connection with Atmospheric New Particle Formation, *Annu Rev Phys Chem*, 65, 21-37, 2014.
- Lehtipalo, K., Leppä, J., Kontkanen, J., Kangasluoma, J., Wimmer, D., Franchin, A., Schobesberger, S., Junninen, H., Petäjä, T., Sipilä, M., Mikkilä, J., Vanhanen, J., Worsnop, D. r., and Kulmala, M.: methods for determining particle size distribution and growth rates between 1 and 3 nm using the Particle Size Magnifier, *Boreal Environ Res*, 19, 215-236, 2014.
- Mazon, S. B., Kontkanen, J., Manninen, H. E., Nieminen, T., Kerminen, V.-M., and Kulmala,

M.: A long-term comparison of nighttime cluster events and daytime ion formation in a boreal forest, *Boeral Environment Research*, 21, 19, 2016.

Yao, L., Garmash, O., Bianchi, F., Zheng, J., Yan, C., Kontkanen, J., Junninen, H., Mazon, S. B., Ehn, M., Paasonen, P., Sipilä, M., Wang, M. Y., Wang, X. K., Xiao, S., Chen, H. F., Lu, Y. Q., Zhang, B. W., Wang, D. F., Fu, Q. Y., Geng, F. H., Li, L., Wang, H. L., Qiao, L. P., Yang, X., Chen, J. M., Kerminen, V. M., Petäjä, T., Worsnop, D. R., Kulmala, M., and Wang, L.: Atmospheric new particle formation from sulfuric acid and amines in a Chinese megacity, *Science*, 361, 278-281, <https://doi.org/10.1126/science.aao4839>, 2018.

Responses to comments from reviewer #2

The manuscript describes the evolution of aerosol size-segregated particle number concentration during winter 2018 in Beijing. The data is separated in two different sets: days when haze is observed, and days with new particle formation (NPF) events. Additionally, the particle size distribution is separated into different modes according to the particle diameter: cluster, nucleation, Aitken and accumulation modes. Trace gases concentrations are used to establish the origin of the aerosol observed and induce a primary or secondary origin of the particles observed in each mode.

The topic of this paper is within the scope of this journal and the dataset used is interesting because particles in a wide size range, including very small particles (1.5 to 1000 nm) are measured. However, I believe that with such an interesting dataset one could expect a more comprehensive study. For example, it would be nice to see the evolution of condensation sinks during NPF and haze days, or calculate growth rates for each mode during NPF days. Additionally, the statistical data analysis is very simplistic, and the authors should reconsider analyzing the data with a different approach. The only statistical tools used for relating trace gases with the different modes are correlation coefficients. Assuming that the processes involved in the formation of the different modes is linear is a big oversimplification. The authors should improve the data analysis or discuss the limitations of the methodology they use.

In general, the manuscript is poorly written. There are grammar mistakes and the language is not fluent. This makes it difficult to follow some parts of the manuscript. The authors should have the paper proof-read and edited by a competent English speaker before publishing it.

Most of the discussions are very short and do not provide much more information than what is presented in the tables or figures.

The figures are good in general. The scales on figures 5 and 6 could be improved, and there are a few technical mistakes and information missing in the figure captions (see comments below).

We would like to thank the referee for the suggestions and careful editorial comments. These comments are valuable and very helpful for revising and improving our paper. We have studied all the comments carefully and made corrections. We would like to thank the referee for the suggestions and careful editorial comments. Our replies (text in blue) to the comments (text in black) item by item and modification in our manuscript (text in red) as per suggestions of the referee are presented as below:

As suggested by both referees, we improved the scope of this manuscript by adding discussions on atmospheric ions in size range of 0.8-7 nm and ion induced nucleation, these discussions improve our understanding of the sources of cluster mode particles. Also, we made a more comprehensive study about traffic-related cluster and nucleation mode particles as suggested by both referees. In addition, we added results on growth rates on both NPF event days of cluster and nucleation mode particles as suggested by the referee.

We agree that correlation coefficients analysis cannot tell much on the evolution of size-segregated particle number concentration accurately because the processes involved in the

formation of different modes should not be linear as pointed out by the referee. By examining responses of size-segregated particle number concentrations to changes in trace gas and PM_{2.5} concentrations (Table R2a and Table R2b), we can get further insights into the main sources of particles in each mode and into the dynamical processes experienced by these particles under different pollution levels. Of course, not all sources or dynamics can be captured using this approach. In addition, due to the complex physical and chemical processes experienced by the particles, the correlation analysis cannot quantify the strength of individual sources or dynamical processes.

According to the reviewer's good instruction, we updated some parts of our manuscript on both languages and scientific discussion as shown in the replies to specific comments.

As per suggestions of both referees, the following discussion on parameter calculations and Figure R2-1 was added to our manuscript as section 2.4.

2.4 Parameter calculation

2.4.1 Calculation of the growth rate

The growth rates of cluster and nucleation mode particles were calculated from positive ion data and particle data from Neutral Cluster and Air Ion Spectrometer (NAIS), respectively, by using the appearance time method introduced by Lehtipalo et al. (2014). In this method, the particle number concentration of particles of size dp is recorded as a function of time, and the appearance time of particles of size dp is determined as the time when their number concentration reaches 50% of its maximum value during new particle formation (NPF) events.

The growth rates (GR) were calculated according to:

$$GR = \frac{dp_2 - dp_1}{t_2 - t_1} \quad (1)$$

where t_2 and t_1 are the appearance times of particles with sizes of dp_2 and dp_1 respectively. Figure R2-1 shows an example of how this method was used.

2.4.2 Calculation of the coagulation sink

The coagulation sink (CoagS) was calculated according to the equation (2) introduced by Kulmala et al. (2012):

$$CoagS_{dp} = \int K(dp, d'p)n(d'p)dd'p \cong \sum_{d'p=dp}^{d'p=max} K(dp, d'p)N_{d'p} \quad (2)$$

where $K(dp, d'p)$ is the coagulation coefficient of particles with sizes of dp and $d'p$, $N_{d'p}$ is the particle number concentration with size of $d'p$.

2.4.3 Calculation of the formation rate

The formation rate of 1.5-nm particles ($J_{1.5}$) was calculated using particle number

concentrations measured with a Particle Sizer Magnifier (PSM). The formation rate of 1.5-nm ions ($J_{1.5}^{\pm}$) was calculated using positive and negative ions data from the Neutral Cluster and Air Ion Spectrometer (NAIS) as well as PSM data. The upper limit used was 3 nm. The values of $J_{1.5}$ and $J_{1.5}^{\pm}$ were calculated following the methods introduced by Kulmala et al. (2012) with equation (3) and equation (4), respectively:

$$J_{dp} = \frac{dN_{dp}}{dt} + CoagS_{dp} \cdot N_{dp} + \frac{GR}{\Delta dp} \cdot N_{dp} \quad (3)$$

where $CoagS_{dp}$ is coagulation sink in the size range of $[dp, dp + \Delta dp]$ and GR is the growth rate.

$$J_{dp}^{\pm} = \frac{dN_{dp}^{\pm}}{dt} + CoagS_{dp} \cdot N_{dp}^{\pm} + \frac{GR}{\Delta dp} \cdot N_{dp}^{\pm} + \alpha \cdot N_{dp}^{\pm} \cdot N_{<dp}^{\mp} - \chi N_{dp} \cdot N_{<dp}^{\pm} \quad (4)$$

The fourth and fifth terms on the right hand side of equation (4) represent ion-ion recombination and charging of neutral particles by smaller ions, respectively, α is the ion-ion recombination coefficient and χ is the ion-aerosol attachment coefficient.

As per suggestions of both referees, the following discussion on atmospheric ions and ion induced nucleation as well as Figure R2-2, Figure R2-3 and Figure R2-4 were added to the manuscript as section 3.5.

3.5 Atmospheric ions and ion induced nucleation in Beijing

In order to estimate the contribution of ions to the total cluster mode particle number concentration and the importance of ion induced nucleation in Beijing, we studied ion number concentrations in the size range of 0.8-7 nm by dividing them into 3 sub-size bins: constant pool (0.8-1.5 nm), charged clusters (1.5-3 nm) and larger ions (3-7 nm). As shown in Figure R2-2, number concentrations of positive ions were higher than those negative ions in all the size bins on both NPF event days and haze days. We will only discuss positive ions here.

The median number concentration of positive ions in the constant pool on NPF event days was only 100 cm^{-3} in Beijing, much less than that in the boreal forest (600 cm^{-3} ; Mazon et al., 2016). Also, the median number concentration of positive charged clusters was 20 cm^{-3} on the NPF event days, and the ratio to the total cluster mode particle number concentration was 0.001 to 0.004 during the NPF time window (Figure R2-3). This ratio is comparable to that observed in San Pietro Capofiume (0.004), in which the anthropogenic pollution level was also high, but clearly lower than that observed in another megacity in China, Nanjing (0.02; Kontkanen et al., 2017). Considerably higher ratios were observed in clean environments, for example during winter in the boreal forest at Hyytiälä, Finland (0.7; Kontkanen et al., 2017). The median number concentration of larger ions (3-7 nm) on the NPF event days was 30 cm^{-3} , a little bit higher than the charged cluster mode particle number concentration, indicating that not all of the larger ions originate from the growth of charged clusters, but rather from charging of neutral particles by smaller ions. On the haze days, charged ion number concentrations were much lower than those on the NPF days, which could be attributed to the higher condensation sink.

The diurnal pattern of the ratio of number concentration between charged and total cluster mode particles was the highest during the night with a maximum of 0.008, and had a trough during

daytime with a minimum of 0.001 on the NPF event days. Such diurnal pattern is similar to earlier observations in Nanjing, San Pietro Capofiume and Hyytiälä (Kontkanen et al., 2017). This ratio reached its minimum around noon, because the total cluster mode particle number concentration reached its maximum around that time due to NPF. The ratio had a small peak at around 9:00, similar to earlier observations in Centreville and Po Valley (Kontkanen et al., 2016; Kontkanen et al., 2017). The possible reason is that charged clusters were activated earlier in the morning than neutral clusters. The ratio increased from the midnight until about 4:00, similar to the number concentration of charged clusters.

As shown in Figure R2-4, the diurnal median of the ratio of formation rate of positive ions of 1.5 nm ($J_{1.5}^+$) to the total clusters of 1.5 nm ($J_{1.5}$) varied from 0.0009 to 0.006. This result is comparable to observations in Shanghai, where the positive ion induced nucleation contributed only 0.05% to the total formation rate of particles of 1.7 -nm ($J_{1.7}$) (Yao et al., 2018).

We updated our discussion in the manuscript from line 252 to line 259 with a more comprehensive study on traffic-related cluster and nucleation mode particles as below:

In Figure R2-4, we show the median diurnal pattern of particle number size distribution on the NPF event days and haze days separately. On the NPF event days, we observed cluster formation from diameters smaller than 3 nm. The growth of newly-formed particles lasted for several hours, resulting in a consecutive increase of the particle number concentrations in all the four modes. During traffic rush hours in the morning and evening, we observed an increase of particle number concentrations in the size range of cluster mode to around 100 nm.

On the haze days, we still observed an increase of particle number concentration in the size range of cluster mode to Aitken mode during rush hours. Traditionally, NPF events occur during the time window between sunrise and sunset by photochemical reactions (Kerminen et al., 2018). The binary or ternary nucleation between sulfuric acid and water, ammonia or amines are usually thought of as sources of atmospheric cluster mode particles, especially in heavily polluted environments (Kulmala et al., 2013; Kulmala et al., 2014; Yao et al., 2018; Chu et al., 2019). The burst of cluster mode particle number concentration outside the traditional NPF time window, especially during the rush hours in the afternoon, suggests a very different source of cluster mode particles from traditional nucleation, e.g. nucleation from gases emitted by traffic (Rönkkö et al., 2017).

As shown in Figure 6, on the NPF event days, the cluster mode particle number concentration started to increase at the time of sunrise and peaked around noon with a wide single peak, showing the typical behavior related to NPF events (Kulmala et al., 2012). Comparatively, on the haze days, the cluster mode particle number concentration showed a double peak pattern similar to the diurnal cycle of NO_x (Figure 5). This observation is consistent with our discussion above that traffic emission possibly contributed to cluster mode particles. By comparing cluster mode particle number concentrations between the haze days and NPF event days, we estimated that traffic-related cluster mode particles could contribute up to 40-50 % of the total cluster mode particle number concentration on the NPF event days.

As per suggestion of the referee, the following discussion on growth rates of cluster and nucleation mode particles on NPF event days as well as Figure R2-5 were added to our

manuscript as section 3.6:

3.6 Particle growth rates

The growth rates of particles generated from NPF events were examined in three size ranges: <3 nm, 3-7 nm and 7- 25 nm (Figure R2-5). The median growth rates of particles in these size ranges were 1.0 nm/h, 2.7 nm/h and 5.5 nm/h, respectively. The growth rate of cluster mode particles was comparable with that observed in Shanghai (1.5 nm/h; Yao et al., 2018). The notable increase of the particle growth rate with an increasing particle size is a very typical feature in the sub-20 nm size range (Kerminen et al., 2018), and it may also extend to larger particle sizes (Paasonen et al., 2018).

Our observations are in line with the reported range of nucleation mode particle growth rates of 0.1-11.2 nm/h in urban areas of Beijing (Wang et al., 2017; Jayaratne et al., 2017). Such growth rates can explain the observed increases of Aitken mode particle number concentrations in the afternoon.

Specific comments

Table 1: It would be useful for the reader if the authors mention in the text the number of days classified as NPF and haze.

Thank you for your suggestions.

We added in line 180 ‘We observed 28 NPF event days and 24 haze days’ as per suggestion of the referee.

I don’t see the definition of the modes. Also, which instrumentation did you use to calculate the different modes number concentrations? There are overlapping size ranges for nucleation and Aitken modes in the instrumentation you described.

The definition of the modes used in our study are introduced on lines 184-186: cluster mode (smaller than 3 nm), nucleation mode (3- 25 nm), Aitken mode (25- 100 nm) and accumulation mode (100- 1000 nm).

As per suggestion of the referee, the following discussion was added to our manuscript in line 186:

We calculated cluster mode particle number concentrations using Particle Size Magnifier (PSM) data, nucleation mode particle number concentration using Neutral Cluster and Air Ion Spectrometer (NAIS) particle mode data, and Aitken and accumulation mode particle number concentrations using Particle Size Distribution (PSD) system data.

The Particle Size Distribution system (PSD) and Neutral Cluster and Air Ion Spectrometer (NAIS) had an overlapping particle size distribution over the mobility diameter range of 3-42 nm. As shown in Figure R2-6, total particle number concentrations from the NAIS and PSD system correlated well with each other on both NPF event days (R^2 was 0.92) and haze days (R^2 was 0.90) in the overlapping size range. The slopes between the total particle number concentration from the PSD system and that from the NAIS were 0.90 and 0.85 on the NPF event days and haze days, respectively. The particle number size distribution in the overlapping

size range of the NAIS and PSD system matched well on both NPF event days and haze days as shown in Figure R2-7.

Section 2.2: Please include the time resolution of the data you use. I could not find this information for the PSD system and trace gases. How did you merge the data when the different instruments have different time resolutions? It is important that you describe this procedure carefully.

The following changes were made to our manuscript as per suggestion of the referee.

Line 145 as ‘In the operation of the PSM, the saturator flow rate scanned from 0.1 to 1.3 lpm and scanned back from 1.3 to 0.1 lpm within 240 s. We averaged the data over 3 scans to make it smoother, and therefore the time resolution of PSM data was 12 minutes.’

Line 151 ‘the time resolution of PSD system data was 5 minutes’.

We added in line 165 that ‘the time resolution of CO, NO_x, and O₃ data were 5 minutes, whereas the time resolution of SO₂ data was 1 hour before 22, January, 2018, and 5 minutes after that.’ as per suggestion to the referee.

When data sets having different time resolutions were used, we chose the smallest time resolution as the common time resolution. Data with higher time resolutions were merged to the common time resolution by taking median numbers between two time points of the new time series.

Line 181: “In general, there were no overlap between NPF and haze periods”. Did you look for NPF events during haze days? If haze and NPF are not 100% mutually excluding it would be interesting to describe these episodes. If they are, then change your sentence to make it clear that there was never an overlap. Also, did you determine haze days or did the China Meteorological Administration do this? If the authors did the classification, they should include the instrumentation used.

We thank the referee for the suggestions. We observed NPF events and haze events occurred on the same day, but never at the same time. We classified haze days not only according to the definition given by the China Meteorological Administration on the visibility and relative humidity but also the time haze lasts. Days were classified as haze days when haze events lasted for at least 12 consecutive hours. According to this classification, we did not observe any overlap between NPF event days and haze days.

As per suggestion of the referee, the following changes has been made in our manuscript:

We will update line 181 with ‘NPF events and haze days as these two phenomena never occurred simultaneously.’

We added in section 2.2 ‘We measured relative humidity (RH, %) and, visibility (km), wind speed (m/s) and wind direction (°) from a weather station on the roof of our station.’

Lines 222-228: The authors should also talk about O₃ here. I only see information for SO₂, CO and NO_x.

We thank the referee for the suggestions, we added the following description to our manuscript

as per suggestion of the referee:

The median concentration of O₃ was 10 ppb on the haze days during our observations, a little bit higher than the severe haze episode in 2013 (<7 ppb; Wang et al., 2014b).

Lines 232-233: NPF does not favor clean environments. In any case, clean environments favor NPF.

We modified the corresponding text correspondingly.

Their lower levels on NPF event days indicates that relatively clean conditions favor NPF events.

Lines 247-251: “NO_x and CO are important precursors of O₃ in Chinese urban areas. Based on our data, O₃, on the other hand, started to increase [...] after the levels of NO_x and CO started to decrease”. Your wording is confusing. It feels like you are suggesting that NO_x and CO are not precursors of O₃. Please reword.

We thank the referee for the suggestion, we rephrased the text as follows.

Earlier observations in urban areas having high NO_x concentrations found that O₃ was consumed by its reaction with NO, while NO₂ works as precursor for O₃ via photochemical reactions (Wang et al., 2017). In our observations, the diurnal pattern of O₃ was opposite to that of NO_x, which is consistent with O₃ loss by large amounts of freshly emitted NO during rush hours and O₃ production by photochemical reactions involving NO₂ after the rush hours in the morning.

Lines 280-284: I don't see Aitken mode concentrations being similar to NO_x evolutions before 9:00. See my comment on Figure 6 below.

We thank the referee for the suggestion. We modified Figure 6 as shown below. We can see Aitken mode number concentration increased during traffic rush time in Figure 6 after we changed the y-scale.

Lines 295-297: Did you measure meteorological parameters or is this a general statement? If it is a general statement change “the wind was” for “the wind is...”.

We thank the referee for the comments. Yes, we measured meteorological parameters.

Line 301: It would be interesting to see the graphs for CS instead of giving only a daily value.

We thank the referee for the comments.

As per suggestion of the referee, we added Figure R2-8 to our manuscript. Figure R2-8 describes the condensation sink on both NPF event days and haze days.

Section 3.3: In line 318 the authors state “In this section, we use CO, SO₂, NO_x and O₃ as tracers”, but there are no comments whatsoever regarding CO or O₃ in this section.

We thank the referee for the comments. Combined with the comments on Table 2, we updated discussion at section 3.3 and added the discussion about the limitation on the method in line 319 as below:

By examining responses of size-segregated particle number concentrations to changes in trace gas and PM_{2.5} concentrations (Table R2a and Table R2b), we can get further insights into the main sources of particles in each mode and into the dynamical processes experienced by these particles under different pollution levels. Of course, not all sources or dynamics can be captured using this approach. In addition, due to the complex physical and chemical processes experienced by the particles, the correlation analysis cannot quantify the strength of individual sources or dynamical processes.

3.3.1 Connection with SO₂

Generally, as shown in Figure 8 (Figure 7 in ACPD version), the SO₂ concentration correlated negatively with both cluster and nucleation mode particle number concentrations. Higher SO₂ concentrations were encountered on more polluted days when NPF events were suppressed due to the high particle loadings, explaining the overall negative correlation. However, if we look at the NPF event days and haze days separately, we cannot see any clear correlation between the SO₂ concentration and cluster mode or nucleation mode particle number concentration, as shown also in Table R2a and Table R2b. This result indicates that during our observations, NPF occurred in relatively clean conditions, but the strength of a NPF event was not sensitive to the regional pollution level as long as NPF was able to occur.

On the NPF event days, the SO₂ concentration correlated positively with the concentrations of both Aitken and accumulation mode particles during the chosen NPF time window, whereas on the haze days no correlation between the SO₂ concentration and Aitken mode particle number concentration could be observed. This suggests that regional and transported pollution contributed to Aitken and accumulation mode particles on the NPF event days, while on haze days the transported and regional pollution was only a prominent factor affecting accumulation mode particle number concentration. In addition, SO₂ contributes to heterogeneous reactions on particle surfaces, explaining that a fraction of accumulation mode particles could have resulted from the growth of Aitken mode particles (Ravishankara., 1997).

3.3.2 Connection with NO_x

As shown in Table R2a, and Figure 9 (Figure 8 in ACPD version), the NO_x concentration correlated negatively with both cluster and nucleation mode particle number concentrations on the NPF event days. Compared with the correlation between SO₂ and cluster and nucleation mode particle number concentrations, this result indicates that local traffic emissions affected cluster and nucleation mode particles more than regional pollution on the NPF event days.

On the haze days, we did not see any correlation between cluster mode particle number concentration and NO_x concentration (Table R2b), although according to our analysis above, traffic emissions can be the source of cluster mode particles during the haze days. One possible reason for this is that the relationship between cluster mode particle number concentration and NO_x concentration was not linear. Earlier studies pointed out that the dilution ratio is the dominant factor affecting the number size distribution of nanoparticles generated from traffic gases emissions (Shi and Harrison, 1999; Shi et al., 2001). Temperature and humidity were also identified as factors affecting nanoparticle number size distribution nucleated from tailpipe emissions (Shi et al., 2001). Such factors above could decrease the correlation coefficients

between cluster and nucleation mode particle number concentrations and NO_x concentration.

The Aitken mode particle number concentration correlated positively with the NO_x concentration on both NPF event days and haze days, suggesting that traffic emissions might be an important source of Aitken mode particles.

The accumulation mode particle number concentration correlated positively with the NO_x concentration on the NPF event days, which is consistent with earlier studies showing that traffic emissions can contribute to accumulation mode particles in urban areas (Vu et al., 2015). On the haze days, accumulation mode particle number concentration correlated less with NO_x than with SO₂, suggesting that regional and transported pollution was more important to accumulation mode particles than traffic emissions.

3.3.3 Connection with CO

CO has some similar sources as NO_x, such as traffic. On the NPF event days, the CO concentration correlated with particle number concentrations in each mode in a very similar way as NO_x did, suggesting that CO and NO_x had common sources, such as traffic emissions, on the NPF event days. This result confirms our analysis above that traffic emissions could suppress NPF and growth on the NPF event days, in addition to which they might be important sources of the Aitken and accumulation mode particles.

On the haze days, CO transported from polluted areas dominated the total CO concentration. The CO concentration had a positive correlation with the accumulation mode particle number concentration, but no clear correlation with the particle number concentration of the three other modes. This result confirms our analysis above that on the haze days, local emissions dominated Aitken particle number concentrations while regional and transported pollutions affected accumulation mode particle number concentrations more than local emissions.

3.3.4 Connection with O₃

Ozone is a secondary pollution trace gas and its concentration represents the oxidization capacity of atmosphere. Earlier observations found that high O₃ concentrations favor NPF by enhancing photochemical reactions (Qi et al., 2015). However, we did not see any correlation between the O₃ concentration and cluster mode particle number concentration, suggesting that O₃ was not the limiting factor for cluster mode particle number concentration.

The O₃ concentration correlated positively with both nucleation and Aitken mode particle number concentration on the NPF event days during the NPF time window, whereas on the haze days O₃ concentration correlated only with the Aitken mode particle number concentration.

The above results suggest that O₃ influences heterogeneous reactions and particle growth rather than the formation of new aerosol particles.

Line 337: Looking at the figure, it doesn't seem to me that SO₂ and cluster and nucleation mode concentrations are correlated, especially for NPF days. What are the correlation coefficients for NPF days and haze days separately? (see also comment for Table 2).

We thank the referee for the comments. Although SO₂ is precursor of sulfuric acid and we would have expected a positive correlation with cluster mode particles, there are other species

involved such as NH_3 , dimethyl amine (DMA), that could limit the process.

As per suggestion of the referee, we will update our discussion in our manuscript as shown in the response to the last comments above.

Lines 400-402: Please elaborate and comment on the correlation with the other modes. $\text{PM}_{2.5}$ is also highly correlated with cluster mode but this is not discussed. Consider showing the correlations in an additional figure.

We thank the referee for the comments. We added correlation coefficient between $\text{PM}_{2.5}$ concentration and every mode on NPF event days and haze days in Table R2a and Table R2b separately. The following discussions and Figure R2-9 were added to our manuscript as section 3.3.5 as per suggestions to the referee:

3.3.5 Connection to $\text{PM}_{2.5}$

As shown in Figure R2-9, $\text{PM}_{2.5}$ concentration correlated negatively with the cluster and nucleation mode particle number concentrations, and positively with the accumulation mode particle number concentration. High $\text{PM}_{2.5}$ concentrations tend to suppress NPF by increasing the sinks of vapors responsible for nucleation and growth of cluster and nucleation mode particles. The particles causing high $\text{PM}_{2.5}$ concentrations also serve as sinks of cluster and nucleation mode particles by coagulation.

As shown in Table R2a and Figure R2-9, the Aitken mode particle number concentration correlated positively with the $\text{PM}_{2.5}$ concentration on the NPF event days. A possible reason for this could be the tight connection between the Aitken and accumulation mode particles on the NPF event days (Table R1a), and the observation that accumulation mode particles are usually the main contributor to $\text{PM}_{2.5}$ in Beijing (Liu et al., 2013). On the haze days, the Aitken mode particle number concentration correlated negatively with the $\text{PM}_{2.5}$ concentration (Table R2b). A possible reason for this is that pre-existing large particles acted as a sink for Aitken mode particles by coagulation as well as a sink for vapors responsible for the growth of smaller particles into the Aitken mode. In addition, while $\text{PM}_{2.5}$ is dominated by regional and transported secondary aerosols, Aitken mode particles mainly originate from local emissions such as traffic and cooking in Beijing (Wu et al., 2007; Wang et al., 2013; Du et al., 2017; de Jesus et al., 2019).

Conclusion: This section is written as a summary. The conclusion should reflect the significance of the results presented in this paper compared with existing observations, and give a message beyond summarizing what has already been said in the previous sections.

We thank the referee for the comments. we revised our conclusion as per suggestion of the referee as below:

4. Summary and conclusions

We measured particle number concentrations over a wide range of particle diameters (1.5-1000 nm) on both NPF event days and haze days in winter Beijing. To our knowledge, this was the first time when cluster mode particle number concentrations have been reported on haze days

in Beijing.

The observed responses of particle number concentrations in different modes (cluster, nucleation, Aitken and accumulation mode) to changes in trace gas and PM_{2.5} concentrations were quite heterogeneous, suggesting different sources and dynamics experienced by each mode. NPF was the dominant source of cluster and nucleation mode particles. Ion-induced nucleation did not play an important role during the NPF events. The growth rates of cluster and nucleation mode particles increased with an increasing particle size. Traffic emissions contributed to every mode and were the dominant source of cluster and nucleation mode particles on the haze days. The main sources of Aitken mode particles were local emissions, while transported and regional pollution as well as growth from the nucleation mode also contributed to the Aitken mode. The main source of accumulation mode particles was regional and transported pollution. PM_{2.5} affected the number concentration of sub-100 nm particles by competing for vapors responsible for particle growth and by acting as sinks for particles by coagulation. The main contributors to the PM_{2.5} mass concentration were accumulation mode particles on the haze days.

As demonstrated here and in many other studies (Brines et al., 2015), ultrafine particles (< 100 nm in diameter) tend to dominate the total aerosol particle number concentration in megacities like Beijing. We should put no less attention on ultrafine particles than larger particles for their large number population. More attention should therefore be put on ultrafine particles in urban environments. We found that both NPF and traffic emissions are important sources of ultrafine particles in Beijing. To improve our understanding on the potential effects of ultrafine particles on health and air quality, we need to do more research on their sources and physical and chemical properties. Laboratory and model analysis on dynamics of ultrafine particles would help us to understand the evolution of particle number size distributions. In addition, to identify and locate other possible sources, long-term observations on ultrafine particles down to the cluster mode as well as source apportionment analyses, such as cluster analysis and receptor model studies, are still needed. Ultrafine particles should also be taken into consideration when making policies to control air pollution. New regulations should be designed to control primary emission sources, such as traffic, or precursor emissions for secondary ultrafine particles involving NPF and subsequent particle growth.

Line 415-416: I do not see in the text where this is discussed (secondary sources contribution to the Aitken mode during haze days).

We thank the referee for the comments. We updated our conclusion and we deleted this sentence about ‘secondary sources contribution to the Aitken mode during haze days’ in our conclusions.

Table 2: I think this table would be more useful if the authors separate the data for haze days and NPF days. Also, what do you mean by “all the data are in log scale”? Please reword. You are showing correlation coefficients here, which are not represented in any scale.

We deleted the words ‘all the data are in log scale’.

As per suggestion of the referee, we separated the data for NPF and haze days by changing Table 2 into Table R2a and Table R2b as shown below.

Figures 1, 2, 3, 4: Are these daily averages? Please specify the data you used to make the plot.

Data in Figure 1,3,4 are raw data we observed. Data in Figure 2 are the median of all the raw data of each mode on NPF event days, haze days and others days separately

Figures 5 and 6: Please specify the time resolution of the data you are showing, and reword “and they are the median data from midnight to midnight”.

We thank the referee for the comments.

As per suggestion of the referee, we changed captions of Figure 5 and 6 as below:

Figure 5. Diurnal variation of trace gas (CO, SO₂, NO_x and O₃ separately) mixing ratios on the NPF event days (green lines) and haze days (grey lines) separately. The time resolution was 30 minutes for every data point. Every data point here represents the median of all data at the same time of the days.

Figure 6. Diurnal variation of particle number concentration of every mode (cluster, nucleation, Aitken and accumulation mode separately) on the NPF event days (green lines) and haze days (grey lines). The time resolution was 30 min for every data point. Every data point here represents the median of all data at the same time of the days.

Figure 5: The scale in the upper left graph is different to the others. If you decide to use the same scale, change it to match the others. If it is not important for you that the graphs have the same scale, change the other scales (especially SO₂ and O₃) so that the variations can be seen more clearly.

We thank the referee for the comments.

As per suggestion of the referee, to make the variations to be seen more clearly, we changed the scales as shown in Figure 5 below.

Figure 6: The scales used here do not allow to see changes in the Aitken and accumulation modes. I would suggest changing the scales on the lower graphs. It is hard to see the changes you mention in the discussion.

As per suggestion of the referee, to make the variations to be visible, we changed the scales as shown in Figure 6 below.

Technical comments

Line 93-94: “.... complicating the story even further”. I would suggest using a different language.

We thank the referee for the comments. We will update the description in our manuscript as below:

While cluster mode particles can grow into the Aitken mode , also other sources like traffic contribute to this mode, making the source identification of the Aitken mode complicated.

Line 153: Please change the verb tense: measures -> measured.

As per suggestion of the referee, we corrected the verb tense.

Lines 169 and 175: Correct the references format.

As per suggestion of the referee, we corrected the reference format.

Line 213-214: Check the Aitken and accumulation median concentrations. Are they exactly the same?

We corrected the median number concentration of Aitken mode on haze days as 16000 cm^{-3} in our manuscript.

Line 300: Change “maybe” for “may be”.

As per suggestion of the referee, we changed ‘maybe’ for ‘may be’ in our manuscript in line 300.

Line 305: Delete “in” between “increase” and “during”.

As per suggestion of the referee, we deleted “in” between “increase” and “during” in line 305.

Line 311: Add in: “... SO₂ participated in the formation...”

As per suggestion of the referee, we added in: “... SO₂ participated in the formation...”

Line 386: “resulting in an increase...”

As per suggestion of the referee, we corrected our words as “resulting in an increase...”

Figure 2: Switch “left” and “right” in the figure caption.

As per suggestion of the referee, we switched “left” and “right” in the figure caption.

Figure 3: Please change the label: OtherS -> Others.

As per suggestion of the referee, we changed the label from “OtherS” to “Others” in Figure 3.

Tables and Figures

Table R1a: Correlation coefficients between particle number concentration of every mode on NPF event days. The time window was 08:00 - 14:00. High correlation coefficients ($|R|>0.5$) are marked with bold and italic.

	Cluster	Nucleation	Aitken	Accumulation
Cluster	1			
Nucleation	0.76 ^a	1		
Aitken	-0.46 ^a	-0.33 ^b	1	
Accumulation	-0.66 ^a	-0.66 ^c	0.7 ^c	1

^a included 516 data points (the time resolution was 12 minutes), ^b included 1251 data points (the time resolution was 5 min), ^c included 1331 data points (the time resolution was 5 min).

Table R1b: Correlation coefficients between particle number concentration of every mode on haze days. The time window was 08:00 - 14:00. High correlation coefficients ($|R|>0.5$) are marked with bold and italic.

	Cluster	Nucleation	Aitken	Accumulation
Cluster	1			
Nucleation	0.74 ^a	1		
Aitken	0.41 ^a	0.48 ^b	1	
Accumulation	-0.22 ^a	-0.33 ^c	-0.5 ^c	1

^a included 342 data points (the time resolution was 12 minutes), ^b included 824 data points (the time resolution was 5 min), ^c included 845 data points (the time resolution was 5 min).

Table R2a: Correlation coefficients between size segregated particle number concentrations and trace gases mixing ratios/ PM_{2.5} concentration on NPF event days. The time window was 08:00 - 14:00. High correlation coefficients ($|R|>0.5$) are marked with bold and italic.

	CO	SO ₂	NO _x	O ₃	PM _{2.5}
--	----	-----------------	-----------------	----------------	-------------------

Cluster	-0.61 ^a	-0.16 ^a	-0.66^a	0.16 ^a	-0.66^c
Nucleation	-0.5 ^b	-0.17 ^b	-0.55^b	0.36 ^b	-0.54^c
Aitken	0.58^b	0.55^b	0.66^b	0.32 ^b	0.33 ^c
Accumulation	0.71^b	0.65^b	0.69^b	0.15 ^b	0.83^c

^a included 665 data points (the time resolution was 12 minutes), ^b included 1620 data points (the time resolution was 5 min), ^c included 151 data points (the time resolution was 1 hour).

Table R2b: Correlation coefficients between size segregated particle number concentrations and trace gases mixing ratios/ PM_{2.5} concentration on haze days. The time window was 08:00 - 14:00. High correlation coefficients ($|R|>0.5$) are marked with bold and italic.

	CO	SO ₂	NO _x	O ₃	PM _{2.5}
Cluster	-0.19 ^a	0.09 ^a	0.02 ^a	0.13 ^a	0.01 ^c
Nucleation	-0.24 ^b	0.07 ^b	0.31 ^b	0.17 ^b	-0.33 ^c
Aitken	0.10 ^b	0.03 ^b	0.44 ^b	0.41 ^b	-0.5 ^c
Accumulation	0.71^b	0.76^b	0.37 ^b	0.17 ^b	0.81^c

^a included 620 data points (the time resolution was 12 minutes), ^b included 1460 data points (the time resolution was 5 min), ^c included 89 data points (the time resolution was 1 hour).

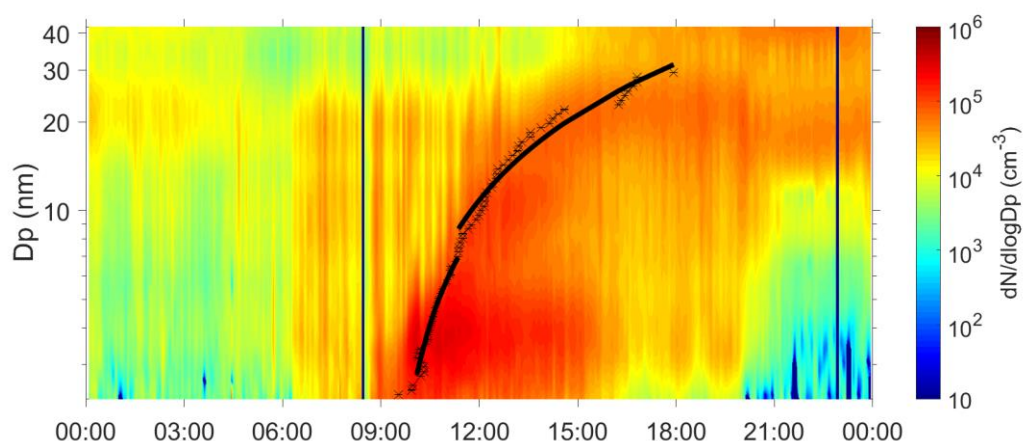


Figure R2-1: An example of how the appearance time method was used to calculate growth rate. The appearance time was recorded as a function of particle diameter as the black stars in the figure. The black lines are the fitted growth periods. The growth rates were calculated by calculating the slopes of the black lines.

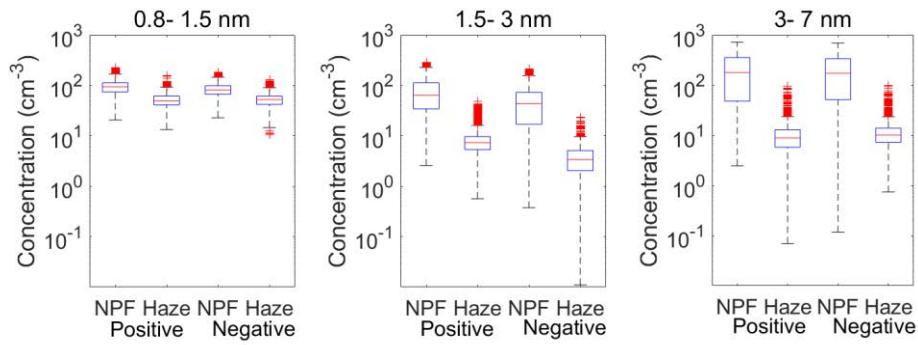


Figure R2-2: Positive and negative ion number concentrations in the size bins of 0.8- 1.5nm, 1.5-3 nm and 3-7 nm on NPF event days and haze days separately. The whiskers include 99.3% of data of every group. Data out of $1.5 \times$ interquartile range are posited outside the whiskers and considered as outliers. The lines in the boxes represent the median value, the lower of the boxes represent 25% of the number concentration, and the upper of the boxes represent 75% of the number concentration. Data marked with red pluses represent outliers.

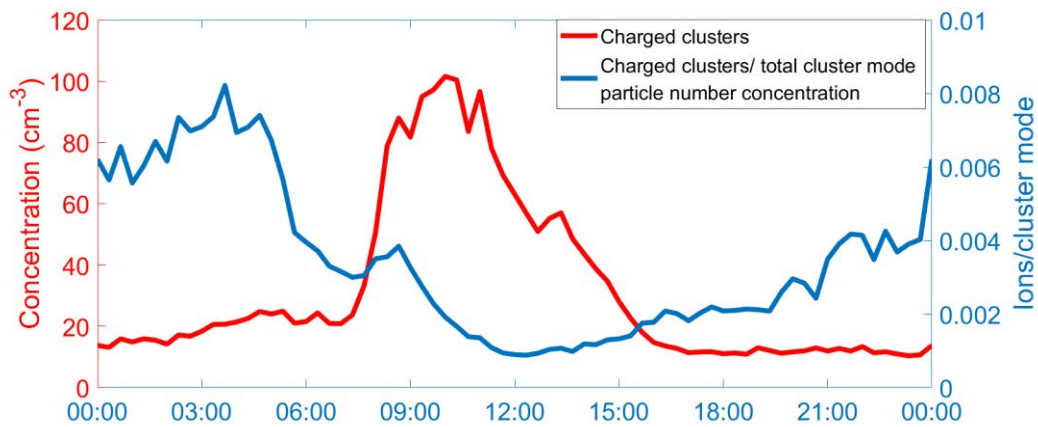


Figure R2-3: Diurnal pattern of charged clusters (1.5-3 nm) number concentration (red line) and ratio of charged clusters to total cluster mode particle number concentration on the NPF event days (blue line). The time resolution of the used data was 12 min.

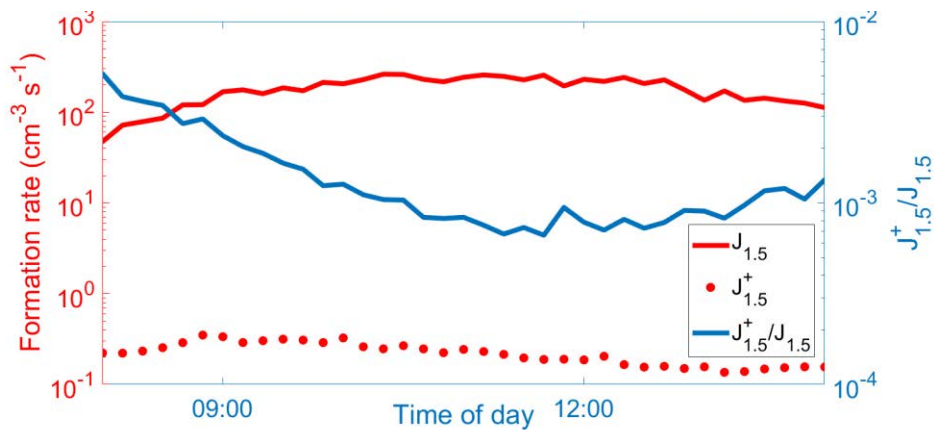


Figure R2-4 : Diurnal pattern of formation rate of positive charged clusters of 1.5 nm (red dots) and neutral clusters of 1.5 nm (red line) and the ratio between them (blue line) on the NPF event days during the NPF time window we chose. The time resolution of the used data was 12 min.

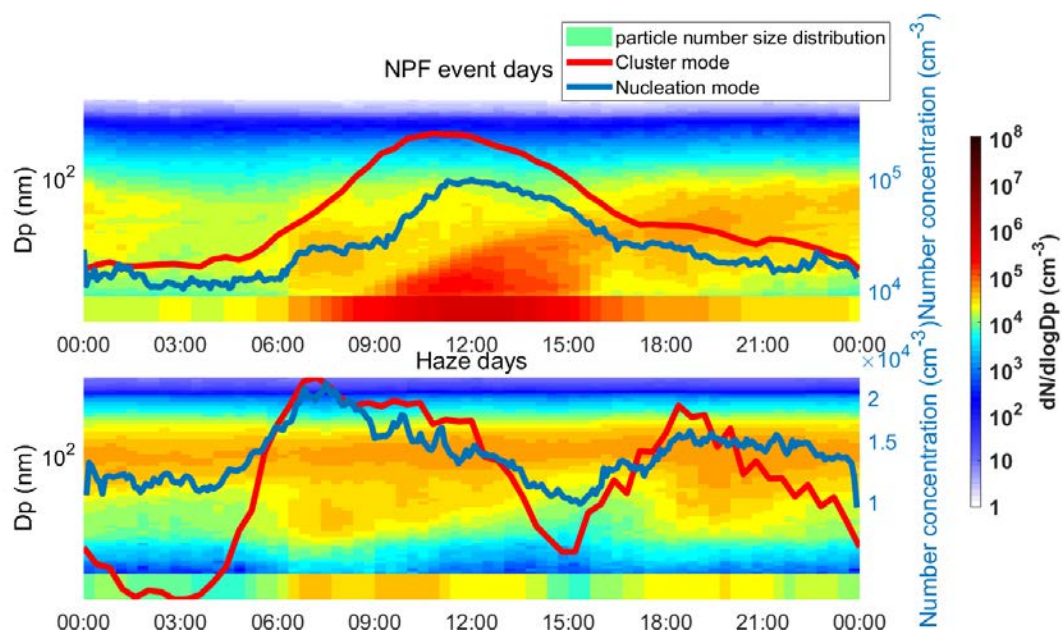


Figure R2-5: Median diurnal patterns of the particle number size distribution over the size range of 1.5-1000 nm and number concentrations of cluster mode (red lines) and nucleation mode (blue lines) particles on the NPF event days (upper panel) and haze days (lower panel). The time resolution for every data point of particle number size distribution and cluster mode particle number concentration was 12 minutes. The time resolution of every data point of nucleation mode particle number concentration was 5 minutes.

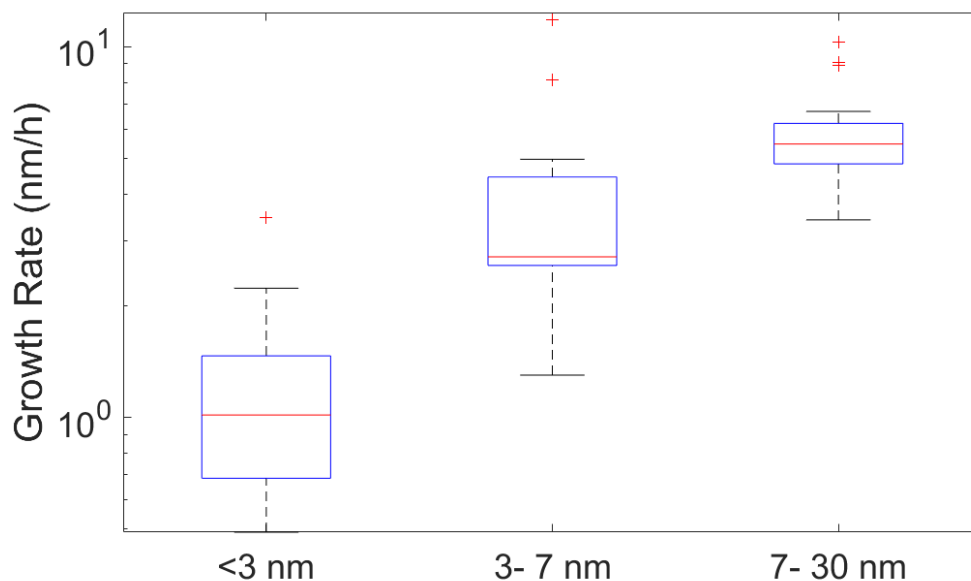


Figure R2-5: Growth rates of cluster mode and nucleation mode particles generated from NPF events. The lines in the boxes represent the median value, the lower of the boxes represent 25% of the growth rates and the upper of the boxes represent 75% of the growth rates. Data marked with red pluses represent outliers.

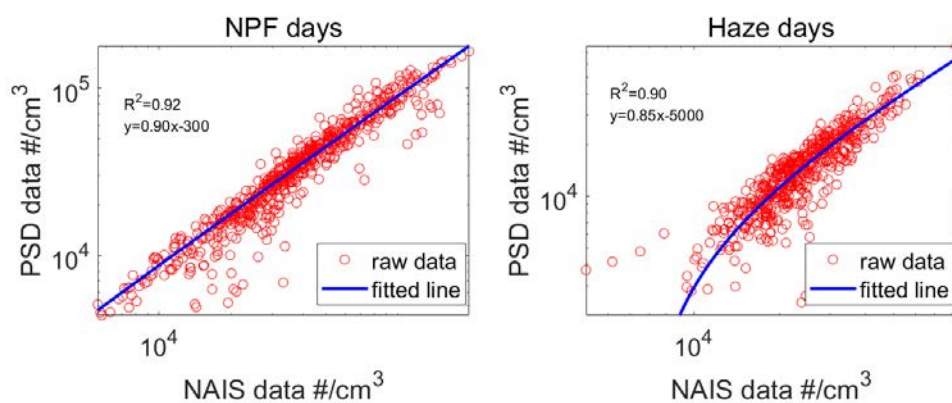


Figure R2-6: Total particle number concentration in size range of 3-42 nm from NAIS and PSD system. There are 1271 data points on the plots of NPF days and 887 data points on the plots of haze days. The time resolution was 5 minutes.

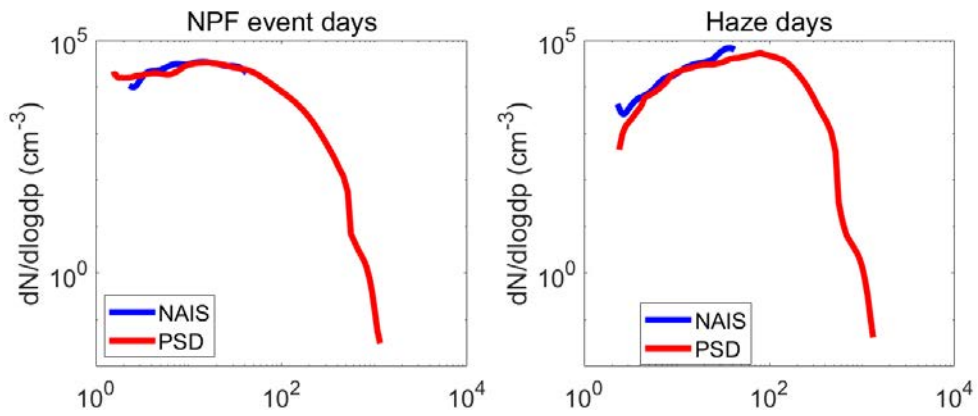


Figure R2-7: Median particle number size distribution of data from NAIS (blue line) and PSD system (red line) on NPF event days (left panel) and haze days (right panel) during our observation. The time resolution we used here for every point was 1h.

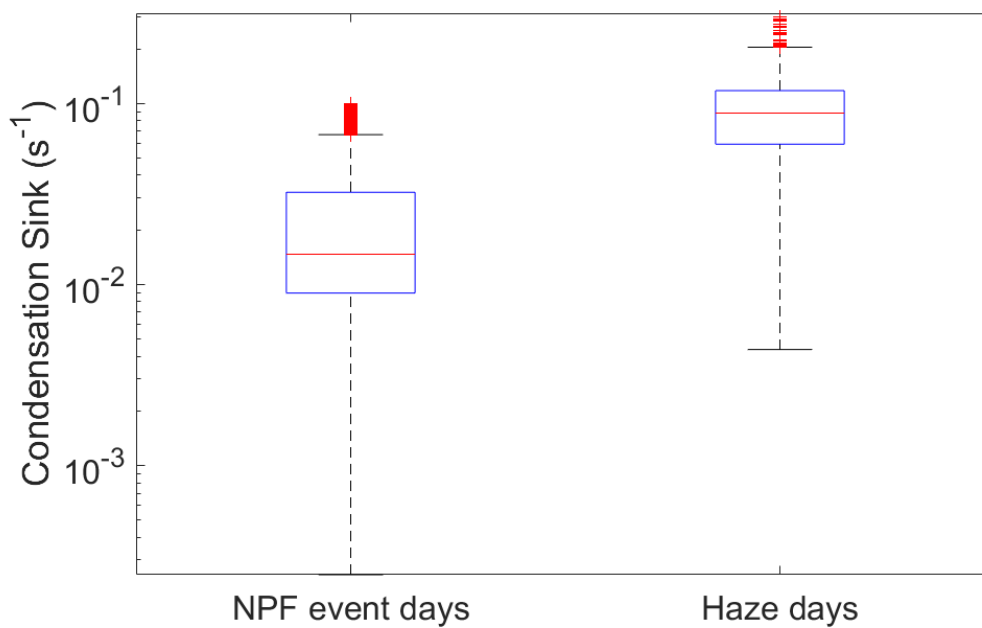


Figure R2-8: Condensation sink on NPF event days and haze days. The lines in the boxes represent the median value, the lower of the boxes represent 25% of the condensation sink and the upper of the boxes represent 75% of the condensation sink. Data marked with red pluses represent outliers.

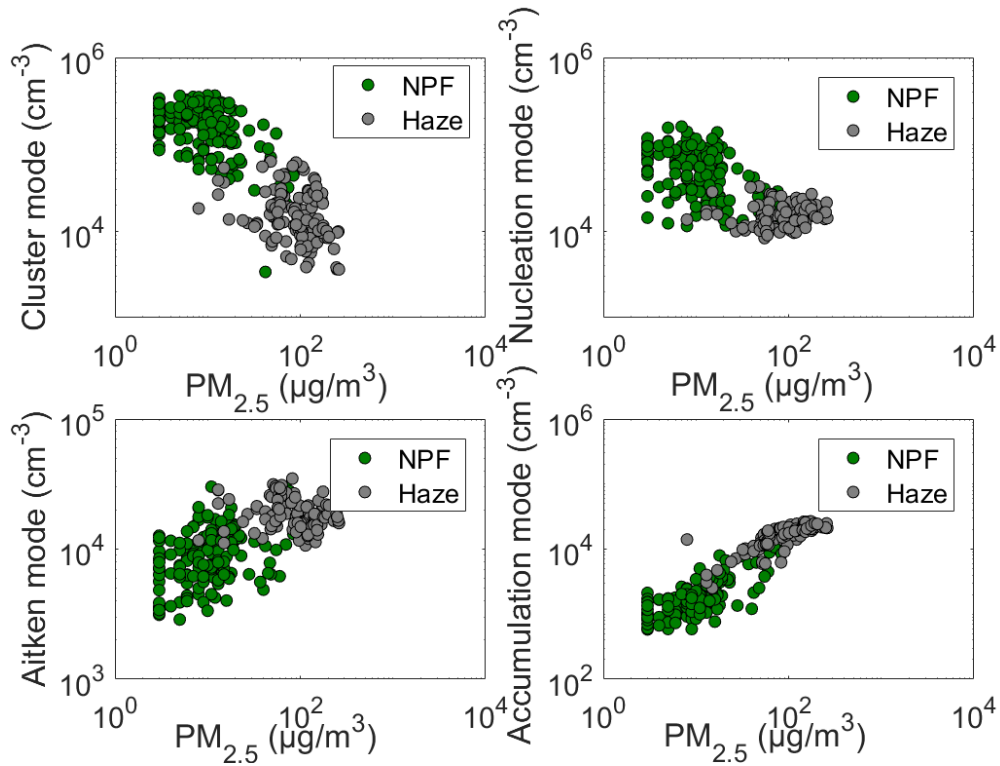


Figure R2-9 : Correlation between $PM_{2.5}$ concentration and particle number concentration in each mode on the NPF event days (green dots) and haze days (grey dots) separately. The time resolution of the data points was 1 hour.

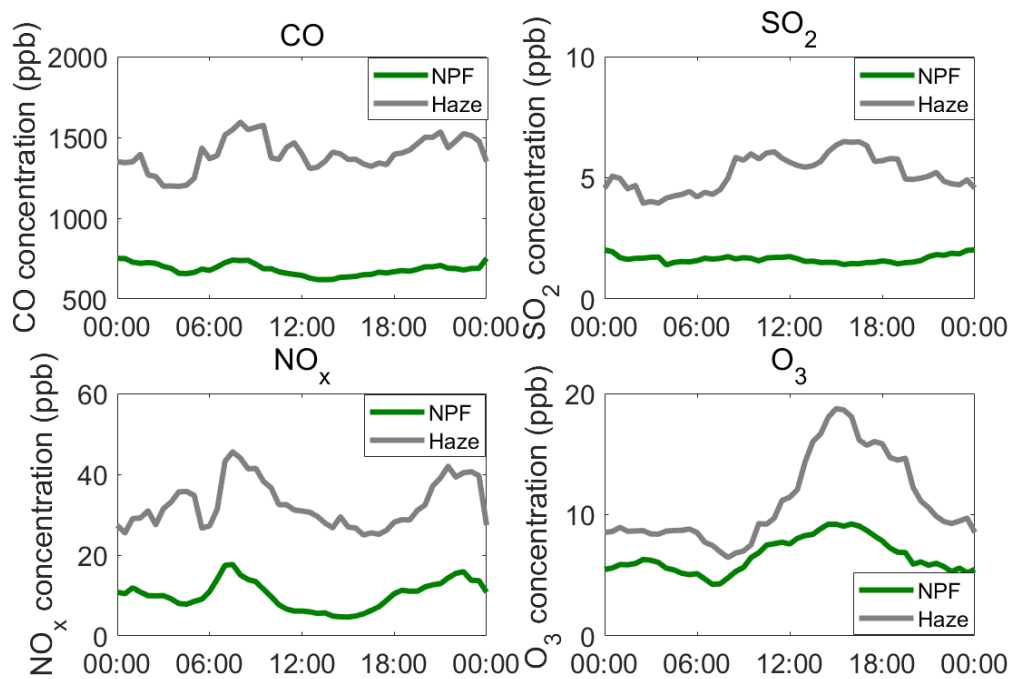


Figure 5. Diurnal variation of trace gas (CO, SO₂, NO_x and O₃ separately) mixing ratios on the NPF event days (green lines) and haze days (grey lines) separately. The time resolution was 30 minutes for every data point. Every data point here represents the median of all data at the same time of the days.

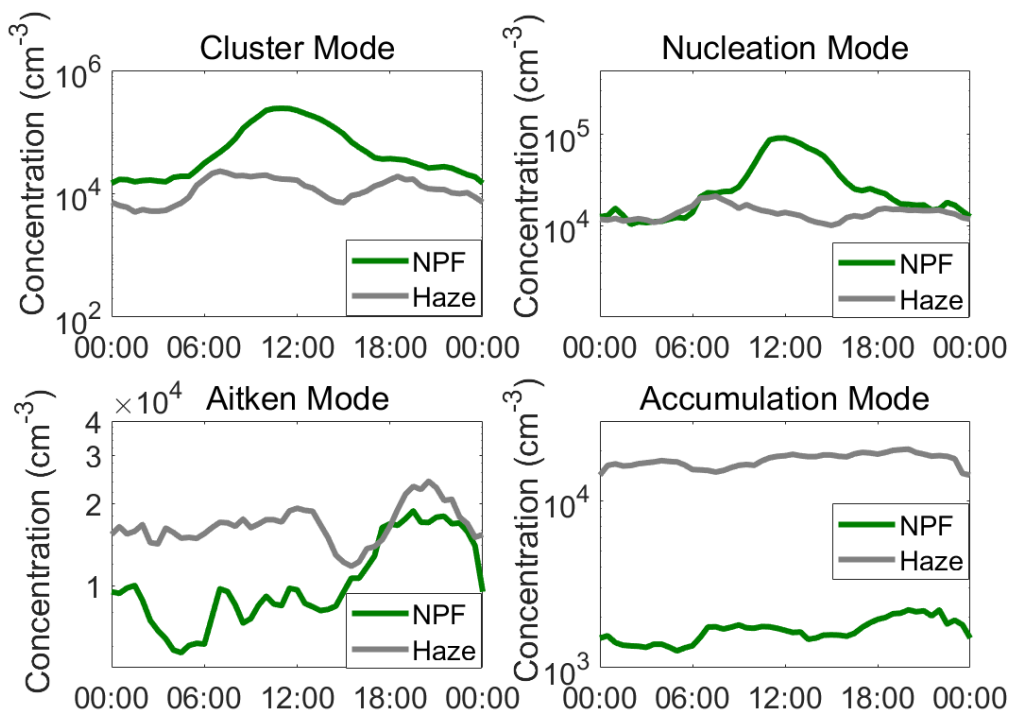


Figure 6. Diurnal variation of particle number concentration of every mode (cluster, nucleation, Aitken and accumulation mode separately) on the NPF event days (green lines) and haze days (grey lines). The time resolution was 30 min for every data point. Every data point here represents the median of all data at the same time of the days.

References

Brines, M., Dall'Osto, M., Beddows, D. C. S., Harrison, R. M., Gomez-Moreno, F., Nunez, L., Artinano, B., Costabile, F., Gobbi, G. P., Salimi, F., Morawska, L., Sioutas, C., and Querol, X.: Traffic and nucleation events as main sources of ultrafine particles in high-insolation developed world cities, *Atmos Chem Phys*, 15, 5929-5945, 2015.

Chu, B. W., Kerminen, V. M., Bianchi, F., Yan, C., Petäjä, T., and Kulmala, M.: Atmospheric new particle formation in China, *Atmos Chem Phys*, 19, 115-138, <https://doi.org/10.5194/acp-19-115-2019>, 2019.

de Jesus, A. L., Rahman, M. M., Mazaheri, M., Thompson, H., Knibbs, L. D., Jeong, C., Evans, G., Nei, W., Ding, A., Qiao, L., Li, L., Portin, H., Niemi, J. V., Timonen, H., Luoma, K., Petäjä, T., Kulmala, M., Kowalski, M., Peters, A., Cyrys, J., Ferrero, L., Manigrasso, M., Avino, P., Buonano, G., Reche, C., Querol, X., Beddows, D., Harrison, R. M., Sowlat, M. H., Sioutas, C., and Morawska, L.: Ultrafine particles and PM_{2.5} in the air of cities around the world: Are they representative of each other?, *Environment International*, 129, 118-135, [10.1016/j.envint.2019.05.021](https://doi.org/10.1016/j.envint.2019.05.021), 2019.

Du, W., Zhao, J., Wang, Y. Y., Zhang, Y. J., Wang, Q. Q., Xu, W. Q., Chen, C., Han, T. T., Zhang, F., Li, Z. Q., Fu, P. Q., Li, J., Wang, Z. F., and Sun, Y. L.: Simultaneous measurements of particle number size distributions at ground level and 260m on a meteorological tower in urban Beijing, China, *Atmos Chem Phys*, 17, 6797-6811, 2017.

Jayarathne, R., Pushpawela, B., He, C. R., Li, H., Gao, J., Chai, F. H., and Morawska, L.: Observations of particles at their formation sizes in Beijing, China, *Atmos Chem Phys*, 17, 8825-8835, 2017.

Kerminen, V. M., Chen, X. M., Vakkari, V., Petäjä, T., Kulmala, M., and Bianchi, F.: Atmospheric new particle formation and growth: review of field observations, *Environ Res Lett*, 13, <https://doi.org/10.1088/1748-9326/aadf3c>, 2018.

Kontkanen, J., Järvinen, E., Manninen, H. E., Lehtipalo, K., Kangasluoma, J., Decesari, S., Gobbi, G. P., Laaksonen, A., Petäjä, T., and Kulmala, M.: High concentrations of sub-3nm clusters and frequent new particle formation observed in the Po Valley, Italy, during the PEGASOS 2012 campaign, *Atmos Chem Phys*, 16, 17, <https://doi.org/10.5194/acp-16-1919-2016>, 2016.

Kerminen, V. M., Chen, X. M., Vakkari, V., Petäjä, T., Kulmala, M., and Bianchi, F.: Atmospheric new particle formation and growth: review of field observations, *Environ Res Lett*, 13, <https://doi.org/10.1088/1748-9326/aadf3c>, 2018.

Kontkanen, J., Lehtipalo, K., Ahonen, L., Kangasluoma, J., Manninen, H. E., Hakala, J., Rose, C., Sellegri, K., Xiao, S., Wang, L., Qi, X. M., Nie, W., Ding, A. J., Yu, H., Lee, S., Kerminen, V. M., Petaja, T., and Kulmala, M.: Measurements of sub-3nm particles using a particle size magnifier in different environments: from clean mountain top to polluted megacities, *Atmos Chem Phys*, 17, 2163-2187, 2017.

Kulmala, M., Petäjä, T., Nieminen, T., Sipilä, M., Manninen, H. E., Lehtipalo, K., Dal Maso, M., Aalto, P. P., Junninen, H., Paasonen, P., Riipinen, I., Lehtinen, K. E. J., Laaksonen, A., and Kerminen, V. M.: Measurement of the nucleation of atmospheric aerosol particles, *Nat Protoc*, 7, 1651-1667, <https://doi.org/10.1038/nprot.2012.091>, 2012.

Kulmala, M., Kontkanen, J., Junninen, H., Lehtipalo, K., Manninen, H. E., Nieminen, T., Petäjä, T., Sipilä, M., Schobesberger, S., Rantala, P., Franchin, A., Jokinen, T., Järvinen, E., Äijälä, M., Kangasluoma, J., Hakala, J., Aalto, P. P., Paasonen, P., Mikkilä, J., Vanhanen, J., Aalto, J., Hakola, H., Makkonen, U., Ruuskanen, T., Mauldin, R. L., Duplissy, J., Vehkamäki, H., Bäck, J., Kortelainen, A., Riipinen, I., Kurtén, T., Johnston, M. V., Smith, J. N., Ehn, M., Mentel, T. F., Lehtinen, K. E. J., Laaksonen, A., Kerminen, V. M., and Worsnop, D. R.: Direct Observations of Atmospheric Aerosol Nucleation, *Science*, 339, 943-946, <https://doi.org/10.1126/science.1227385>, 2013.

Kulmala, M., Petaja, T., Ehn, M., Thornton, J., Sipilä, M., Worsnop, D. R., and Kerminen, V. M.: Chemistry of Atmospheric Nucleation: On the Recent Advances on Precursor Characterization and Atmospheric Cluster Composition in Connection with Atmospheric New Particle Formation, *Annu Rev Phys Chem*, 65, 21-37, 2014.

Lehtipalo, K., Leppä, J., Kontkanen, J., Kangasluoma, J., Wimmer, D., Franchin, A., Schobesberger, S., Junninen, H., Petäjä, T., Sipilä, M., Mikkilä, J., Vanhanen, J., Worsnop, D. r., and Kulmala, M.: methods for determining particle size distribution and growth rates between 1 and 3 nm using the Particle Size Magnifier, *Boreal Environ Res*, 19 215-236, 2014.

Liu, X. G., Li, J., Qu, Y., Han, T., Hou, L., Gu, J., Chen, C., Yang, Y., Liu, X., Yang, T., Zhang, Y., Tian, H., and Hu, M.: Formation and evolution mechanism of regional haze: a case study in the megacity Beijing, China, *Atmos Chem Phys*, 13, 4501-4514, 2013.

Mazon, S. B., Kontkanen, J., Manninen, H. E., Nieminen, T., Kerminen, V.-M., and Kulmala, M.: A long-term comparison of nighttime cluster events and daytime ion formation in a boreal forest, *Boeral Environment Research*, 21, 19, 2016.

Paasonen, P., Peltola, M., Kontkanen, J., Junninen, H., Kerminen, V.-M., and Kulmala, M.: Comprehensive analysis of particle growth rates from nucleation mode to cloud condensation nuclei in boreal forest, *Atmos Chem Phys*, 18, 12085-12103, 10.5194/acp-18-12085-2018, 2018.

Qi, X. M. D., A. J., Nie, W., Petaja, T., Kerminen, V. M., Herrmann, E., Xie, Y. N., Zheng, L. F., Manninen, H., Aalto, P., Sun, J. N., Xu, Z. N., Chi, X. G., Huang, X., Boy, M., Virkkula, A., Yang, X. Q., Fu, C. B., and Kulmala, M.: Aerosol size distribution and new particle formation in the western Yangtze River Delta of China: 2 years of measurements at the SORPES station, *Atmos Chem Phys*, 15, 12445-12464, 2015.

Rönkkö, T., Kuuluvainen, H., Karjalainen, P., Keskinen, J., Hillamo, R., Niemi, J. V., Pirjola, L., Timonen, H. J., Saarikoski, S., Saukko, E., Järvinen, A., Silvennoinen, H., Rostedt, A., Olin, M., Yli-Ojanperä, J., Nousiainen, P., Kousa, A., and Dal Maso, M.: Traffic is a major source of atmospheric nanocluster aerosol, *P Natl Acad Sci USA*, 114, 7549-7554, <https://doi.org/10.1073/pnas.1700830114>, 2017.

Shi, J. P., Evans, D. E., Khan, A. A., and Harrison, R. M.: Sources and concentration of nanoparticles (< 10 nm diameter) in the urban atmosphere, *Atmospheric Environment*, 35, 1193-1202, 2001.

Tuomi, T. J.: Atmospheric electrode effect: Approximate theory and wintertime observations, pure and applied geophysics, 119, 15, <https://doi.org/10.1007/BF00878719>, 1980.

Vu, T. V., Delgado-Saborit, J. M., and Harrison, R. M.: Review: Particle number size distributions from seven major sources and implications for source apportionment studies, *Atmospheric Environment*, 122, 114-132, 10.1016/j.atmosenv.2015.09.027, 2015.

Wang, Z. B., Hu, M., Wu, Z. J., Yue, D. L., He, L. Y., Huang, X. F., Liu, X. G., and Wiedensohler, A.: Long-term measurements of particle number size distributions and the relationships with air mass history and source apportionment in the summer of Beijing, *Atmos Chem Phys*, 13, 10159-10170, 2013.

Wang, Z. B., Wu, Z. J., Yue, D. L., Shang, D. J., Guo, S., Sun, J. Y., Ding, A. J., Wang, L., Jiang, J. K., Guo, H., Gao, J., Cheung, H. C., Morawska, L., Keywood, M., and Hu, M.: New particle formation in China: Current knowledge and further directions, *Science of the Total Environment*, 577, 258-266, 2017.

Wu, Z. J., Hu, M., Liu, S., Wehner, B., Bauer, S., Ssling, A. M., Wiedensohler, A., Petaja, T., Dal Maso, M., and Kulmala, M.: New particle formation in Beijing, China: Statistical analysis of a 1-year data set, *J Geophys Res-Atmos*, 112, 2007.

Yao, L., Garmash, O., Bianchi, F., Zheng, J., Yan, C., Kontkanen, J., Junninen, H., Mazon, S. B., Ehn, M., Paasonen, P., Sipilä, M., Wang, M. Y., Wang, X. K., Xiao, S., Chen, H. F., Lu, Y. Q., Zhang, B. W., Wang, D. F., Fu, Q. Y., Geng, F. H., Li, L., Wang, H. L., Qiao, L. P., Yang, X., Chen, J. M., Kerminen, V. M., Petäjä, T., Worsnop, D. R., Kulmala, M., and Wang, L.: Atmospheric new particle formation from sulfuric acid and amines in a Chinese megacity, *Science*, 361, 278-281, <https://doi.org/10.1126/science.aao4839>, 2018.

Marked-up manuscript

1 Variation of size-segregated particle number concentrations in winter

2 Beijing

3 Ying Zhou¹, Lubna Dada^{1,2*}, Yiliang Liu³, Yueyun Fu⁴, Juha Kangasluoma^{1,2}, Tommy
4 Chan¹, Chao Yan², Biwu Chu², Kaspar R Daellenbach², Federico Bianchi², Tom
5 Kokkonen², Yongchun Liu¹, Joni Kujansuu^{1,2}, Veli-Matti Kerminen², Tuukka Petäjä²,
6 Lin Wang³, Jingkun Jiang⁴, Markku Kulmala^{1,2*}

7 ¹Aerosol and Haze Laboratory, Beijing Advanced Innovation Center for Soft Matter Science and
8 Engineering, Beijing University of Chemical Technology, Beijing, China

9 ²Institute for Atmospheric and Earth System Research / Physics, Faculty of Science, University of
10 Helsinki, Finland

11 ³Shanghai Key Laboratory of Atmospheric Particle Pollution and Prevention (LAP³), Department of
12 Environmental Science & Engineering, Jingwan Campus, Fudan University, Shanghai 200438, China

13 ⁴School of Environment, Tsinghua University, Beijing, China

14

15 *Correspondences are to Lubna Dada: lubna.dada@helsinki.fi and Markku Kulmala:
16 markku.kulmala@helsinki.fi

17 Abstract

18 ~~Aerosol~~ The spatial and temporal variability of the number ~~concentration~~ varying
19 spatially and temporally size distribution of aerosol particles is ~~a good~~ an indicator of
20 the dynamic behavior of Beijing's atmospheric cocktail. This variation
21 ~~represents~~ reflects the strength of different ~~contributing~~ primary and secondary sources,
22 such as traffic and new particle formation, ~~respectively~~ as well as the main processes
23 affecting the particle population. In this paper, we report size-segregated particle
24 number concentrations observed at ~~a newly~~ developed Beijing station during ~~the~~ winter
25 of 2018. Our measurements ~~cover~~ covered particle number size distributions ~~of particles~~
26 ~~in a~~ over the diameter range ~~between~~ of 1.5 nm ~~and~~ – 1 μm (cluster mode, nucleation
27 mode, Aitken mode and accumulation mode), thus being descriptive of a major fraction
28 of the processes ~~happening~~ taking place in the atmosphere of Beijing. Here we ~~aim to~~
29 explain ~~focus on explaining~~ the concentration ~~variation~~ variations in the observed
30 particle modes by relating them to ~~the~~ potential aerosol sources ~~as well as to~~
31 ~~understand~~ and sinks, and on understanding the ~~connection~~ connections between
32 ~~the~~ these modes. We ~~focused on two types of days (considered haze days and new~~
33 ~~particle formation)~~ and divided the data accordingly: event days separately. Our results
34 show that during ~~the~~ new particle formation (NPF) event days, ~~an increase~~ increases in
35 ~~the~~ cluster mode ~~particles was~~ particle number concentration were observed. ~~In contrast,~~

36 ~~whereas~~ during ~~the~~ haze days ~~we observed a high concentration concentrations~~ of
37 accumulation mode particles: ~~were present~~. There was a ~~clear correlation tight~~
38 ~~connection~~ between the cluster ~~mode~~ and nucleation ~~modes during mode on both~~ NPF
39 ~~days, while it was absent during event and~~ haze days. In addition, we correlated the
40 ~~particle number concentrations in~~ different modes with concentrations of trace gases
41 and other parameters measured at our station. Our results show that ~~the particle number~~
42 ~~concentration in all the~~ modes ~~in the sub-micron size range~~ correlated with NO_x, which
43 ~~clearly~~ reflects the contribution of traffic to ~~all particle sizes the whole sub-micron size~~
44 ~~range. We also estimated the contribution of ion-induced nucleation in Beijing, and~~
45 ~~found this contribution to be negligible.~~

46 1 Introduction

47 Atmospheric aerosols are the main ingredient of China's pollution cocktail (Kulmala
48 2015). ~~They~~ Aerosols have gained increasing attention due to their effects on human
49 health, climate and visibility (Lelieveld et al., 2015, IPCC 2007). Currently, air quality
50 standards for cities in China consider particle mass instead of number concentration
51 (WHO, 2000), which may ignore the ~~potential adverse~~ effect of ultra-fine particles ~~on~~
52 ~~health~~ (diameter less than 100 nm). ~~However, it~~ It has been shown that ultra-fine
53 particles can penetrate deep into the respiratory tract, ending up to the blood circulation,
54 which ~~allow allows~~ them to deposit into the brain (Oberdörster et al., 2004). Indeed,
55 studies have pointed out that ultra-fine particles, which contribute to a negligible
56 fraction of the mass concentration, dominate the total number concentration in urban
57 areas (von Bismarck-Osten et al., 2013; Wehner et al., 2004; Wu et al., 2008). Due to
58 their high ~~concentration concentrations~~, ultrafine particles' toxicological ~~effect is~~
59 ~~enlarged effects are enhanced~~ by their large total surface area (Kreyling et al., 2004).

60 Apart from their health effects, the temporal and spatial variation of particle number
61 concentrations of different sizes is a good ~~estimate indicator~~ of the strength of their
62 emission sources. ~~The aerosols~~ Aerosols are emitted either directly as primary particles,
63 such as sea salt or dust particles as a result of natural phenomena (Solomos et al., 2011),
64 or ~~nano-particles could also form they can be formed~~ through new particle formation
65 (Kulmala, 2003; Kulmala et al., 2004; Kulmala et al., 2013; Kerminen et al., 2018; Chu
66 et al., 2019). ~~The newly~~ Newly formed particles can grow up ~~into diameters of~~ 20-100
67 nm within a day (Kulmala et al., 2004), and ~~are they have been~~ found to contribute to
68 a major fraction of ~~the global~~ cloud condensation nuclei population (CCN), thus
69 indirectly affecting the climate (Kerminen et al., 2012). For all aforementioned reasons,
70 and in order to form a collective, ~~and~~ complete picture about atmospheric aerosol
71 particles, to understand their origin and potential impacts at a specific location, the
72 whole size distribution of these ~~atmospheric~~ particles needs to be studied.

73 Recently, due to urbanization and increased population, megacities have increased their
74 contribution to atmospheric aerosol pollution massively (Baklanov et al., 2016).
75 Interestingly, more people live ~~inside~~ eastern Asia (specifically, China and India)
76 ~~rather than~~ outside this region (<https://www.unfpa.org/swop>). Therefore, it is important
77 to study the contributions of different sources to size-segregated number concentrations
78 in order to inspire policy makers and the public on measures that need to be taken in
79 order to reduce particulate pollution. Many studies in various cities in China have
80 tackled this topic. For instance, ~~a~~-two-years ~~observation of~~ observations of particle
81 number size distributions at a site in northern Beijing reported that traffic emissions
82 ~~are were~~ the major source of nucleation (3-20 nm) and Aitken (20-100 nm) mode
83 particles in urban Beijing (Wang et al., 2013). On ~~another~~ the other hand, ~~a~~ research
84 conducted in western downtown of Nanjing reported that local new particle formation
85 events ~~are were~~ the main contributors of both nucleation (5-20 nm) mode and CCN
86 particle populations (Dai et al., 2017). ~~Moreover, an observation~~ Measurements
87 of nucleation mode particle ~~concentration~~ concentrations in urban Hong Kong reported the
88 dominant contribution of combustion sources to the nucleation mode (5.5-10 nm)
89 (Wang et al., 2014a). ~~Also, an observation~~, whereas observations in urban Guangzhou
90 found that accumulation and secondary transformation of particles ~~are were~~ the main
91 reasons for high ~~concentration~~ concentrations of accumulation mode particles (100-660
92 nm) (Yue et al., 2010). However, only a few studies in China have reported
93 measurements of cluster mode ~~particles~~-(sub-3 nm) particles and related them to new
94 particle formation events (Cai et al., 2017; Xiao et al., 2015; Yao et al., 2018; Yu et al.,
95 2016).

96 The observation of sub-3 nm particles and ions ~~was has been~~ made possible by recent
97 major ~~instrumentation development~~ developments in instrumentations, such as the
98 particle size magnifier (PSM) (Vanhanen et al., 2011), diethylene glycol-based scanning
99 mobility particle sizer (DEG-SMPS) (Jiang et al., 2011), and Neutral Cluster and Air
100 Ion Spectrometers (NAIS) (Manninen et al., 2016; Mirme et al., 2007).

101 In ~~a~~-complicated ~~environment such as in~~ environments like Beijing, it is very hard to
102 relate each particle mode to a specific source. Indeed, ~~many several~~ sources could
103 contribute to aerosol particles in the same size range. For instance, cluster mode
104 particles mainly originate from ~~the~~-secondary gas-to-particle transformation
105 ~~process~~ processes (Kulmala et al. 2013), although recently also traffic has been
106 identified as a source for these ~~small sized~~-particles (Rönkkö et al., 2017). While
107 ~~these cluster mode~~ particles can grow ~~to nucleation into the Aitken~~ mode sizes, also
108 other sources ~~such as black carbon from~~ like traffic contribute to Aitken this mode,
109 ~~complicating making~~ the ~~story even further~~ source identification of the Aitken mode
110 complicated (Pirjola et al., 2012). Various anthropogenic activities and biogenic
111 processes contribute to accumulation mode particle sizes. Thus, correlating trace gases
112 and aerosol concentrations of different sizes during different time periods help

113 ~~narrow~~narrowing down these aerosol sources.

114 In this study, we analyzed the number concentration of four sub-micron aerosol modes:
115 cluster mode (sub-3 nm), nucleation mode (3-25 nm), Aitken mode (25-100 nm), and
116 accumulation mode (100-1000 nm). Our aims ~~are~~were i) to investigate the number
117 concentration variations of ~~the size-segregated~~ aerosol number concentrations for each
118 ~~modes~~mode, ii) to explore the relationships between the different modes under different
119 atmospheric conditions, iii) to connect the number size distribution modes with multiple
120 trace gases (NO_x, SO₂, CO and O₃) and PM_{2.5} (particulate matter with aerodynamic
121 diameter less than 2.5 μm), and iv) to quantify the contribution of NPF and haze
122 formation to different particle modes in winter time in Beijing. Our work increases ~~our~~
123 understanding of the sources of the different sized particles in Beijing, China, and
124 the work complements studies in other megacities.

125 2 Materials and Methods

126 2.1 Description of SMEAR Beijing station

127 Beijing, as the capital of China, accommodates more than 20 million people within 16.8
128 thousand square kilometers and only 1.4 thousand square kilometers for urban areas,
129 with an expanding economic activity, construction and industry. Beijing, as one of the
130 largest megacities in the world, is located in the Northern Chinese Plain, and is one of
131 the most industrialized regions in China. Mountains surround Beijing from the west,
132 north and north-west.

133 For our study, we analyzed data collected at the newly-developed station which is part
134 of the Aerosol and Haze Laboratory in Beijing. The urban station follows ~~from~~ the
135 concept of Station for Measuring Ecosystem and Atmospheric Relations (SMEAR)
136 (Hari and Kulmala, 2005). Our station is located on the western campus of Beijing
137 University of Chemical Technology (BUCT). It is constructed on the fifth floor of the
138 teaching building on the campus ~~and the~~. The sampling lines extend to the rooftop of
139 the building around 20 m above the ground level, going directly through windows for
140 selected instruments. The station represents a typical area in urban Beijing subject to
141 pollution sources, such as traffic, cooking and long-range transport of pollution. The
142 campus is surrounded by highways and main roads from the Easteast (3rd ring main
143 road), north (Zizhu road) and south-east (Zizhu Bridge). From the east, west and south,
144 the campus is surrounded by residential and commercial areas.

145 Measurements at SMEAR Beijing started on 16 January, 2018 (Lu et al., 2018). ~~and~~
146 continueOur measurements continued until present, except during the necessary
147 instruments² maintenance and unavoidable factors such as power cuts (~~Lu et al., 2018~~).

148 The data included in this study were collected between 16 January and 15 March 2018,
149 being representative of Beijing winter conditions.

150 2.2 Instrumentation

151 For a comprehensive measurement of particles, a full set of particle measuring
152 instrumentation was operated. First, a nano-condensation nucleus counter system
153 (nCNC) consisting of a Particle Sizer Magnifier (PSM, model A10, Airmodus Oy,
154 Finland) and butanol condensation particle counter (CPC) (model A20, Airmodus Oy,
155 Finland) measured the number concentration of small clusters ~~for~~ particles of 1.2-2.5
156 nm (in mobility diameter) (Vanhanen et al., 2011). To minimize the sampling losses,
157 the PSM was sampling horizontally ~~from~~through a window to the north through a short
158 stainless steel sampling inlet extending ~1.2 m outward from the building. The length
159 of the sampling tube was 1.33 m and ~~the~~its inner diameter ~~is~~was 0.8 cm. To further
160 improve the sampling efficiency, a core sampling tube (Kangasluoma et al., 2016) was
161 utilized. The total flow rate was 7.5 liters per minute (lpm), from which 5 lpm was used
162 as a transport flow while the nCNC sample flow rate was 2.5 lpm. In the operation of
163 the PSM ~~the saturator flow scanned from 0.1 to 1.3 lpm within 240s.~~, the saturator flow
164 rate scanned from 0.1 to 1.3 lpm and scanned back from 1.3 to 0.1 lpm within 240 s.
165 We averaged the data over 3 scans to make it smoother, and therefore the time resolution
166 of PSM data was 12 minutes. The data were inverted with a kernel function method.
167 When comparing the particle number concentrations obtained with the expectation-
168 maximization method, the cluster mode particle number concentration was, on average,
169 twice higher on the NPF event days and eleven times higher on the haze days (Cai et
170 al., 2018). Therefore, there is some uncertainty in the reported cluster mode particle
171 concentrations.

172 A particle size distribution (PSD) system measured ~~aerosol~~the particle number size
173 distribution in the size range of 3 nm-10000 nm (Liu et al., 2016). It included a nano-
174 scanning mobility particle sizer (nano SMPS, 3-55 nm, mobility diameter), a long
175 SMPS (25-650 nm, mobility diameter) and an aerodynamic particle sizer (APS, 0.55
176 μm -10 μm , aerodynamic diameter). The PSD system sampled from the rooftop ~~with an~~
177 ~~around~~using a 3-~~m~~-long sampling tube. A cyclone that removed particles larger than
178 10 μm was added in front of the sample line. The time resolution of PSD system data
179 was 5 minutes.

180 A Neutral Cluster and Air Ion Spectrometer (NAIS, model 4-11, Airel, Estonia)
181 ~~measures total particle~~measured number size ~~distribution~~distributions of particles (2.5-
182 42 nm ~~(, mobility diameter),~~) and ions ~~of~~ (0.7-42 nm, ~~(mobility diameter)~~) (Manninen
183 et al., 2016; Mirme and Mirme, 2013). It switched between detecting either naturally
184 charged ions or total particles (including the uncharged fraction) with unipolar charging.
185 It measured 2 min in the neutral mode, 2 min in the ion mode and then offset for 30

186 seconds for every measurement cycle. The NAIS was sampling horizontally from the
187 north window. The copper ~~4 cm sampling tube with an~~ outer diameter ~~sampling tube of~~
188 4 cm extended 1.6 m outside the window. To increase the sampling efficiency, the
189 sampling flow rate was ~~60~~54 lpm.

190 The trace gas monitors measured carbon monoxide (CO), sulfur dioxide (SO₂), nitrogen
191 oxides (NO_x) and ozone (O₃) concentrations with Thermo Environmental Instruments
192 models 48i, 43i-TLE, 42i, 49i, respectively. They all sampled through a common inlet
193 through the roof of the building. The length of the sampling tube was approximately 3
194 m. The time resolution of CO, NO_x, and O₃ data were 5 minutes, whereas the time
195 resolution of SO₂ data was 1 hour before 22 January, 2018, and 5 minutes after that.

196 The PM_{2.5} data ~~was~~were obtained from the nearest national monitor station, Wanliu
197 station, around 3 km north ~~from~~of our station. The PM_{2.5} data from Wanliu station
198 compared nicely ~~to~~with the PM_{2.5} data from three other adjacent national stations. The
199 ~~data~~was time resolution of the PM_{2.5} data was 1 hour, and these data were recorded
200 every hour. Detailed information is reported in ~~(Cao et al., (2014).~~

201 We measured the relative humidity (RH, %), visibility (km), wind speed (m/s) and wind
202 direction (°) from a weather station on the roof of our station.

203 When data sets having different time resolutions were used, we chose the smallest time
204 resolution as the common time resolution. Data with higher time resolutions were
205 merged to the common time resolution by taking median numbers between two time
206 points of the new time series.

207 2.3 NPF events and haze days classification

208 We classified days into “NPF event days” and “haze days”. The days that did not fit
209 either of these two categories ~~were~~were marked as “Other ~~day~~days”, and they were
210 excluded from our future analysis unless otherwise specified. We observed 28 NPF
211 event days and 24 haze days in total. Table 1 describes the specific calendar of events
212 with the aforementioned categories of days.

213 We identified the NPF event days following the method introduced in (Dal Maso et al.,
214 2005), which requires an appearance of a new mode below 25 nm and that the new
215 mode shows signs of growth ~~and spans for~~ several hours (Dal Maso et al., 2005;
216 Kulmala et al., 2012). Haze ~~day~~events were identified ~~with~~as having a visibility less
217 than 10 km ~~with~~and ambient relative humidity below 80% (China Meteorological
218 Administration). ~~In this study,~~Individual days were classified as haze days when ~~the~~
219 haze event lasted for at least 12 consecutive hours. ~~In general,~~During our study periods,
220 there ~~were~~was no overlap between the NPF events and haze ~~periods~~days, as these two
221 phenomena never occurred simultaneously. While the NPF events appeared right after
222 sunrise and lasted for several hours, the haze events did not have any specific ~~hour,~~

and time of appearance but lasted for from a few hours up to several days.

The particle number size distribution was divided into 4 modes according to their diameter: cluster mode (sub-3 nm), nucleation mode (3-25 nm), Aitken mode (25-100 nm), and accumulation mode (100-1000 nm). Moreover, since in Beijing, new particle formation events were only observed during daytime, our analysis concentrated mostly on the time period 8:00 to 14:00, unless specified otherwise. We calculated cluster mode particle number concentrations using Particle Size Magnifier (PSM) data, nucleation mode particle number concentration using Neutral Cluster and Air Ion Spectrometer (NAIS) particle mode data, and Aitken and accumulation mode particle number concentrations using Particle Size Distribution (PSD) system data. The Particle Size Distribution system (PSD) and Neutral Cluster and Air Ion Spectrometer (NAIS) had an overlapping particle size distribution over the mobility diameter range of 3-42 nm. As shown in Figure S1, total particle number concentrations from the NAIS and PSD system correlated well with each other on both NPF event days (R^2 was 0.92) and haze days (R^2 was 0.90) in the overlapping size range. The slopes between the total particle number concentration from the PSD system and that from the NAIS were 0.90 and 0.85 on the NPF event days and haze days, respectively. The particle number size distribution in the overlapping size range of the NAIS and PSD system matched well on both NPF event days and haze days as shown in Figure S2.

Moreover, since new particle formation events were only observed during daytime in Beijing, our analysis concentrated mostly on the time period 8:00 to 14:00, unless specified otherwise.

2.4 Parameter calculation

2.4.1 Calculation of the growth rate

The growth rates of cluster and nucleation mode particles were calculated from positive ion data and particle data from Neutral Cluster and Air Ion Spectrometer (NAIS), respectively, by using the appearance time method introduced by Lehtipalo et al. (2014). In this method, the particle number concentration of particles of size dp is recorded as a function of time, and the appearance time of particles of size dp is determined as the time when their number concentration reaches 50% of its maximum value during new particle formation (NPF) events.

The growth rates (GR) were calculated according to:

$$GR = \frac{dp_2 - dp_1}{t_2 - t_1} \quad (1)$$

where t_2 and t_1 are the appearance times of particles with sizes of dp_2 and dp_1 respectively. Figure S3 shows an example of how this method was used.

2.4.2 Calculation of the coagulation sink

The coagulation sink (CoagS) was calculated according to the equation (2) introduced by Kulmala et al. (2012):

$$CoagS_{dp} = \int K(dp, d'p)n(d'p)dd'p \cong \sum_{d'p=dp}^{d'p=max} K(dp, d'p)N_{d'p} \quad (2)$$

where $K(dp, d'p)$ is the coagulation coefficient of particles with sizes of dp and $d'p$, $N_{d'p}$ is the particle number concentration with size of $d'p$.

2.4.3 Calculation of the formation rate

The formation rate of 1.5-nm particles ($J_{1.5}$) was calculated using particle number concentrations measured with a Particle Sizer Magnifier (PSM). The formation rate of 1.5-nm ions ($J_{1.5}^{\pm}$) was calculated using positive and negative ions data from the Neutral Cluster and Air Ion Spectrometer (NAIS) as well as PSM data. The upper limit used was 3 nm. The values of $J_{1.5}$ and $J_{1.5}^{\pm}$ were calculated following the methods introduced by Kulmala et al. (2012) with equation (3) and equation (4), respectively:

$$J_{dp} = \frac{dN_{dp}}{dt} + CoagS_{dp} \cdot N_{dp} + \frac{GR}{\Delta dp} \cdot N_{dp} \quad (3)$$

where $CoagS_{dp}$ is the coagulation sink in the size range of $[dp, dp + \Delta dp]$ and GR is the growth rate.

$$J_{dp}^{\pm} = \frac{dN_{dp}^{\pm}}{dt} + CoagS_{dp} \cdot N_{dp}^{\pm} + \frac{GR}{\Delta dp} \cdot N_{dp}^{\pm} + \alpha \cdot N_{dp}^{\pm} \cdot N_{<dp}^{\mp} - \chi N_{dp} \cdot N_{<dp}^{\pm} \quad (4)$$

The fourth and fifth terms on the right hand side of equation (4) represent ion-ion recombination and charging of neutral particles by smaller ions, respectively. α is the ion-ion recombination coefficient and χ is the ion-aerosol attachment coefficient.

3 Results and discussion

3.1 General character of particle modes and trace gases

3.1.1 Sub-micron particles and PM2.5

Particle number concentrations of different modes varied depending on the period, as

284 shown in Figure 1. We observed that the cluster and nucleation mode particle
285 concentrations were the highest on the NPF event days. In fact, the cluster and
286 nucleation mode particles dominated the total particle number concentration with an
287 average contribution of 96% (Figure 2). On the haze days, the average contribution
288 levels of the four modes were about equal. Aitken and accumulation mode particles
289 contributed to 52% of the total particle number concentration on the haze days, as
290 compared to 4% on the NPF event days.

291 On the haze days, we observed a surprising concentration of cluster mode particles;
292 ~~which indicates that the clusters in this size range were still produced even during haze.~~
293 ~~These high spite of the high concentrations were still present regardless of the high~~
294 ~~loadings of Aitken and accumulation particles, which.~~ Since large particles are
295 expected to efficiently scavenge ~~the~~ clusters and ~~the~~ smallest growing particles by
296 coagulation (Kerminen et al., 2001; Kulmala et al., 2017). ~~The clusters during haze days~~
297 ~~could be attributed to a), this is indicative of either airborne cluster formation which do~~
298 ~~not grow further (Kulmala et al., 2007), but also to) or vehicular source emissions~~
299 ~~of cluster clusters and nucleation mode particles (e.g. Rönkkö et al., 2017).) during haze.~~
300 The ratio between nucleation mode and cluster mode particle median number
301 concentration was close to unity (0.84)), which might indicate ~~a concurrent~~ their
302 common source on haze days, in comparison to the smaller ratio of 0.3 during the NPF
303 days. It is therefore likely that the primary particles dominated the nucleation mode on
304 the haze days, while the growth of cluster mode ~~to~~ particles into nucleation mode
305 explains the nucleation mode particles on NPF days.

306 The median concentrations of Aitken and accumulation mode particles were
307 ~~17500~~ 16000 cm^{-3} and 17500 cm^{-3} , respectively, ~~during on the~~ haze days and 8240 cm^{-3}
308 and 1670 cm^{-3} , respectively, ~~during on the~~ NPF event days. Overall, these concentrations
309 were a factor of 2.1 and 10.5 times higher on the haze days than on the NPF event days.
310 The $\text{PM}_{2.5}$ mass concentration was clearly higher ~~during on the~~ haze days ~~than~~
311 ~~during compared with the~~ NPF event days (Figure 3). The $\text{PM}_{2.5}$ mass concentration in
312 urban areas is dominated by accumulation mode particles ~~while the, with a clearly~~
313 smaller a contribution ~~of by~~ ultrafine (cluster, nucleation and Aitken mode) particles
314 ~~tends to remain relatively little~~ (Feng et al., 2010).

315 **3.1.2 Trace gases**

316 In this work, we considered four trace gases (SO_2 , CO, NO_x and O_3) in our analysis
317 (Figure 4), as these compounds are most commonly used to evaluate air quality and
318 pollution sources in China (Hao and Wang, 2005; Han et al., 2011). During our
319 observation period, the median concentrations of SO_2 , CO, NO_x on haze days were 5.1,
320 1400 and 27 ppb, respectively. While ~~still~~ high, these concentrations are lower than the
321 corresponding concentrations (18, 2200, 75 ppb, respectively) during the extremely
322 severe haze episode that took place in Beijing in January 2013 (Wang et al., 2014b).

323 The median concentration of O₃ was 10 ppb on the haze days during our observations,
324 a little bit higher than the severe haze episode in 2013 (<7 ppb; Wang et al., 2014b).

325 The median levels of SO₂, CO, NO_x and O₃ were 230%, 50%, 100% and 50% higher,
326 respectively, on the haze days than on the NPF days. SO₂, CO and NO_x are usually
327 considered tracers of primary pollution, so their lower levels on the NPF event days
328 ~~than on haze days indicate~~indicates that ~~new particle formation events favor~~ relatively
329 clean ~~environment~~conditions favor NPF events (Vahlsing and Smith, 2012; Tian et al.,
330 2018).

331

332 3.2 Diurnal behavior

333 In order to draw a clear picture of the evolution of size-segregated particle number
334 concentrations, we analyzed the diurnal concentration behavior of ~~each of the~~ different
335 trace gases (Figure 5) ~~as well as those of~~ and particle modes (Figure 6).

336 Since trace gases have more definitive sources than particles, we can get some insights
337 ~~on insight into~~ particle sources by comparing ~~the their~~ diurnal patterns ~~together~~-with
338 those of particles in different modes. For instance, CO is usually emitted as the by-
339 product of inefficient combustion, of biomass ~~burning as well as or~~ fossil fuel
340 ~~combustion fuels~~ (Pétron et al., 2004; Lowry et al., 2016). ~~NO_x and CO had~~ We observed
341 similar diurnal patterns. ~~We observed a concurrent~~ for NO_x and CO, with an increase
342 ~~with during the~~ morning rush ~~hour~~hours followed by another peak at around 15:00. ~~The~~
343 ~~similar diurnal patterns of CO and NO_x suggest that they have,~~ suggesting similar
344 sources. Due to lower human activities and traffic during ~~the night~~nighttime, lower
345 concentrations of NO_x and CO were observed. ~~Many~~Earlier observations point out that
346 ~~NO_x and CO are important precursors of O₃ in Chinese urban areas~~ having high NO_x
347 concentrations found that O₃ was consumed by its reaction with NO, while NO₂ works
348 as precursor for O₃ via photochemical reactions (Wang et al., 2017). ~~Based on our data,~~
349 ~~O₃, on the other hand, started to~~ In our observations, the diurnal pattern of O₃ was
350 opposite to that of NO_x, which is consistent with O₃ loss by large amounts of freshly
351 emitted NO during rush hours and O₃ production by photochemical reactions involving
352 NO₂ after the rush hours in the morning.

353 In Figure 7, we show the median diurnal pattern of particle number size distribution on
354 the NPF event days and haze days separately. On the NPF event days, we observed
355 cluster formation from diameters smaller than 3 nm. The growth of newly-formed
356 particles lasted for several hours, resulting in a consecutive increase of the particle
357 number concentrations in all the four modes. During traffic rush hours in the morning
358 and evening, we observed an increase of particle number concentrations in the size
359 range of cluster mode to around 8:00 after the levels of NO_x and CO started to decrease.

360 ~~Ozone had the opposite diurnal pattern to that of NO_x 100 nm.~~

361 ~~On the haze days, we still observed an increase of particle number concentration in the~~
362 ~~size range of cluster mode to Aitken mode during rush hours. Traditionally, NPF events~~
363 ~~occur during the time window between sunrise and ~~CO~~ representing the well-known~~
364 ~~NO_x cycle (Wang sunset by photochemical reactions (Kerminen et al., 2017)-2018).~~
365 ~~The binary or ternary nucleation between sulfuric acid and water, ammonia or amines~~
366 ~~are usually thought of as sources of atmospheric cluster mode particles, especially in~~
367 ~~heavily polluted environments (Kulmala et al., 2013; Kulmala et al., 2014; Yao et al.,~~
368 ~~2018; Chu et al., 2019). The burst of cluster mode particle number concentration outside~~
369 ~~the traditional NPF time window, especially during the rush hours in the afternoon,~~
370 ~~suggests a very different source of cluster mode particles from traditional nucleation,~~
371 ~~e.g. nucleation from gases emitted by traffic (Rönkkö et al., 2017).~~

372 ~~Interestingly, on~~As shown in Figure 6, on the NPF event days, the cluster mode particle
373 ~~number concentration started to increase at the time of sunrise and peaked around noon~~
374 ~~with a wide single peak, showing the typical behavior related to NPF events (Kulmala~~
375 ~~et al., 2012). Comparatively, on the~~ haze days, the cluster mode particle number
376 ~~concentration showed a double peak pattern similar to the diurnal cycle of NO_x~~
377 ~~(FiguresFigure 5-& 6). This observation suggests in consistent with our discussion~~
378 ~~above that traffic emission possibly contributed to cluster mode particles. By comparing~~
379 ~~cluster mode particle number concentrations between the haze days and NPF event days,~~
380 ~~we estimated that the clusters on haze days had similar sources as NO_x, plausibly related~~
381 ~~to combustion. Comparatively, on NPF event days, the cluster mode particle number~~
382 ~~concentration showed a wide single peak. The cluster mode particle number~~
383 ~~concentration started to increase at the same time as sunrise, and the peak around noon,~~
384 ~~showing the typical behavior related to the NPF process (Kulmala et al., 2012). traffic-~~
385 ~~related cluster mode particles could contribute up to 40-50 % of the total cluster mode~~
386 ~~particle number concentration on the NPF event days.~~

387 ~~Similarly, Similar to the cluster mode, the~~ nucleation mode ~~also~~ had a single peak on the
388 ~~NPF event days. Nucleation mode particle number concentration concentrations~~ started
389 ~~to increase shortly after the increase of corresponding increases in~~ the cluster mode,
390 ~~which could be attributed to the growth of formed particles from the cluster mode~~
391 ~~particles into the nucleation mode. The observed peak however has of the nucleation~~
392 ~~mode particle number concentrations had~~ a shoulder ~~at~~ around 7:00 - 9:00 ~~am~~ which is
393 ~~concurrent with the morning peak of the NO_x, thus originating concentration, which~~
394 ~~indicates a contribution from traffic to the nucleation mode. It is important to note,~~
395 ~~however, that the height of the peak this shoulder of the nucleation mode is was~~ only 20%
396 ~~of the maximum nucleation mode particle number concentration. Our These~~ results
397 ~~showsuggest that, compared with atmospheric NPF, traffic contributes contributed~~
398 ~~much less to the nucleation mode particle number concentration than an NPF event.~~

399 During the haze days, the diurnal pattern of the nucleation mode ~~overlapped with~~
400 particle number concentration reminded that of NO_x ~~with, showing~~ no ~~clear major~~ peak
401 during the ~~day. Our observation daytime between the rush hours.~~ This suggests that the
402 nucleation mode ~~number concentration was dominated by particles were dominantly~~
403 from traffic emissions on the haze days. Additionally, it is important to note that during
404 ~~haze days, when the main contributor of the nucleation mode particles was traffic~~the
405 haze days, we observed different maximum concentrations for morning versus evening
406 peaks, implying a higher contribution of traffic in the morning than in the afternoon.
407 ~~The~~This result is in line with the diurnal cycle of NO_x during the haze days.

408 On the NPF even days, Aitken mode particles ~~on NPF days~~ are mainly attributed to two
409 different sources ~~which are~~ hard to ~~distinguish~~be distinguished from each other. ~~The~~
410 ~~Aitken mode particles can be the result of:~~ primary ~~or~~and secondary sources, such as
411 combustion and growth of newly formed particles, respectively. In comparison to the
412 cluster and nucleation modes, ~~which that~~ had ~~a more~~ pronounced diurnal cycles during
413 the NPF event days, the Aitken mode particle number concentration had a pattern
414 similar ~~pattern~~asto NO_x before 9:00 in the morning. This implies that ~~the~~ traffic
415 emissions ~~are~~were important sources to maintain Aitken mode particle concentrations
416 in the morning hours. The Aitken mode particle number concentration increased during
417 the afternoon hours. ~~This is associated with, probably due to the~~ growth of the
418 nucleation mode particles via multicomponent condensation ~~into the Aitken mode sizes.~~
419 ~~This is verified by a~~and possibly some other gas-to-particle conversion pathways. ~~The~~
420 concurrent decrease of the nucleation mode particle number concentration. supports
421 this view. The Aitken mode particle number concentration increase in the
422 ~~afternoon~~evening was concurrent with ~~an~~the increase of CO and NO_x, which could be
423 attributed to combustion sources (Roberts and Jones, 2004; Koponen et al., 2001).
424 ~~Similarly, Aitken mode particle concentrations, peak around 20:00 simultaneously with~~
425 ~~a peak of CO. On~~

426 On the haze days, the Aitken mode particle number ~~concentrations~~concentration
427 experienced ~~a negligible~~little change before about 14:00. ~~Even when, contrary to both~~
428 CO and NO_x ~~concentration began to decrease, which implies less~~concentrations,
429 indicating a small contribution ~~of~~by primary sources. ~~during that time of the day.~~ It is
430 important to mention that the growth of particles is not ~~only~~ limited to the days when
431 new particle formation ~~occurred~~occurs. In fact, on the haze days, the wind was typically
432 more stagnant, reducing the vertical mixing of ~~the~~ pollutants and their horizontal
433 advection (Zheng et al., 2015). The increase of Aitken mode particle number
434 concentration started at around 16:00 and ~~the concentration~~ peaked at around 20:00
435 similar to the NPF event days. ~~If~~This is concurrent with the increase ~~time of in the~~ NO_x
436 and CO, ~~this increase maybe~~ concentrations, which might be attributed ~~into~~to traffic
437 ~~emission~~emissions.

438 The concentration of accumulation mode particles was an order of magnitude higher

439 during ~~the~~ haze days ~~than during compared with the~~ NPF days, ~~representing causing a~~
440 higher condensation sink (~~on average~~ 0.02015 s^{-1} for ~~the~~ NPF event days and 0.110 s^{-1}
441 for ~~the~~ haze days ~~on average~~), ~~as shown in Figure S4~~), and thus introducing a reason
442 why NPF ~~does did~~ not ~~happentake place~~ on ~~the~~ haze days (Kulmala et al., 2017). The
443 concentration, on the other hand, did not experience much diurnal variation ~~during the~~
444 ~~day~~. There was a slight increase in the accumulation mode particle number
445 concentration during the morning rush ~~hour, hours~~ starting at around 6:00. ~~This is~~
446 concurrent with the increase in the Aitken mode particle number concentration,
447 ~~simultaneous with traffic rush hours in Beijing~~. The second slight increase started at
448 around 16:00, two hours later than that of the Aitken mode, suggesting ~~thea~~ secondary
449 contribution to accumulation mode particles. On the NPF event days, the
450 accumulation ~~Accumulation~~ mode ~~also~~ had the similar diurnal pattern as SO_2 ~~on NPF~~
451 ~~event days~~, implying that SO_2 participated in the formation of accumulation mode on
452 the NPF event days.

453 3.3 Correlation between the particle modes and trace gas and $\text{PM}_{2.5}$ concentrations

454 Beijing's atmosphere is a very complicated environment (Kulmala, 2015). Aerosol
455 particles in the atmosphere of Beijing are subject to ~~e.g.~~ aerosol dynamical processes,
456 surface reactions, coagulation, deposition ~~or and~~ transport, thus hindering direct
457 connection with their sources based on physical size ~~distribution~~ distributions only.
458 However, by correlating each particle mode to various trace gases, we can get
459 indications on the sources of ~~the~~ particles. In this section, we use CO , SO_2 , NO_x and O_3
460 as tracers. ~~By evaluating their correlation coefficients with the size-segregated particle~~
461 ~~number concentration (Table 2), we can infer the particle sources. CO , SO_2 and NO_x~~
462 ~~are primary pollutants emitted from various combustion sources. Our results show that~~
463 ~~these trace gases have a high positive correlation with accumulation mode particles~~
464 ~~($R > 0.75$) and negative correlation with cluster and nucleation modes generally.~~

465 ~~Figures 7 and 8 show correlation between the size-segregate particle number~~
466 ~~concentrations and SO_2 and NO_x concentration, respectively. By examining responses~~
467 ~~of size-segregated particle number concentrations to changes in trace gas and $\text{PM}_{2.5}$~~
468 ~~concentrations (Table 2a and Table 2b), we can get further insights into the main sources~~
469 ~~of particles in each mode and into the dynamical processes experienced by these~~
470 ~~particles under different pollution levels. Of course, not all sources or dynamics can be~~
471 ~~captured using this approach. In addition, due to the complex physical and chemical~~
472 ~~processes experienced by the particles, the correlation analysis cannot quantify the~~
473 ~~strength of individual sources or dynamical processes.~~

474 3.3.1 Connection with SO₂

475 SO₂ is a key precursor for H₂SO₄ through photochemical reactions in Beijing, which is
476 in turn a requirement for new particle formation in megacity environments (Wang et al.,
477 2013; Yao et al., 2018). Although being a very important precursor of NPF, ~~the~~-SO₂
478 ~~concentration was had~~ lower concentrations on the NPF event days than on the haze
479 days, ~~relating high~~ (Figure 8). High concentrations of SO₂ have been ascribed to
480 regional pollution and anthropogenic condensation sink even in semi-pristine
481 environments (Dada et al., 2017). ~~Our observation can be explained by the fact that~~
482 ~~during haze, SO₂ partitions to the particle and liquid phase oxidation much faster than~~
483 ~~gas phase oxidation of SO₂ to H₂SO₄.~~ Earlier observations report that the main sources
484 of SO₂ are power plants, traffic and industry, and it so SO₂ can be used as a tracer for
485 regional pollution (Yang et al., 2018; Lu et al., 2010).

486 ~~Table 2 and~~ Generally, as shown in Figure 7 ~~show negative correlations between 8, the~~
487 SO₂ concentration ~~and correlated negatively with both~~ cluster and nucleation mode
488 particle number concentrations, ~~while a highly positive correlation between~~. Higher
489 SO₂ concentrations were encountered on more polluted days when NPF events were
490 suppressed due to the high particle loadings, explaining the overall negative correlation.
491 However, if we look at the NPF event days and haze days separately, we cannot see any
492 clear correlation between the SO₂ concentration and ~~accumulation~~ cluster mode or
493 nucleation mode particle number concentration (~~R = -0.88~~), and ~~PM_{2.5} mass~~
494 ~~concentration (R = 0.80)~~. So, when, as shown also in Table 2a and Table 2b. This result
495 indicates that during our observations, NPF occurred in relatively clean conditions, but
496 the strength of a NPF event was not sensitive to the regional pollution level as long as
497 NPF was able to occur.

498 On the NPF event days, the SO₂ concentration correlated positively with the
499 concentrations of both Aitken and accumulation mode particles during the chosen NPF
500 time window, whereas on the haze days no correlation between the SO₂ concentration
501 ~~was high, the and~~ Aitken mode particle number concentration could be observed. This
502 suggests that regional and transported pollution contributed to Aitken and accumulation
503 mode ~~particle concentration was also high, indicated with high condensation sink yet~~
504 ~~not limiting aerosol formation.~~

505 ~~SO₂ had the highest positive correlation coefficient with the particles on the NPF event~~
506 ~~days, while on haze days the transported and regional pollution was only a prominent~~
507 ~~factor affecting~~ accumulation mode particle number concentration ~~among all the four~~
508 ~~trace gases. This result suggests that the sources of accumulation mode particles during~~
509 ~~the time window we chose were more similar to sources of SO₂, attributed to fossil fuel~~
510 ~~combustion and linked to regional pollution. However,~~. In addition, SO₂ contributes to
511 heterogeneous reactions on particle surfaces, explaining that a fraction of accumulation
512 mode particles could have resulted from the growth of Aitken mode particles
513 (Ravishankara., 1997).

514 3.3.2 Connection with NO_x

515 NO_x is usually considered as the pollution tracer mainly from traffic (Beevers et al.,
516 2012). As shown in Table 22a and Figure 8 show negative correlation coefficients
517 between 9, the NO_x and concentration correlated negatively with both cluster and
518 nucleation mode particle number ~~concentration concentrations~~ concentrations on the NPF event days.
519 Compared with the correlation between SO₂ and cluster and positive correlation
520 coefficients between Aitken and accumulation nucleation mode particle number
521 ~~concentration concentrations~~, this result indicates that local traffic emissions affected
522 cluster and nucleation mode particles more than regional pollution on the NPF event
523 days.

524 ~~As shown in Table 2, the positive correlation coefficient between Aitken mode particle~~
525 ~~number concentration and NO_x is the highest among all four trace gases. As we~~
526 ~~mentioned before, traffic is identified as an important source of Aitken and nucleation~~
527 ~~mode particles. Given that our station is so close to the highway (around 100 m), NO_x~~
528 ~~concentration is affected by local traffic emissions.—~~

529 ~~As shown in Figure 8, the higher NO_x concentration was associated with less cluster~~
530 ~~mode particle number concentration during the NPF event days. However, on haze days~~
531 ~~the cluster mode particle number concentration seemed not to be sensitive to NO_x~~
532 ~~concentration, which is in contradiction to our previous understanding that gas phase~~
533 ~~NO_x can suppress the formation of clusters by suppressing NPF event (Lehtipalo et al.,~~
534 ~~2018). However, there might be other sources of cluster mode other than the NPF events~~
535 ~~as well as compensating vapors that can contribute to clusters formation.~~

536 ~~The negative correlation between the NO_x concentration and nucleation mode particle~~
537 ~~number concentration on the NPF event days can be explained by less cluster mode~~
538 ~~particles, which act as an important seed for nucleation mode particles. However, on~~
539 ~~haze days, the negative correlation was slightly higher. On the haze days, primary~~
540 ~~sources dominated the whole nucleation mode.~~

541 ~~The positive correlation between Aitken mode particle number concentration and NO_x~~
542 ~~concentration on both the NPF event days and the haze days suggests that traffic is one~~
543 ~~of the major sources of Aitken mode in urban Beijing.—~~

544 On the haze days, we did not see any correlation between the cluster mode particle
545 number concentration and NO_x concentration (Table 2b), although according to our
546 analysis above, traffic emissions can be the source of cluster mode particles during the
547 haze days. One possible reason for this is that the relationship between cluster mode
548 particle number concentration and NO_x concentration was not linear. Earlier studies
549 pointed out that the dilution ratio is the dominant factor affecting the number size
550 distribution of nanoparticles generated from traffic gases emissions (Shi and Harrison,

1999; Shi et al., 2001). Temperature and humidity were also identified as factors affecting nanoparticle number size distribution nucleated from tailpipe emissions (Shi et al., 2001). Such factors would decrease the correlation between the cluster and nucleation mode particle number concentrations and NO_x concentration.

The Aitken mode particle number concentration correlated positively with the NO_x concentration on both NPF event days and haze days, suggesting that traffic emissions might be an important source of Aitken mode particles.

The accumulation mode particle number concentration correlated positively with the NO_x concentration on the NPF event days, which is consistent with earlier studies showing that traffic emissions can contribute to accumulation mode particles in urban areas (Vu et al., 2015). On the haze days, the accumulation mode particle number concentration correlated less with NO_x than with SO₂, suggesting that regional and transported pollution was a more important contributor to accumulation mode particles than traffic emissions.

3.3.3 Connection with CO

CO has some similar sources as NO_x, such as traffic. On the NPF event days, the CO concentration correlated with particle number concentrations in each mode in a very similar way as NO_x did, suggesting that CO and NO_x had common sources, such as traffic emissions, on the NPF event days. This result confirms our analysis above that traffic emissions could suppress NPF and growth on the NPF event days, in addition to which they might be important sources of the Aitken and accumulation mode particles.

On the haze days, CO transported from polluted areas dominated the total CO concentration. The CO concentration had a positive correlation with the accumulation mode particle number concentration, but no clear correlation with the particle number concentration of the three other modes. This result confirms our analysis above that on the haze days, local emissions dominated Aitken particle number concentrations while regional and transported pollutions affected accumulation mode particle number concentrations more than local emissions.

3.3.4 Connection with O₃

Ozone is a secondary pollution trace gas and its concentration represents the oxidization capacity of atmosphere. Earlier observations found that high O₃ concentrations favor NPF by enhancing photochemical reactions (Qi et al., 2015). However, we did not see any correlation between the O₃ concentration and cluster mode particle number concentration, suggesting that O₃ was not the limiting factor for cluster mode particle number concentration.

586 The O₃ concentration correlated positively with both nucleation and Aitken mode
587 particle number concentration on the NPF event days during the NPF time window,
588 whereas on the haze days O₃ concentration correlated only with the Aitken mode
589 particle number concentration.

590 The above results suggest that O₃ influences heterogeneous reactions and particle
591 growth rather than the formation of new aerosol particles.

592 3.3.5 Connection to PM_{2.5}

593 As shown in Figure 10, the PM_{2.5} concentration correlated negatively with the cluster
594 and nucleation mode particle number concentrations, and positively with the
595 accumulation mode particle number concentration. High PM_{2.5} concentrations tend to
596 suppress NPF by increasing the sinks of vapors responsible for nucleation and growth
597 of cluster and nucleation mode particles. The particles causing high PM_{2.5}
598 concentrations also serve as sinks of cluster and nucleation mode particles by
599 coagulation.

600 As shown in Table 2a and Figure 12, the Aitken mode particle number concentration
601 correlated positively with the PM_{2.5} concentration on the NPF event days. A possible
602 reason for this could be the tight connection between the Aitken and accumulation mode
603 particles on the NPF event days (Table 3a), and the observation that accumulation mode
604 particles are usually the main contributor to PM_{2.5} in Beijing (Liu et al., 2013). On the
605 haze days, the Aitken mode particle number concentration correlated negatively with
606 the PM_{2.5} concentration (Table 2b). A possible reason for this is that pre-existing large
607 particles acted as a sink for Aitken mode particles by coagulation as well as a sink for
608 vapors responsible for the growth of smaller particles into the Aitken mode. In addition,
609 while PM_{2.5} is dominated by regional and transported secondary aerosols, Aitken mode
610 particles mainly originate from local emissions such as traffic and cooking in Beijing
611 (Wu et al., 2007; Wang et al., 2013; Du et al., 2017; de Jesus et al., 2019).

612 **3.4 Correlation between different particle modes**

613 ~~The correlation between size-segregated particle number concentrations (Table 3 and~~
614 ~~Figure 9) can give us an indication of dynamical behavior of fine particles in the~~
615 ~~atmosphere aerosols. Generally, pre-existing accumulation mode particles and PM_{2.5}~~
616 ~~act as coagulation sink and suppress the concentration of cluster mode and nucleation~~
617 ~~mode particles. The particle number concentrations between adjacent modes were~~
618 ~~highly correlated except for nucleation mode and Aitken modes. The Aitken mode~~
619 ~~particles have two different sources e.g. primary emissions and new particle formation~~
620 ~~events, also they do not necessarily coincide in time. On the other hand, fresh nucleation~~
621 ~~mode particles must growth fast enough to survive from coagulation scavenging. Only~~

622 ~~under favorable conditions, nucleation mode particles can grow into Aitken mode~~
623 ~~particles, resulting increase in Aitken mode number concentration (Kerminen et al.,~~
624 ~~2001).~~

625 ~~Cluster mode particle number concentrations were positively correlated with nucleation~~
626 ~~mode particle number concentrations on haze days because the traffic emissions were~~
627 ~~a main primary source of these two modes. On NPF event days, the positive correlation~~
628 ~~coefficient ($R = 0.84$) between these two modes can be attributed to the growth of~~
629 ~~clusters into larger particles.~~

630 ~~Accumulation mode particle number concentration was positively correlated with~~
631 ~~Aitken mode particle number concentration on the NPF event days, implying~~
632 ~~transformation from Aitken mode to accumulation mode. While on haze days, higher~~
633 ~~Aitken mode particle number concentration was not concurrent with higher~~
634 ~~accumulation mode particle number concentration. The median Aitken mode particle~~
635 ~~number concentration was twice on haze days of NPF event days while accumulation~~
636 ~~mode particle number concentration was 10.5 times on haze days of NPF event days,~~
637 ~~representing the transformation from Aitken mode to accumulation mode. The high~~
638 ~~correlation coefficient between accumulation mode particle number concentration and~~
639 ~~$PM_{2.5}$ mass concentration implied accumulation mode mainly contributed to $PM_{2.5}$.~~

640 Table 3a and Table 3b as well as Figure 11 show the correlation between particle
641 number concentrations in different modes. On the NPF event days, cluster and
642 nucleation mode particle number concentrations correlated positively with each other
643 due to their common dominant source, NPF. Both cluster and nucleation mode particle
644 number concentrations correlated negatively with the Aitken and accumulation mode
645 particle number concentrations because, as discussed earlier, high concentrations of
646 large particles tend to suppress NPF and subsequent growth of newly-formed particles.

647 On the NPF event days, Aitken and accumulation mode particle number concentrations
648 correlated positively with each other, as well as with the SO_2 and NO_x concentration.
649 This suggests that on the NPF event days, Aitken and accumulation mode particles both
650 formed during regional transportation as secondary particles and were emitted by traffic
651 as primary particles.

652 On the haze days, cluster and nucleation mode particle number concentrations
653 correlated positively with each other, and with the Aitken mode particle number
654 concentration. This is suggestive of a similar dominating sources for these particle,
655 most likely traffic emissions. Similar to the NPF event days, cluster and nucleation
656 mode particle number concentrations correlated negatively with the accumulation mode
657 particle number concentration, even though this correlation was rather weak (Table 3b).

658 As expected based on the discussion in section 3.3.5, the Aitken mode particle number
659 concentration had a negative correlation with the accumulation mode particle number
660 concentration on the haze days.

4— Conclusion

We investigated the variation of size-segregated particle number concentrations on both NPF and haze days observed during winter 2018 in Beijing. Cluster and nucleation modes contributed to 96% of total sub-micro particle number concentration on NPF days. On haze days, these two modes contributed 48% of the total number concentration while Aitken and accumulation modes contributed to the rest.

Cluster and nucleation modes particle number concentration showed a clear diurnal variation on NPF event days with a typical behavior of NPF events, suggesting NPF event was the main source of these two modes while on the haze days these two modes showed similar diurnal pattern as NO_x , suggesting traffic contributed to these modes.

On NPF event days, the diurnal pattern of Aitken mode particle number concentration showed an increase during traffic rush hour and transformation from nucleation mode. On haze days, the diurnal pattern of Aitken mode particle number concentration still implied secondary sources contribution to this mode. Aitken mode number concentration was highly correlated with NO_x concentration, suggesting traffic emissions contributed to the concentration in this mode.

Accumulation mode particle number concentration showed a similar diurnal pattern as Aitken mode, but no variation on haze days. Accumulation mode was correlated with SO_2 , suggesting a character of regional pollution. Accumulation mode mostly contributed to $\text{PM}_{2.5}$ mass concentration.

3.5 Atmospheric ions and ion induced nucleation in Beijing

In order to estimate the contribution of ions to the total cluster mode particle number concentration and the importance of ion induced nucleation in Beijing, we studied ion number concentrations in the size range of 0.8-7 nm by dividing them into 3 sub-size bins: constant pool (0.8-1.5 nm), charged clusters (1.5-3 nm) and larger ions (3-7 nm). As shown in Figure 12, number concentrations of positive ions were higher than those negative ions in all the size bins on both NPF event days and haze days. We will only discuss positive ions here.

The median number concentration of positive ions in the constant pool on NPF event days was only 100 cm^{-3} in Beijing, much less than that in the boreal forest (600 cm^{-3} ; Mazon et al., 2016). Also, the median number concentration of positive charged clusters was 20 cm^{-3} on the NPF event days, and the ratio to the total cluster mode particle number concentration was 0.001 to 0.004 during the NPF time window (Figure 13). This ratio is comparable to that observed in San Pietro Capofiume (0.004), in which the anthropogenic pollution level was also high, but clearly lower than that observed in

696 another megacity in China, Nanjing (0.02; Kontkanen et al., 2017). Considerably higher
697 ratios were observed in clean environments, for example during winter in the boreal
698 forest at Hyytiälä, Finland (0.7; Kontkanen et al., 2017). The median number
699 concentration of larger ions (3-7 nm) on the NPF event days was 30 cm⁻³, a little bit
700 higher than the charged cluster mode particle number concentration, indicating that not
701 all of the larger ions originate from the growth of charged clusters, but rather from
702 charging of neutral particles by smaller ions. On the haze days, charged ion number
703 concentrations were much lower than those on the NPF days, which could be attributed
704 to the higher condensation sink.

705 The diurnal pattern of the ratio of number concentration between charged and total
706 cluster mode particles was the highest during the night with a maximum of 0.008, and
707 had a trough during daytime with a minimum of 0.001 on the NPF event days. Such
708 diurnal pattern is similar to earlier observations in Nanjing, San Pietro Capofiume and
709 Hyytiälä (Kontkanen et al., 2017). This ratio reached its minimum around noon,
710 because the total cluster mode particle number concentration reached its maximum
711 around that time due to NPF. The ratio had a small peak at around 9:00, similar to earlier
712 observations in Centreville and Po Valley (Kontkanen et al., 2016; Kontkanen et al.,
713 2017). The possible reason is that charged clusters were activated earlier in the morning
714 than neutral clusters. The ratio increased from the midnight until about 4:00, similar to
715 the number concentration of charged clusters.

716 As shown in Figure 14, the diurnal median of the ratio between the formation rate of
717 positive ions of 1.5 nm ($J_{1.5}^+$) and the total formation rate clusters of 1.5 nm ($J_{1.5}$) varied
718 from 0.0009 to 0.006. This result is comparable to observations in Shanghai, where the
719 positive ion induced nucleation contributed only 0.05% to the total formation rate of
720 1.7-nm particles ($J_{1.7}$) (Yao et al., 2018).

721 **3.6 Particle growth rates**

722 The growth rates of particles generated from NPF events were examined in three size
723 ranges: <3 nm, 3-7 nm and 7- 25 nm (Figure 15). The median growth rates of particles
724 in these size ranges were 1.0 nm/h, 2.7 nm/h and 5.5 nm/h, respectively. The growth
725 rate of cluster mode particles was comparable with that observed in Shanghai (1.5 nm/h;
726 Yao et al., 2018). The notable increase of the particle growth rate with an increasing
727 particle size is a very typical feature in the sub-20 nm size range (Kerminen et al., 2018),
728 and it may also extend to larger particle sizes (Paasonen et al., 2018).

729 Our observations are in line with the reported range of nucleation mode particle growth
730 rates of 0.1-11.2 nm/h in urban areas of Beijing (Wang et al., 2017b; Jayaratne et al.,
731 2017). Such growth rates can explain the observed increases of Aitken mode particle
732 number concentrations in the afternoon.

733 4 Summary and conclusions

734 We measured particle number concentrations over a wide range of particle diameters
735 (1.5-1000 nm) on both NPF event days and haze days in winter Beijing. To our
736 knowledge, this was the first time when cluster mode particle number concentrations
737 have been reported on haze days in Beijing.

738 The observed responses of particle number concentrations in different modes (cluster,
739 nucleation, Aitken and accumulation mode) to changes in trace gas and PM_{2.5}
740 concentrations were quite heterogeneous, suggesting different sources and dynamics
741 experienced by each mode. NPF was the dominant source of cluster and nucleation
742 mode particles. Ion-induced nucleation did not play an important role during the NPF
743 events. The growth rates of cluster and nucleation mode particles increased with an
744 increasing particle size. Traffic emissions contributed to every mode and were the
745 dominant source of cluster and nucleation mode particles on the haze days. The main
746 sources of Aitken mode particles were local emissions, while transported and regional
747 pollution as well as growth from the nucleation mode also contributed to the Aitken
748 mode. The main source of accumulation mode particles was regional and transported
749 pollution. PM_{2.5} affected the number concentration of sub-100 nm particles by
750 competing for vapors responsible for particle growth and by acting as sinks for particles
751 by coagulation. The main contributors to the PM_{2.5} mass concentration were
752 accumulation mode particles on the haze days.

753 As demonstrated here and in many other studies (e.g. Brines et al., 2015), ultrafine
754 particles (< 100 nm in diameter) tend to dominate the total aerosol particle number
755 concentration in megacities like Beijing. More attention should therefore put on
756 ultrafine particles in urban environments. We found that both NPF and traffic emissions
757 are important sources of ultrafine particles in Beijing. To improve our understanding on
758 the potential effects of ultrafine particles on health and air quality, we need to do more
759 research on their sources and physical and chemical properties. Laboratory and model
760 analysis on dynamics of ultrafine particles would help us to understand the evolution
761 of particle number size distributions. In addition, to identify and locate other possible
762 sources, long-term observations on ultrafine particles down to the cluster mode as well
763 as source apportionment analyses, such as cluster analysis and receptor model studies,
764 are still needed. Ultrafine particles should also be taken into consideration when making
765 policies to control air pollution. New regulations should be designed to control primary
766 emission sources, such as traffic, or precursor emissions for secondary ultrafine
767 particles involving NPF and subsequent particle growth.

768 **5 Acknowledgments**

769 This study received funding from Beijing University of Chemical Technology. This
770 research has received funding from the National Natural Science Foundation of China
771 (41877306). The work is supported by Academy of Finland via Center of Excellence in
772 Atmospheric Science (project no. 272041) and European Research Council via ATM-
773 GTP 266 (742206). LD received funding from the ATM-DP program at university of
774 Helsinki. KRD acknowledges support by the Swiss National Science postdoc mobility
775 grant P2EZP2_181599. LW acknowledges support by National Key R&D Program of
776 China (2017YFC0209505) and the National Natural Science Foundation of China.

777 *Author contributions.* YZ, YiL, YF, JuK contributed to data collection. YZ, TC, LD
778 contributed to data inversion. YZ and LD contributed to analyzing the data. CY, BC,
779 KRD, FB, TK, YoL, JoK contributed to maintaining the station. YZ, LD, JuK, VMK
780 wrote the paper. TP, LW, JJ, MK provided helpful scientific discussions. All co-authors
781 reviewed the manuscript.

782 *Competing interests.* The authors declare that they have no conflict of interest.

783 *Data availability:* Particle number concentrations are available upon contacting
784 yingzhouahl@163.com or lubna.dada@helsinki.fi.

785

786 **6 References**

- 787 Baklanov, A., Molina, L. T., and Gauss, M.: Megacities, air quality and climate,
 788 Atmospheric Environment, 126, 235-249,
 789 <https://doi.org/10.1016/j.atmosenv.2015.11.059>, 2016.
- 790 Beevers, S. D., Westmoreland, E., de Jong, M. C., Williams, M. L., and Carslaw, D. C.:
 791 Trends in NO_x and NO₂ emissions from road traffic in Great Britain,
 792 Atmospheric Environment, 54, 107-116,
 793 <https://doi.org/10.1016/j.atmosenv.2012.02.028>, 2012.
- 794 Brines, M., Dall'Osto, M., Beddows, D. C. S., Harrison, R. M., Gomez-Moreno, F.,
 795 Nunez, L., Artinano, B., Costabile, F., Gobbi, G. P., Salimi, F., Morawska, L.,
 796 Sioutas, C., and Querol, X.: Traffic and nucleation events as main sources of
 797 ultrafine particles in high-insolation developed world cities, Atmos Chem Phys,
 798 15, 5929-5945, 2015.
- 799 Cai, R. L., Yang, D. S., Fu, Y. Y., Wang, X., Li, X. X., Ma, Y., Hao, J. M., Zheng, J.,
 800 and Jiang, J. K.: Aerosol surface area concentration: a governing factor in new
 801 particle formation in Beijing, Atmos Chem Phys, 17, 12327-12340,
 802 <https://doi.org/10.5194/acp-2017-467>, 2017.
- 803 Cai, R. L., Yang, D. S., Ahonen, L. R., Shi, L. L., Korhonen, F., Ma, Y., Hao, J. M.,
 804 Petaja, T., Zheng, J., Kangasluoma, J., and Jiang, J. K.: Data inversion methods
 805 to determine sub-3 nm aerosol size distributions using the particle size magnifier,
 806 Atmos Meas Tech, 11, 4477-4491, 2018.
- 807 Cao, C., Jiang, W. J., Wang, B. Y., Fang, J. H., Lang, J. D., Tian, G., Jiang, J. K., and
 808 Zhu, T. F.: Inhalable Microorganisms in Beijing's PM_{2.5} and PM₁₀ Pollutants
 809 during a Severe Smog Event, Environ Sci Technol, 48, 1499-1507,
 810 <https://doi.org/10.1021/es4048472>, 2014.
- 811 Chu, B. W., Kerminen, V. M., Bianchi, F., Yan, C., Petäjä, T., and Kulmala, M.:
 812 Atmospheric new particle formation in China, Atmos Chem Phys, 19, 115-138,
 813 <https://doi.org/10.5194/acp-19-115-2019>, 2019.
- 814 Dada, L., Paasonen, P., Nieminen, T., Mazon, S. B., Kontkanen, J., Peräkylä, O.,
 815 Lehtipalo, K., Hussein, T., Petäjä, T., Kerminen, V. M., Bäck, J., and Kulmala,
 816 M.: Long-term analysis of clear-sky new particle formation events and nonevents
 817 in Hyytiälä, Atmos Chem Phys, 17, 6227-6241, [https://doi.org/10.5194/acp-17-](https://doi.org/10.5194/acp-17-6227-2017)
 818 [6227-2017](https://doi.org/10.5194/acp-17-6227-2017), 2017.
- 819 Dai, L., Wang, H. L., Zhou, L. Y., An, J. L., Tang, L. L., Lu, C. S., Yan, W. L., Liu, R.
 820 Y., Kong, S. F., Chen, M. D., Lee, S. H., and Yu, H.: Regional and local new
 821 particle formation events observed in the Yangtze River Delta region, China, J
 822 Geophys Res-Atmos, 122, 2389-2402, <https://doi.org/10.1002/2016JD026030>,
 823 2017.
- 824 Dal Maso, M., Kulmala, M., Riipinen, I., Wagner, R., Hussein, T., Aalto, P. P., and
 825 Lehtinen, K. E. J.: Formation and growth of fresh atmospheric aerosols: eight
 826 years of aerosol size distribution data from SMEAR II, Hyytiälä, Finland, Boreal
 827 Environ Res, 10, 323-336, 2005.

828 [de Jesus, A. L., Rahman, M. M., Mazaheri, M., Thompson, H., Knibbs, L. D., Jeong,](#)
829 [C., Evans, G., Nei, W., Ding, A., Qiao, L., Li, L., Portin, H., Niemi, J. V., Timonen](#)
830 [H., Luoma, K., Petäjä, T., Kulmala, M., Kowalski, M., Peters, A., Cyrus, J.,](#)
831 [Ferrero, L., Manigrasso, M., Avino, P., Buonano, G., Reche, C., Querol, X.,](#)
832 [Beddows, D., Harrison, R. M., Sowlat, M. H., Sioutas, C., and Morawska, L.:](#)
833 [Ultrafine particles and PM2.5 in the air of cities around the world: Are they](#)
834 [representative of each other?, *Environment International*, 129, 118-135,](#)
835 [10.1016/j.envint.2019.05.021, 2019.](#)

836 [Du, W., Zhao, J., Wang, Y. Y., Zhang, Y. J., Wang, Q. Q., Xu, W. Q., Chen, C., Han, T.](#)
837 [T., Zhang, F., Li, Z. Q., Fu, P. Q., Li, J., Wang, Z. F., and Sun, Y. L.:](#)
838 [Simultaneous](#)
839 [measurements of particle number size distributions at ground level and 260m on](#)
840 [a meteorological tower in urban Beijing, China, *Atmos Chem Phys*, 17, 6797-](#)
841 [6811, 2017.](#)

841 Feng, X., Dang, Z., Huang, W., Shao, L., and Li, W.: Microscopic morphology and size
842 distribution of particles in PM2.5 of Guangzhou City, *Journal of Atmospheric*
843 *Chemistry*, 64, 37-51, <http://doi.org/10.1007/s10874-010-9169-7>, 2010.

844 Han, S. Q., Bian, H., Feng, Y. C., Liu, A. X., Li, X. J., Zeng, F., and Zhang, X. L.:
845 Analysis of the Relationship between O3, NO and NO2 in Tianjin, China, *Aerosol*
846 *Air Qual Res*, 11, 128-139, <https://doi.org/10.4209/aaqr.2010.07.0055>, 2011.

847 Hao, J. M., and Wang, L. T.: Improving urban air quality in China: Beijing case study,
848 *J Air Waste Manage*, 55, 1298-1305,
849 <https://doi.org/10.1080/10473289.2005.10464726>, 2005.

850 Hari, P., and Kulmala, M.: Station for measuring ecosystem-atmosphere relations
851 (SMEAR II), *Boreal Environ Res*, 10, 315-322, 2005.

852 IPCC. IPCC, 2007: summary for policymakers. *Climate change 2007*, 93-129.

853 [Jayaratne, R., Pushpawela, B., He, C. R., Li, H., Gao, J., Chai, F. H., and Morawska,](#)
854 [L.: Observations of particles at their formation sizes in Beijing, China, *Atmos*](#)
855 [Chem Phys, 17, 8825-8835, 2017.](#)

856 Jiang, J. K., Zhao, J., Chen, M. D., Eisele, F. L., Scheckman, J., Williams, B. J., Kuang,
857 C. A., and McMurry, P. H.: First Measurements of Neutral Atmospheric Cluster
858 and 1-2 nm Particle Number Size Distributions During Nucleation Events,
859 *Aerosol Science and Technology*, 45, ii-V,
860 <https://doi.org/10.1080/02786826.2010.546817>, 2011.

861 Kangasluoma, J., Franchin, A., Duplissy, J., Ahonen, L., Korhonen, F., Attoui, M.,
862 Mikkilä, J., Lehtipalo, K., Vanhanen, J., Kulmala, M., and Petäjä, T.: Operation
863 of the Airmodus A11 nano Condensation Nucleus Counter at various inlet
864 pressures and various operation temperatures, and design of a new inlet system,
865 *Atmos Meas Tech*, 9, 2977-2988, <https://doi.org/10.5194/amt-9-2977-2016>, 2016.

866 Kerminen, V. M., Pirjola, L., and Kulmala, M.: How significantly does coagulation
867 scavenging limit atmospheric particle production?, *J Geophys Res-Atmos*, 106,
868 24119-24125, <https://doi.org/10.1029/2001jd000322>, 2001.

869 Kerminen, V. M., Paramonov, M., Anttila, T., Riipinen, I., Fountoukis, C., Korhonen,
870 H., Asmi, E., Laakso, L., Lihavainen, H., Swietlicki, E., Svenningsson, B., Asmi,
871 A., Pandis, S. N., Kulmala, M., and Petäjä, T.: Cloud condensation nuclei

872 production associated with atmospheric nucleation: a synthesis based on existing
873 literature and new results, *Atmos Chem Phys*, 12, 12037-12059,
874 <https://doi.org/10.5194/acp-12-12037-2012>, 2012.

875 Kerminen, V. M., Chen, X. M., Vakkari, V., Petäjä, T., Kulmala, M., and Bianchi, F.:
876 Atmospheric new particle formation and growth: review of field observations,
877 *Environ Res Lett*, 13, <https://doi.org/10.1088/1748-9326/aadf3c>, 2018.

878 [Kontkanen, J., Järvinen, E., Manninen, H. E., Lehtipalo, K., Kangasluoma, J., Decesari,](#)
879 [S., Gobbi, G. P., Laaksonen, A., Petäjä, T., and Kulmala, M.: High concentrations](#)
880 [of sub-3nm clusters and frequent new particle formation observed in the Po Valley,](#)
881 [Italy, during the PEGASOS 2012 campaign, *Atmos Chem Phys*, 16, 17,](#)
882 [<https://doi.org/10.5194/acp-16-1919-2016>, 2016.](#)

883 [Kontkanen, J., Lehtipalo, K., Ahonen, L., Kangasluoma, J., Manninen, H. E., Hakala,](#)
884 [J., Rose, C., Sellegri, K., Xiao, S., Wang, L., Qi, X. M., Nie, W., Ding, A. J., Yu,](#)
885 [H., Lee, S., Kerminen, V. M., Petaja, T., and Kulmala, M.: Measurements of sub-](#)
886 [3nm particles using a particle size magnifier in different environments: from](#)
887 [clean mountain top to polluted megacities, *Atmos Chem Phys*, 17, 2163-2187,](#)
888 [<https://doi.org/10.5194/acp-17-2163-2017>.](#)

889 Koponen, I. K., Asmi, A., Keronen, P., Puhto, K., and Kulmala, M.: Indoor air
890 measurement campaign in Helsinki, Finland 1999 - the effect of outdoor air
891 pollution on indoor air, *Atmospheric Environment*, 35, 1465-1477,
892 [https://doi.org/10.1016/s1352-2310\(00\)00338-1](https://doi.org/10.1016/s1352-2310(00)00338-1), 2001.

893 Kreyling, W. G., Semmler, M., and Möller, W.: Dosimetry and toxicology of ultrafine
894 particles, *J Aerosol Med*, 17, 140-152,
895 <https://doi.org/10.1089/0894268041457147>, 2004.

896 Kulmala, M.: How particles nucleate and grow, *Science*, 302, 1000-1001,
897 <https://doi.org/10.1126/science.1090848>, 2003.

898 Kulmala, M., Vehkamäki, H., Petäjä, T., Dal Maso, M., Lauri, A., Kerminen, V. M.,
899 Birmili, W., and McMurry, P. H.: Formation and growth rates of ultrafine
900 atmospheric particles: a review of observations, *J Aerosol Sci*, 35, 143-176,
901 <https://doi.org/10.1016/j.jaerosci.2003.10.003>, 2004.

902 Kulmala, M., Riipinen, I., Sipilä, M., Manninen, H. E., Petäjä, T., Junninen, H., Dal
903 Maso, M., Mordas, G., Mirme, A., Vana, M., Hirsikko, A., Laakso, L., Harrison,
904 R. M., Hanson, I., Leung, C., Lehtinen, K. E. J., and Kerminen, V. M.: Toward
905 direct measurement of atmospheric nucleation, *Science*, 318, 89-92,
906 <https://doi.org/10.1126/science.1144124>, 2007.

907 Kulmala, M., Petäjä, T., Nieminen, T., Sipilä, M., Manninen, H. E., Lehtipalo, K., Dal
908 Maso, M., Aalto, P. P., Junninen, H., Paasonen, P., Riipinen, I., Lehtinen, K. E. J.,
909 Laaksonen, A., and Kerminen, V. M.: Measurement of the nucleation of
910 atmospheric aerosol particles, *Nat Protoc*, 7, 1651-1667,
911 <https://doi.org/10.1038/nprot.2012.091>, 2012.

912 Kulmala, M., Kontkanen, J., Junninen, H., Lehtipalo, K., Manninen, H. E., Nieminen,
913 T., Petäjä, T., Sipilä, M., Schobesberger, S., Rantala, P., Franchin, A., Jokinen, T.,
914 Järvinen, E., Äijälä, M., Kangasluoma, J., Hakala, J., Aalto, P. P., Paasonen, P.,
915 Mikkilä, J., Vanhanen, J., Aalto, J., Hakola, H., Makkonen, U., Ruuskanen, T.,

916 Mauldin, R. L., Duplissy, J., Vehkamäki, H., Bäck, J., Kortelainen, A., Riipinen,
917 I., Kurtén, T., Johnston, M. V., Smith, J. N., Ehn, M., Mentel, T. F., Lehtinen, K.
918 E. J., Laaksonen, A., Kerminen, V. M., and Worsnop, D. R.: Direct Observations
919 of Atmospheric Aerosol Nucleation, *Science*, 339, 943-946,
920 <https://doi.org/10.1126/science.1227385>, 2013.

921 Kulmala, M., Petaja, T., Ehn, M., Thornton, J., Sipila, M., Worsnop, D. R., and
922 Kerminen, V. M.: Chemistry of Atmospheric Nucleation: On the Recent
923 Advances on Precursor Characterization and Atmospheric Cluster Composition
924 in Connection with Atmospheric New Particle Formation, *Annu Rev Phys Chem*,
925 65, 21-37, 2014.

926 Kulmala, M.: Atmospheric chemistry: China's choking cocktail, *Nature*, 526, 497-499,
927 <https://doi.org/10.1038/526497a>, 2015.

928 Kulmala, M., Kerminen, V. M., Petäjä, T., Ding, A. J., and Wang, L.: Atmospheric gas-
929 to-particle conversion: why NPF events are observed in megacities?, *Faraday*
930 *Discuss*, 200, 271-288, <https://doi.org/10.1039/C6FD00257A>, 2017.

931 Lehtipalo, K., Leppä, J., Kontkanen, J., Kangasluoma, J., Wimmer, D., Franchin, A.,
932 Schobesberger, S., Junninen, H., Petäjä, T., Sipilä, M., Mikkilä, J., Vanhanen, J.,
933 Worsnop, D. r., and Kulmala, M.: methods for determining particle size
934 distribution and growth rates between 1 and 3 nm using the Particle Size
935 Magnifier, *Boreal Environ Res*, 19, 215-236, 2014.

936 Lehtipalo, K., Yan, C., Dada, L., Bianchi, F., Xiao, M., Wagner, R., Stolzenburg, D.,
937 Ahonen, L. R., Amorim, A., Baccarini, A., Bauer, P. S., Baumgartner, B., Bergen,
938 A., Bernhammer, A. K., Breitenlechner, M., Brilke, S., Buchholz, A., Mazon, S.
939 B., Chen, D. X., Chen, X. M., Dias, A., Dommen, J., Draper, D. C., Duplissy, J.,
940 Ehn, M., Finkenzeller, H., Fischer, L., Frege, C., Fuchs, C., Garmash, O., Gordon,
941 H., Hakala, J., He, X. C., Heikkinen, L., Heinritzi, M., Helm, J. C., Hofbauer, V.,
942 Hoyle, C. R., Jokinen, T., Kangasluoma, J., Kerminen, V. M., Kim, C., Kirkby, J.,
943 Kontkanen, J., Kurten, A., Lawler, M. J., Mai, H. J., Mathot, S., Mauldin, R. L.,
944 Molteni, U., Nichman, L., Nie, W., Nieminen, T., Ojdanic, A., Onnela, A.,
945 Passananti, M., Petäjä, T., Piel, F., Pospisilova, V., Quéléver, L. L. J., Rissanen,
946 M. P., Rose, C., Sarnela, N., Schallhart, S., Schuchmann, S., Sengupta, K., Simon,
947 M., Sipilä, M., Tauber, C., Tomé, A., Tröstl, J., Väisänen, O., Vogel, A. L.,
948 Volkamer, R., Wagner, A. C., Wang, M. Y., Weitz, L., Wimmer, D., Ye, P. L.,
949 Ylisirnio, A., Zha, Q. Z., Carslaw, K. S., Curtius, J., Donahue, N. M., Flagan, R.
950 C., Hansel, A., Riipinen, I., Virtanen, A., Winkler, P. M., Baltensperger, U.,
951 Kulmala, M., and Worsnop, D. R.: Multicomponent new particle formation from
952 sulfuric acid, ammonia, and biogenic vapors, *Sci Adv*, 4,
953 <https://doi.org/10.1126/sciadv.aau5363>, 2018.

954 Lelieveld, J., Evans, J. S., Fnais, M., Giannadaki, D., and Pozzer, A.: The contribution
955 of outdoor air pollution sources to premature mortality on a global scale, *Nature*,
956 525, 367-371, <https://doi.org/10.1038/nature15371>, 2015.

957 Liu, X. G., Li, J., Qu, Y., Han, T., Hou, L., Gu, J., Chen, C., Yang, Y., Liu, X., Yang, T.,
958 Zhang, Y., Tian, H., and Hu, M.: Formation and evolution mechanism of regional

959 [haze: a case study in the megacity Beijing, China, Atmos Chem Phys, 13, 4501-](#)
960 [4514, 2013.](#)

961 Liu, J. Q., Jiang, J. K., Zhang, Q., Deng, J. G., and Hao, J. M.: A spectrometer for
962 measuring particle size distributions in the range of 3 nm to 10 μ m, Front Env
963 Sci Eng, 10, 63-72, <https://doi.org/10.1007/s11783-014-0754-x>, 2016.

964 Lowry, D., Lanoiselle, M. E., Fisher, R. E., Martin, M., Fowler, C. M. R., France, J. L.,
965 Hernandez-Paniagua, I. Y., Novelli, P. C., Sriskantharajah, S., O'Brien, P., Rata,
966 N. D., Holmes, C. W., Fleming, Z. L., Clemitshaw, K. C., Zazzeri, G., Pommier,
967 M., McLinden, C. A., and Nisbet, E. G.: Marked long-term decline in ambient
968 CO mixing ratio in SE England, 1997-2014: evidence of policy success in
969 improving air quality, Sci Rep-Uk, 6, <https://doi.org/10.1038/srep25661>, 2016.

970 Lu, Y., Yan, C., Fu, Y., Chen, Y., Liu, Y., Yang, G., Wang, Y., Bianchi, F., Chu, B., Zhou,
971 Y., Yin, R., Baalbaki, R., Garmash, O., Deng, C., Wang, W., Liu, Y., Petäjä, T.,
972 Kerminen, V. M., Jiang, J., Kulmala, M., and Wang, L.: A proxy for atmospheric
973 daytime gaseous sulfuric acid concentration in urban Beijing, Atmos. Chem. Phys.
974 Discuss., 2018, 1-31, <https://doi.org/10.5194/acp-2018-1132>, 2018.

975 Lu, Z., Streets, D. G., Zhang, Q., Wang, S., Carmichael, G. R., Cheng, Y. F., Wei, C.,
976 Chin, M., Diehl, T., and Tan, Q.: Sulfur dioxide emissions in China and sulfur
977 trends in East Asia since 2000, Atmos Chem Phys, 10, 6311-6331,
978 <https://doi.org/10.5194/acp-10-6311-2010>, 2010.

979 Manninen, H. E., Mirme, S., Mirme, A., Petäjä, T., and Kulmala, M.: How to reliably
980 detect molecular clusters and nucleation mode particles with Neutral cluster and
981 Air Ion Spectrometer (NAIS), Atmos Meas Tech, 9, 3577-3605,
982 <https://doi.org/10.5194/amt-9-3577-2016>, 2016.

983 [Mazon, S. B., Kontkanen, J., Manninen, H. E., Nieminen, T., Kerminen, V.-M., and](#)
984 [Kulmala, M.: A long-term comparison of nighttime cluster events and daytime](#)
985 [ion formation in a boreal forest, Boeral Environment Research, 21, 19, 2016.](#)

986 Mirme, A., Tamm, E., Mordas, G., Vana, M., Uin, J., Mirme, S., Bernotas, T., Laakso,
987 L., Hirsikko, A., and Kulmala, M.: A wide-range multi-channel air ion
988 spectrometer, Boreal Environ Res, 12, 247-264, 2007.

989 Mirme, S., and Mirme, A.: The mathematical principles and design of the NAIS - a
990 spectrometer for the measurement of cluster ion and nanometer aerosol size
991 distributions, Atmos Meas Tech, 6, 1061-1071, [https://doi.org/10.5194/amt-6-](https://doi.org/10.5194/amt-6-1061-2013)
992 [1061-2013](#), 2013.

993 Oberdörster, G., Sharp, Z., Atudorei, V., Elder, A., Gelein, R., Kreyling, W., and Cox,
994 C.: Translocation of inhaled ultrafine particles to the brain, Inhal Toxicol, 16, 437-
995 445, <https://doi.org/10.1080/08958370490439597>, 2004.

996 [Paasonen, P., Peltola, M., Kontkanen, J., Junninen, H., Kerminen, V.-M., and Kulmala,](#)
997 [M.: Comprehensive analysis of particle growth rates from nucleation mode to](#)
998 [cloud condensation nuclei in boreal forest, Atmos Chem Phys, 18, 12085-12103,](#)
999 [10.5194/acp-18-12085-2018, 2018.](#)

1000 Pétron, G., Granier, C., Khatatov, B., Yudin, V., Lamarque, J. F., Emmons, L., Gille, J.,
1001 and Edwards, D. P.: Monthly CO surface sources inventory based on the 2000-

1002 2001 MOPITT satellite data, *Geophys Res Lett*, 31,
1003 <https://doi.org/10.1029/2004gl020560>, 2004.

1004 Pirjola, L., Lähde, T., Niemi, J. V., Kousa, A., Rönkkö, T., Karjalainen, P., Keskinen, J.,
1005 Frey, A., and Hillamo, R.: Spatial and temporal characterization of traffic
1006 emissions in urban microenvironments with a mobile laboratory, *Atmospheric*
1007 *Environment*, 63, 156-167, <https://doi.org/10.1016/j.atmosenv.2012.09.022>,
1008 2012.

1009 [Qi, X. M. D., A. J., Nie, W., Petaja, T., Kerminen, V. M., Herrmann, E., Xie, Y. N.,](#)
1010 [Zheng, L. F., Manninen, H., Aalto, P., Sun, J. N., Xu, Z. N., Chi, X. G., Huang,](#)
1011 [X., Boy, M., Virkkula, A., Yang, X. Q., Fu, C. B., and Kulmala, M.: Aerosol size](#)
1012 [distribution and new particle formation in the western Yangtze River Delta of](#)
1013 [China: 2 years of measurements at the SORPES station, *Atmos Chem Phys*, 15,](#)
1014 [12445-12464, 2015.](#)

1015 Ravishankara, A.R.: Heterogeneous and Multiphase Chemistry in the Troposphere,
1016 *Science* 276, 1058-1065, <https://doi.org/10.1126/science.276.5315.1058>, 1997.

1017 Roberts, D. L., and Jones, A.: Climate sensitivity to black carbon aerosol from fossil
1018 fuel combustion, *J Geophys Res-Atmos*, 109,
1019 <https://doi.org/10.1029/2004jd004676>, 2004.

1020 Rönkkö, T., Kuuluvainen, H., Karjalainen, P., Keskinen, J., Hillamo, R., Niemi, J. V.,
1021 Pirjola, L., Timonen, H. J., Saarikoski, S., Saukko, E., Järvinen, A., Silvennoinen,
1022 H., Rostedt, A., Olin, M., Yli-Ojanperä, J., Nousiainen, P., Kousa, A., and Dal
1023 Maso, M.: Traffic is a major source of atmospheric nanocluster aerosol, *P Natl*
1024 *Acad Sci USA*, 114, 7549-7554, <https://doi.org/10.1073/pnas.1700830114>, 2017.

1025 [Shi, J. P., and Harrison, R. M.: Investigation of Ultrafine Particle Formation during](#)
1026 [Diesel Exhaust Dilution, *Environ. Sci. Technol.*, 33, 7, 1999.](#)

1027 [Shi, J. P., Evans, D. E., Khan, A. A., and Harrison, R. M.: Sources and concentration of](#)
1028 [nanoparticles \(< 10 nm diameter\) in the urban atmosphere, *Atmospheric*](#)
1029 [*Environment*, 35, 1193-1202, 2001.](#)

1030 Solomos, S., Kallos, G., Kushta, J., Astitha, M., Tremback, C., Nenes, A., and Levin,
1031 Z.: An integrated modeling study on the effects of mineral dust and sea salt
1032 particles on clouds and precipitation, *Atmos Chem Phys*, 11, 873-892,
1033 <https://doi.org/10.5194/acp-11-873-2011>, 2011.

1034 Tian, X., Xie, P. H., Xu, J., Li, A., Wang, Y., Qin, M., and Hu, Z. K.: Long-term
1035 observations of tropospheric NO₂, SO₂ and HCHO by MAX-DOAS in Yangtze
1036 River Delta area, China, *J Environ Sci-China*, 71, 207-221,
1037 <https://doi.org/10.1016/j.jes.2018.03.006>, 2018.

1038 Vahlsing, C., and Smith, K. R.: Global review of national ambient air quality standards
1039 for PM₁₀ and SO₂ (24 h), *Air Qual Atmos Hlth*, 5, 393-399,
1040 <https://doi.org/10.1007/s11869-010-0131-2>, 2012.

1041 Vanhanen, J., Mikkilä, J., Lehtipalo, K., Sipilä, M., Manninen, H. E., Siivola, E., Petäjä,
1042 T., and Kulmala, M.: Particle Size Magnifier for Nano-CN Detection, *Aerosol*
1043 *Science and Technology*, 45, 533-542,
1044 <https://doi.org/10.1080/02786826.2010.547889>, 2011.

- 1045 von Bismarck-Osten, C., Birmili, W., Ketzel, M., Massling, A., Petäjä, T., and Weber,
1046 S.: Characterization of parameters influencing the spatio-temporal variability of
1047 urban particle number size distributions in four European cities, *Atmospheric*
1048 *Environment*, 77, 415-429, <https://doi.org/10.1016/j.atmosenv.2013.05.029>,
1049 2013.
- 1050 [Vu, T. V., Delgado-Saborit, J. M., and Harrison, R. M.: Review: Particle number size](#)
1051 [distributions from seven major sources and implications for source apportionment](#)
1052 [studies, Atmospheric Environment, 122, 114-132,](#)
1053 [10.1016/j.atmosenv.2015.09.027, 2015.](#)
- 1054 Wang, D. W., Guo, H., Cheung, K., and Gan, F. X.: Observation of nucleation mode
1055 particle burst and new particle formation events at an urban site in Hong Kong,
1056 *Atmospheric Environment*, 99, 196-205,
1057 <https://doi.org/10.1016/j.atmosenv.2014.09.074>, 2014a.
- 1058 Wang, T., Xue, L. K., Brimblecombe, P., Lam, Y. F., Li, L., and Zhang, L.: Ozone
1059 pollution in China: A review of concentrations, meteorological influences,
1060 chemical precursors, and effects, *Science of the Total Environment*, 575, 1582-
1061 1596, <https://doi.org/10.1016/j.scitotenv.2016.10.081>, 2017.
- 1062 Wang, Y. S., Yao, L., Wang, L. L., Liu, Z. R., Ji, D. S., Tang, G. Q., Zhang, J. K., Sun,
1063 Y., Hu, B., and Xin, J. Y.: Mechanism for the formation of the January 2013 heavy
1064 haze pollution episode over central and eastern China, *Sci China Earth Sci*, 57,
1065 14-25, <https://doi.org/10.1007/s11430-013-4773-4>, 2014b.
- 1066 Wang, Z. B., Hu, M., Wu, Z. J., Yue, D. L., He, L. Y., Huang, X. F., Liu, X. G., and
1067 Wiedensohler, A.: Long-term measurements of particle number size distributions
1068 and the relationships with air mass history and source apportionment in the
1069 summer of Beijing, *Atmos Chem Phys*, 13, 10159-10170,
1070 <https://doi.org/10.5194/acp-13-10159-2013>, 2013.
- 1071 Wehner, B., Wiedensohler, A., Tuch, T. M., Wu, Z. J., Hu, M., Slanina, J., and Kiang,
1072 C. S.: Variability of the aerosol number size distribution in Beijing, China: New
1073 particle formation, dust storms, and high continental background, *Geophys Res*
1074 *Lett*, 31, <https://doi.org/10.1029/2004GL021596>, 2004.
- 1075 WHO. Health and health behaviour among young people: health behaviour in school-
1076 aged children: a WHO cross-national study (HBSC), international report; WHO:
1077 2000.
- 1078 Wu, Z. J., Hu, M., Liu, S., Wehner, B., Bauer, S., Ssling, A. M., Wiedensohler, A., Petaja,
1079 T., Dal Maso, M., and Kulmala, M.: New particle formation in Beijing, China:
1080 Statistical analysis of a 1-year data set, *J Geophys Res-Atmos*, 112, 2007.
- 1081 Wu, Z. J., Hu, M., Lin, P., Liu, S., Wehner, B., and Wiedensohler, A.: Particle number
1082 size distribution in the urban atmosphere of Beijing, China, *Atmospheric*
1083 *Environment*, 42, 7967-7980, <https://doi.org/10.1016/j.atmosenv.2008.06.022>,
1084 2008.
- 1085 Xiao, S., Wang, M. Y., Yao, L., Kulmala, M., Zhou, B., Yang, X., Chen, J. M., Wang,
1086 D. F., Fu, Q. Y., Worsnop, D. R., and Wang, L.: Strong atmospheric new particle
1087 formation in winter in urban Shanghai, China, *Atmos Chem Phys*, 15, 1769-1781,
1088 <https://doi.org/10.5194/acp-15-1769-2015>, 2015.

1089 Yang, M., Ma, T. M., and Sun, C. W.: Evaluating the impact of urban traffic investment
1090 on SO₂ emissions in China cities, *Energy Policy*, 113, 20-27,
1091 <https://doi.org/10.1016/j.enpol.2017.10.039>, 2018.

1092 Yao, L., Garmash, O., Bianchi, F., Zheng, J., Yan, C., Kontkanen, J., Junninen, H.,
1093 Mazon, S. B., Ehn, M., Paasonen, P., Sipilä, M., Wang, M. Y., Wang, X. K., Xiao,
1094 S., Chen, H. F., Lu, Y. Q., Zhang, B. W., Wang, D. F., Fu, Q. Y., Geng, F. H., Li,
1095 L., Wang, H. L., Qiao, L. P., Yang, X., Chen, J. M., Kerminen, V. M., Petäjä, T.,
1096 Worsnop, D. R., Kulmala, M., and Wang, L.: Atmospheric new particle formation
1097 from sulfuric acid and amines in a Chinese megacity, *Science*, 361, 278-281,
1098 <https://doi.org/10.1126/science.aao4839>, 2018.

1099 Yu, H., Zhou, L. Y., Dai, L., Shen, W. C., Dai, W., Zheng, J., Ma, Y., and Chen, M. D.:
1100 Nucleation and growth of sub-3nm particles in the polluted urban atmosphere of
1101 a megacity in China, *Atmos Chem Phys*, 16, 2641-2657,
1102 <http://doi.org/10.5194/acp-16-2641-2016>, 2016.

1103 Yue, D. L., Hu, M., Wu, Z. J., Guo, S., Wen, M. T., Nowak, A., Wehner, B.,
1104 Wiedensohler, A., Takegawa, N., Kondo, Y., Wang, X. S., Li, Y. P., Zeng, L. M.,
1105 and Zhang, Y. H.: Variation of particle number size distributions and chemical
1106 compositions at the urban and downwind regional sites in the Pearl River Delta
1107 during summertime pollution episodes, *Atmos Chem Phys*, 10, 9431-9439,
1108 <https://doi.org/10.5194/acp-10-9431-2010>, 2010.

1109 Zheng, G. J., Duan, F. K., Su, H., Ma, Y. L., Cheng, Y., Zheng, B., Zhang, Q., Huang,
1110 T., Kimoto, T., Chang, D., Pöschl, U., Cheng, Y. F., and He, K. B.: Exploring the
1111 severe winter haze in Beijing: the impact of synoptic weather, regional transport
1112 and heterogeneous reactions, *Atmos Chem Phys*, 15, 2969-2983,
1113 <https://doi.org/10.5194/acp-15-2969-2015>, 2015.

1114

1115

1116

1117

1118 Tables and Figures

1119 Table 1. Calendar of ~~events~~ different types of days during our ~~observation~~ observations.
1120 NPF event days are marked in green, and haze days are marked in grey. ~~Missing,~~
1121 whereas missing or undefined days are marked in white.

1122

January						
25	26	27	28	29	30	31
1	2	3	4	5	6	7
8	9	10	11	12	13	14
15	16	17	18	19	20	21
22	23	24	25	26	27	28
29	30	31	1	2	3	4
M	T	W	T	F	S	S

February						
29	30	31	1	2	3	4
5	6	7	8	9	10	11
12	13	14	15	16	17	18
19	20	21	22	23	24	25
26	27	28	1	2	3	4
5	6	7	8	9	10	11
M	T	W	T	F	S	S

March						
26	27	28	1	2	3	4
5	6	7	8	9	10	11
12	13	14	15	16	17	18
19	20	21	22	23	24	25
26	27	28	29	30	31	1
2	3	4	5	6	7	8
M	T	W	T	F	S	S

1123

1124

1125 ~~Table 2. Correlation coefficients between size segregated number concentrations /~~
 1126 ~~PM_{2.5} and trace gases mixing ratios. The time window is 08:00 – 14:00. All the data are~~
 1127 ~~in log scale, high correlation coefficients ($|R| > 0.7$) have been marked in blue and the~~
 1128 ~~extremely high correlation coefficient ($|R| > 0.8$) is marked in red. The R between trace~~
 1129 ~~gases / PM_{2.5} and Cluster mode include 1770 data points (12 minutes averaged value)~~
 1130 ~~for each parameter, R between trace gases / PM_{2.5} and Nucleation, Aitken and~~
 1131 ~~Accumulation mode includes 4248 data points (5 minutes averaged value) for each~~
 1132 ~~parameter.~~

R	CO	SO ₂	NO _x	O ₃
Cluster	-0.71	-0.65	-0.71	0.06
Nucleation	-0.60	-0.60	-0.68	0.07
Aitken	0.61	0.61	0.79	-0.28
Accumulation	0.79	0.88	0.78	0.16
PM _{2.5}	0.77	0.80	0.70	0.36

1133 Table 2a: Correlation coefficients between size segregated particle number
 1134 concentrations and trace gases mixing ratios/ PM_{2.5} concentration on the NPF event
 1135 days. The time window was 08:00 - 14:00. High correlation coefficients ($|R| > 0.5$) are
 1136 marked with bold and italic.

	<u>CO</u>	<u>SO₂</u>	<u>NO_x</u>	<u>O₃</u>	<u>PM_{2.5}</u>
<u>Cluster</u>	<u>-0.61^a</u>	<u>-0.16^a</u>	<u>-0.66^a</u>	<u>0.16^a</u>	<u>-0.66^c</u>
<u>Nucleation</u>	<u>-0.5^b</u>	<u>-0.17^b</u>	<u>-0.55^b</u>	<u>0.36^b</u>	<u>-0.54^c</u>
<u>Aitken</u>	<u>0.58^b</u>	<u>0.55^b</u>	<u>0.66^b</u>	<u>0.32^b</u>	<u>0.33^c</u>
<u>Accumulation</u>	<u>0.71^b</u>	<u>0.65^b</u>	<u>0.69^b</u>	<u>0.15^b</u>	<u>0.83^c</u>

1137 ^a included 665 data points (the time resolution was 12 minutes), ^b included 1620 data
 1138 points (the time resolution was 5 min), ^c included 151 data points (the time resolution
 1139 was 1 hour).

1140

1141 Table 2b: Correlation coefficients between size segregated particle number
 1142 concentrations and trace gases mixing ratios/ PM_{2.5} concentration on haze days. The
 1143 time window was 08:00 - 14:00. High correlation coefficients ($|R| > 0.5$) are marked
 1144 with bold and italic.

	<u>CO</u>	<u>SO₂</u>	<u>NO_x</u>	<u>O₃</u>	<u>PM_{2.5}</u>
<u>Cluster</u>	<u>-0.19^a</u>	<u>0.09^a</u>	<u>0.02^a</u>	<u>0.13^a</u>	<u>0.01^c</u>
<u>Nucleation</u>	<u>-0.24^b</u>	<u>0.07^b</u>	<u>0.31^b</u>	<u>0.17^b</u>	<u>-0.33^c</u>
<u>Aitken</u>	<u>0.10^b</u>	<u>0.03^b</u>	<u>0.44^b</u>	<u>0.41^b</u>	<u>-0.5^c</u>
<u>Accumulation</u>	<u>0.71^b</u>	<u>0.76^b</u>	<u>0.37^b</u>	<u>0.17^b</u>	<u>0.81^c</u>

1145 ^a included 620 data points (the time resolution was 12 minutes), ^b included 1460 data
1146 points (the time resolution was 5 min), ^c included 89 data points (the time resolution
1147 was 1 hour).

1148 ^a included 665 data points (the time resolution was 12 minutes), ^b included 1620 data
1149 points (the time resolution was 5 min), ^c included 151 data points (the time resolution
1150 was 1 hour).

1151

1152 ~~Table 3: Correlation coefficient between size segregated particle number~~
1153 ~~concentrations / PM_{2.5}. The time window is 08:00–14:00. All the data are in log scale;~~
1154 ~~high correlation coefficients ($|R|>0.8$) have been marked in blue. And the extremely~~
1155 ~~high correlation coefficients are marked in red ($|R|>0.9$). The R between Cluster and~~
1156 ~~other modes / PM_{2.5} include 1770 data points (12 minutes averaged value) for each~~
1157 ~~parameter. R between any modes else than Cluster mode include 4248 data points (5~~
1158 ~~minutes averaged value) for each parameter.~~

<u>R</u>	<u>Cluster</u>	<u>Nucleation</u>	<u>Aitken</u>	<u>Accumulation</u>	<u>PM_{2.5}</u>
<u>Cluster</u>	<u>1</u>				
<u>Nucleation</u>	<u>0.84</u>	<u>1</u>			
<u>Aitken</u>	<u>-0.53</u>	<u>-0.47</u>	<u>1</u>		
<u>Accumulatio</u> <u>n</u>	<u>-0.84</u>	<u>-0.72</u>	<u>0.66</u>	<u>1</u>	
<u>PM_{2.5}</u>	<u>-0.84</u>	<u>-0.71</u>	<u>0.47</u>	<u>0.92</u>	<u>1</u>

1159

1160

1161 Table 3a: Correlation coefficients between particle number concentration of every
 1162 mode on NPF event days. The time window was 08:00 - 14:00. High correlation
 1163 coefficients ($|R|>0.5$) are marked with bold and italic.

	<u>Cluster</u>	<u>Nucleation</u>	<u>Aitken</u>	<u>Accumulation</u>
<u>Cluster</u>	<u>1</u>			
<u>Nucleation</u>	<u>0.76^a</u>	<u>1</u>		
<u>Aitken</u>	<u>-0.46^a</u>	<u>-0.33^b</u>	<u>1</u>	
<u>Accumulation</u>	<u>-0.66^a</u>	<u>-0.66^c</u>	<u>0.7^c</u>	<u>1</u>

1164 ^a included 516 data points (the time resolution was 12 minutes), ^b included 1251 data
 1165 points (the time resolution was 5 min), ^c included 1331 data points (the time
 1166 resolution was 5 min).

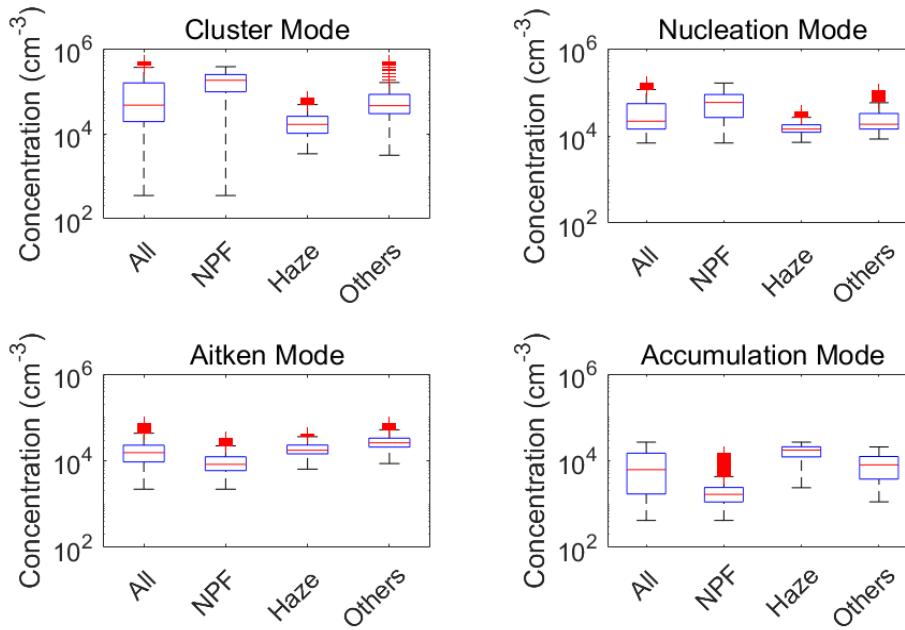
1167

1168 Table 3b: Correlation coefficients between particle number concentration of every
 1169 mode on haze days. The time window was 08:00 - 14:00. High correlation
 1170 coefficients ($|R|>0.5$) are marked with bold and italic.

	<u>Cluster</u>	<u>Nucleation</u>	<u>Aitken</u>	<u>Accumulation</u>
<u>Cluster</u>	<u>1</u>			
<u>Nucleation</u>	<u>0.74^a</u>	<u>1</u>		
<u>Aitken</u>	<u>0.41^a</u>	<u>0.48^b</u>	<u>1</u>	
<u>Accumulation</u>	<u>-0.22^a</u>	<u>-0.33^c</u>	<u>-0.5^c</u>	<u>1</u>

1171 ^a included 342 data points (the time resolution was 12 minutes), ^b included 824 data
 1172 points (the time resolution was 5 min), ^c included 845 data points (the time resolution
 1173 was 5 min).

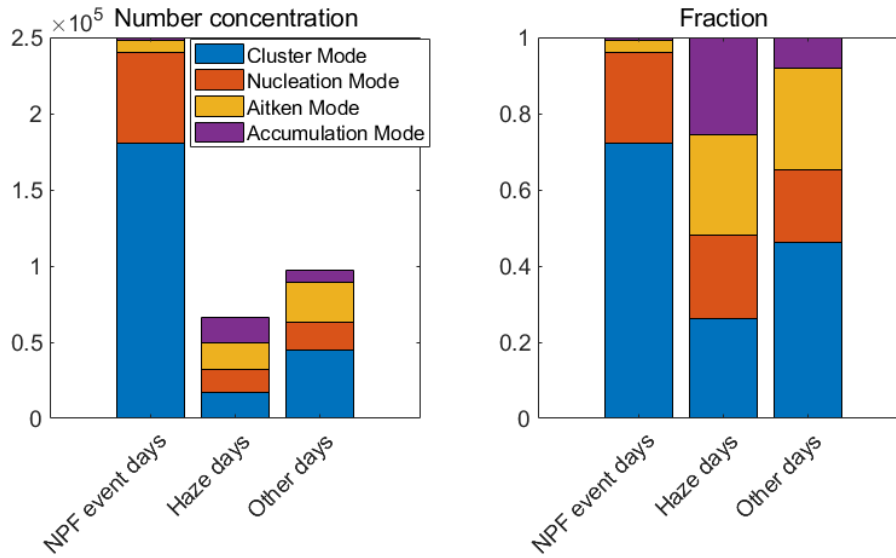
1174



1175

1176 Figure 1. Particle number concentrations in the cluster, nucleation, Aitken and
 1177 accumulation mode on all the days, NPF event days, haze days and other days. The
 1178 whiskers include 99.3% of data of every group. Data out of 1.5 ~~×~~ interquartile range
 1179 are posited outside the whiskers and considered as outliers. ~~This figure shows median~~
 1180 ~~and percentiles of size-segregated particle number concentration.~~ The lines in the boxes
 1181 represent the median value, the lower of the boxes represent 25% of the ~~mixing-ratio~~
 1182 ~~particle number concentration~~ and the upper of the boxes represent 75% of the ~~mixing~~
 1183 ~~ratio-particle number concentration.~~ Data marked with red pluses represent outliers.

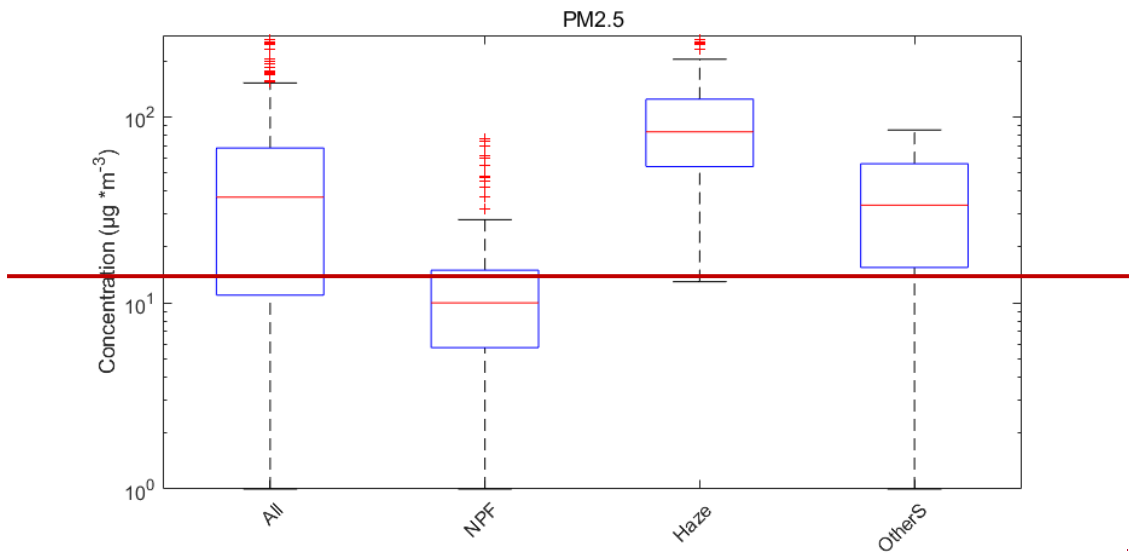
1184



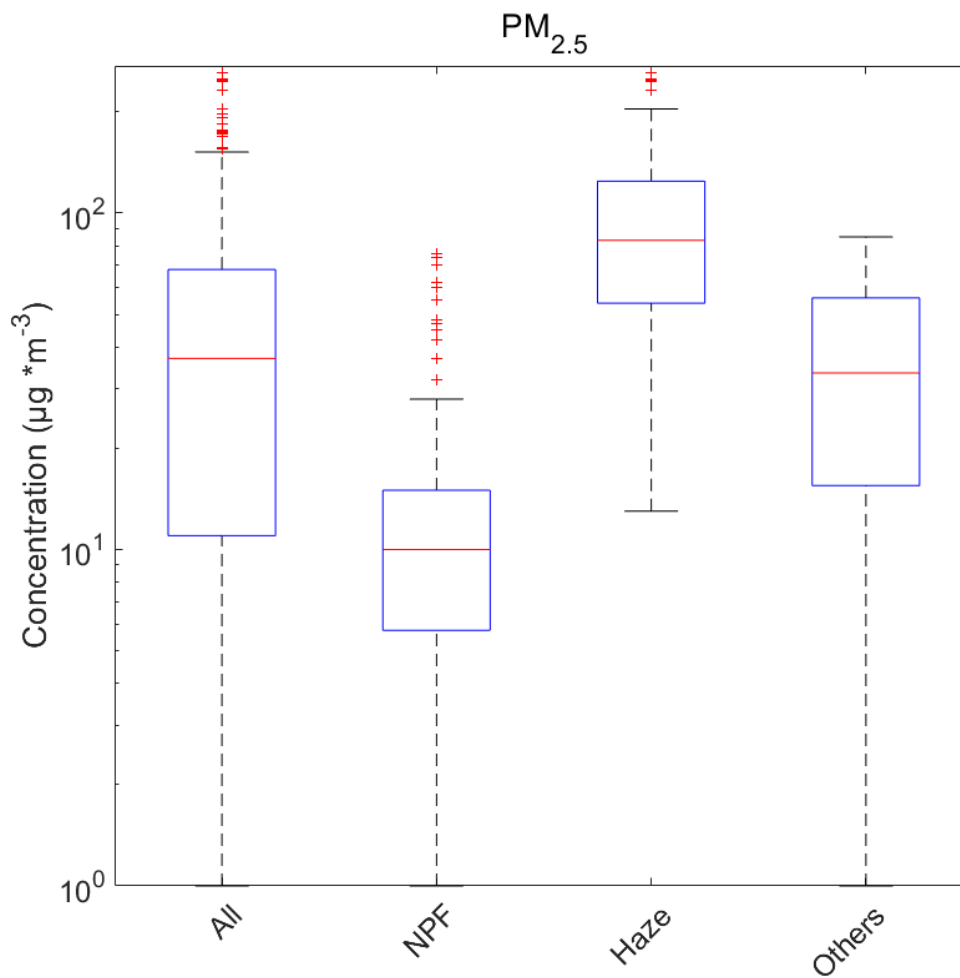
1185

1186 Figure 2. ~~Fractions of each mode under different conditions. The plot on the right is~~
 1187 ~~the median size-segregated number concentrations on (left) and the median fraction of each~~
 1188 ~~mode to the total particle number concentration (right) on the~~ NPF event days, haze
 1189 days and other days. ~~The plot on the left is the fraction of median number concentration~~
 1190 ~~of each mode.~~

1191



1192



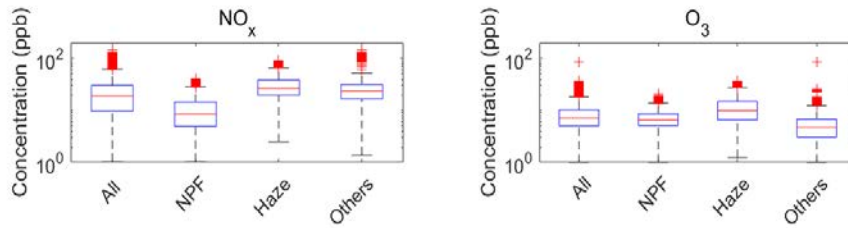
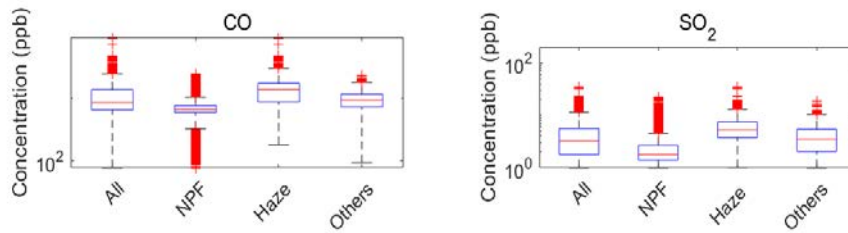
1193

1194 Figure 3. General character of the PM_{2.5} mass concentration on all the days, NPF event
 1195 days, haze days, and others days ~~separately. This figure shows. The boxes show the~~
 1196 median (red line) and 25% and 75% percentiles of the PM_{2.5} mass concentration. The
 1197 lines in the boxes represent the median value, the lower of the boxes represent 25% of

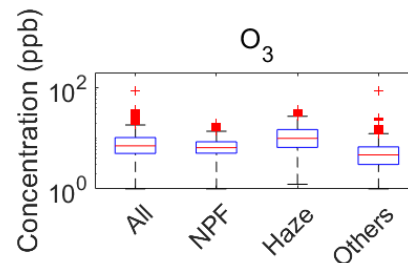
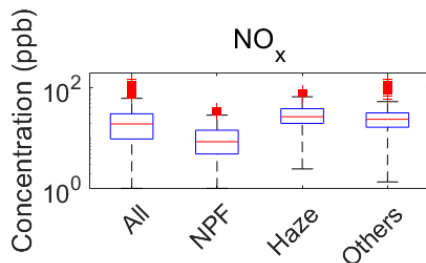
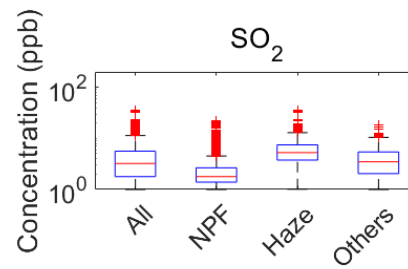
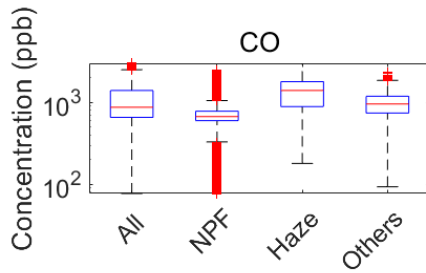
1198 ~~the data and the upper of the boxes represent 75% of the data.~~ Data marked with red
1199 pluses represent outliers as in Figure 1.

1200

1201



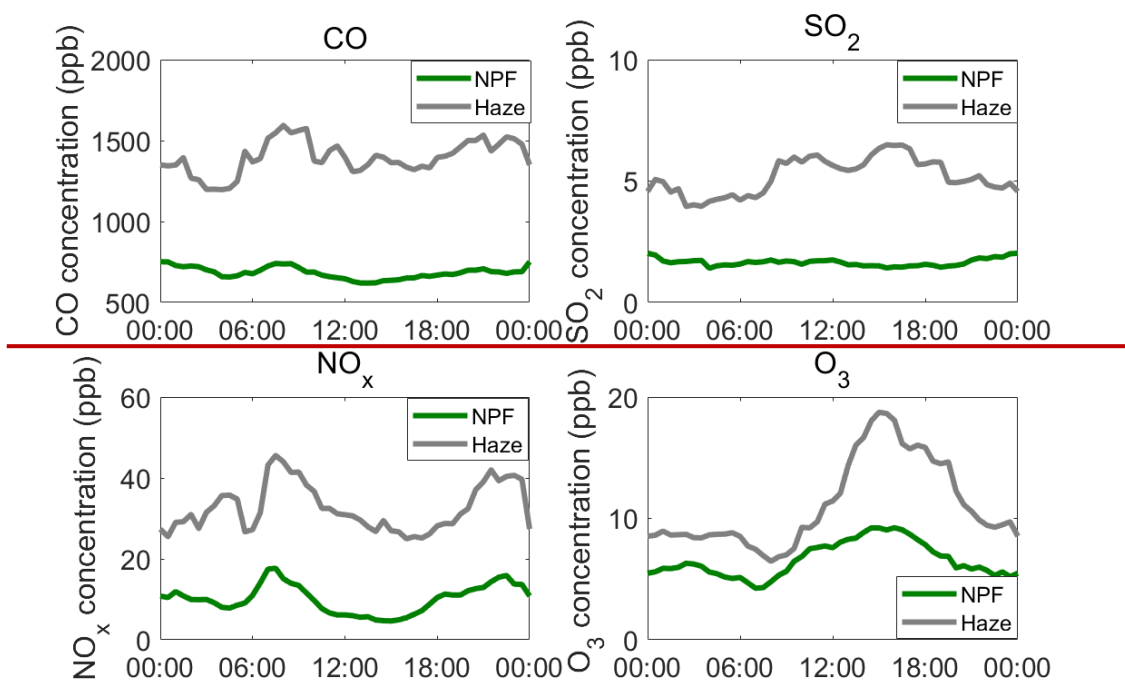
1202



1203

1204 Figure 4. Trace gases mixing ratios of CO, SO₂, NO_x and O₃ on all the days, NPF event
 1205 days, haze days and other days. ~~This figure shows median and percentiles of trace~~
 1206 ~~gases. The lines in the boxes represent the median value, the lower of the boxes~~
 1207 ~~represent The boxes show the median (red line) and 25% of the data and the upper of~~
 1208 ~~the boxes represent and 75% percentiles of the datamixing ratios.~~ Data marked with red
 1209 pluses represent outliers as in Figure 1.

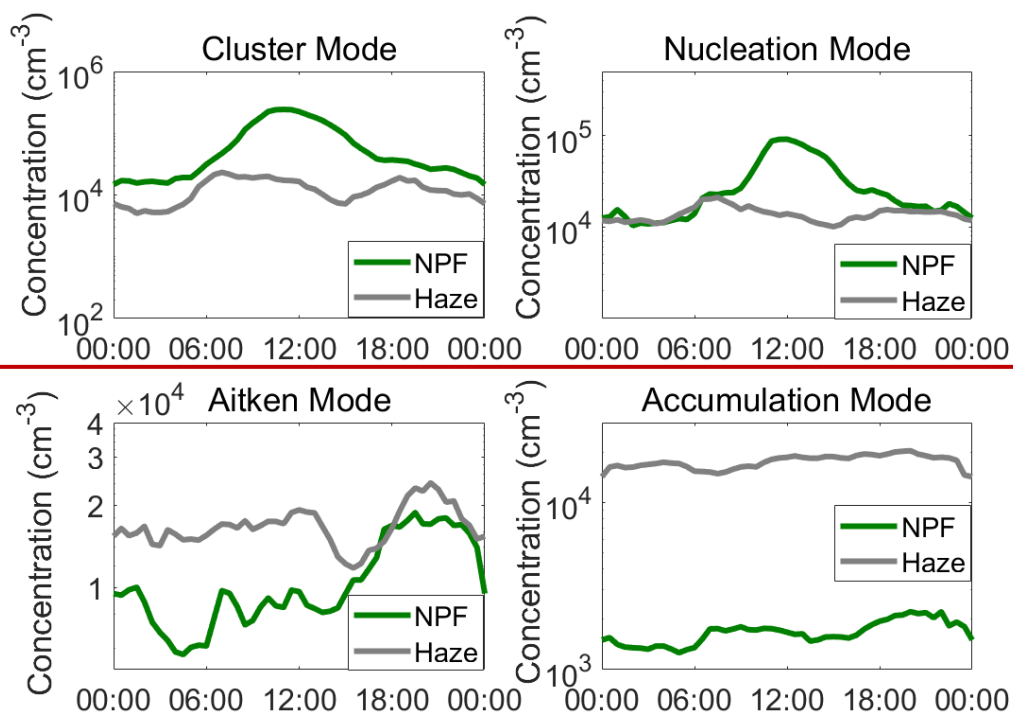
1210



1212

1213 Figure 5. Diurnal variation of trace gasesgas (CO, SO₂, NO_x and O₃ separately)
 1214 mixing ratioratios on haze days (grey lines) and the NPF event days (green lines), and
 1215 they are the median data from midnight to midnight) and haze days (grey lines)
 1216 separately. The time resolution was 30 minutes for every data point. Every data point
 1217 here represents the median of all data at the same time of the days.

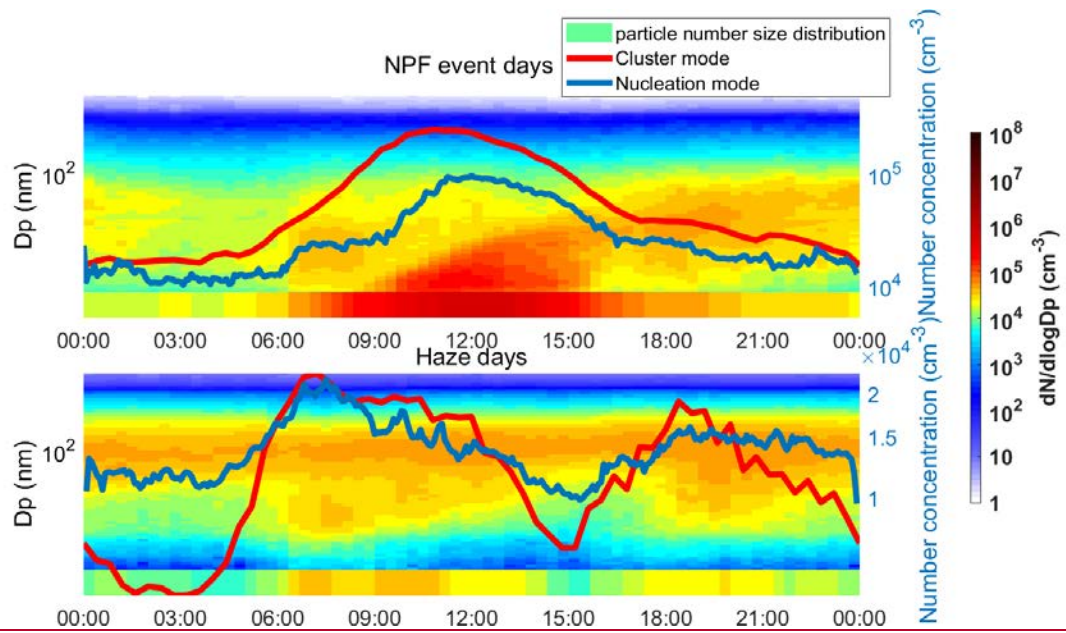
1218



1220

1221 Figure 6. Diurnal variation of ~~particles~~ particle number concentration of every mode
 1222 (cluster, nucleation, Aitken and accumulation mode separately) ~~number concentration~~
 1223 ~~on haze days (grey lines) and on the~~ NPF event days (green lines), and they are the
 1224 median data from midnight to midnight) and haze days (grey lines). The time
 1225 resolution was 30 min for every data point. Every data point here represents the
 1226 median of all data at the same time of the days.

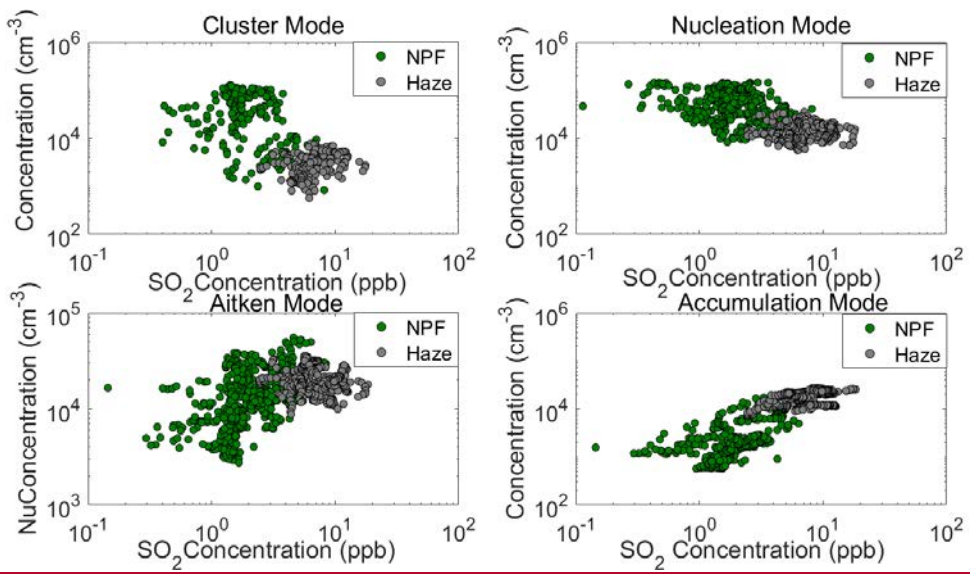
1227



1228
 1229
 1230
 1231
 1232
 1233
 1234
 1235
 1236
 1237

Figure 7. Median diurnal patterns of the particle number size distribution over the size range of 1.5-1000 nm and number concentrations of cluster mode (red lines) and nucleation mode (blue lines) particles on the NPF event days (upper panel) and haze days (lower panel). The time resolution for every data point of particle number size distribution and cluster mode particle number concentration was 12 minutes. The time resolution of every data point of nucleation mode particle number concentration was 5 minutes.

1238

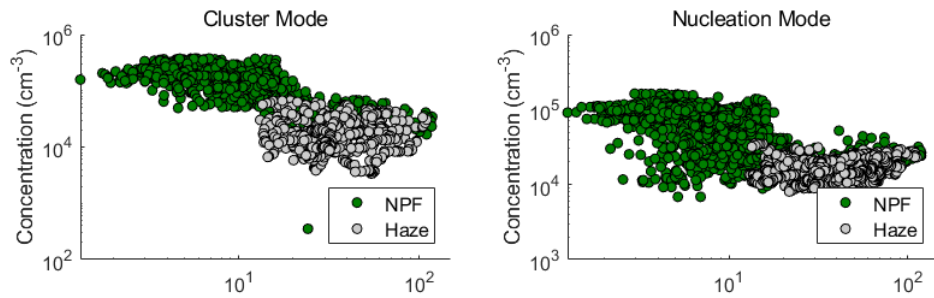


1239

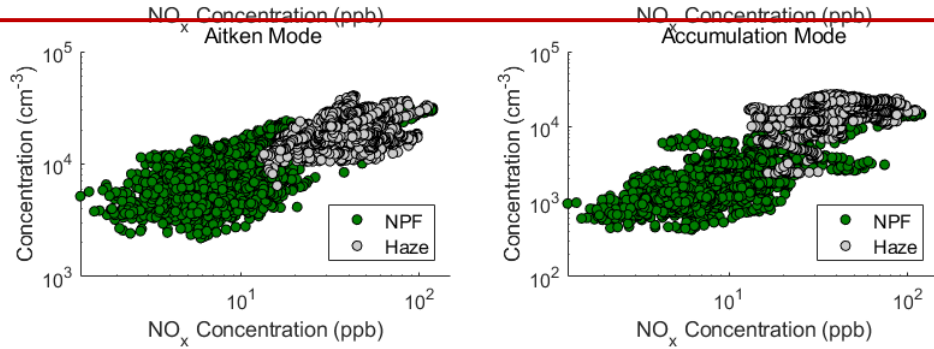
1240 **Figure 8.** Relation between the SO₂ concentration and particle number concentration in
1241 each mode. The time resolution of the data points ~~are~~was 1 hour.

1242

1243

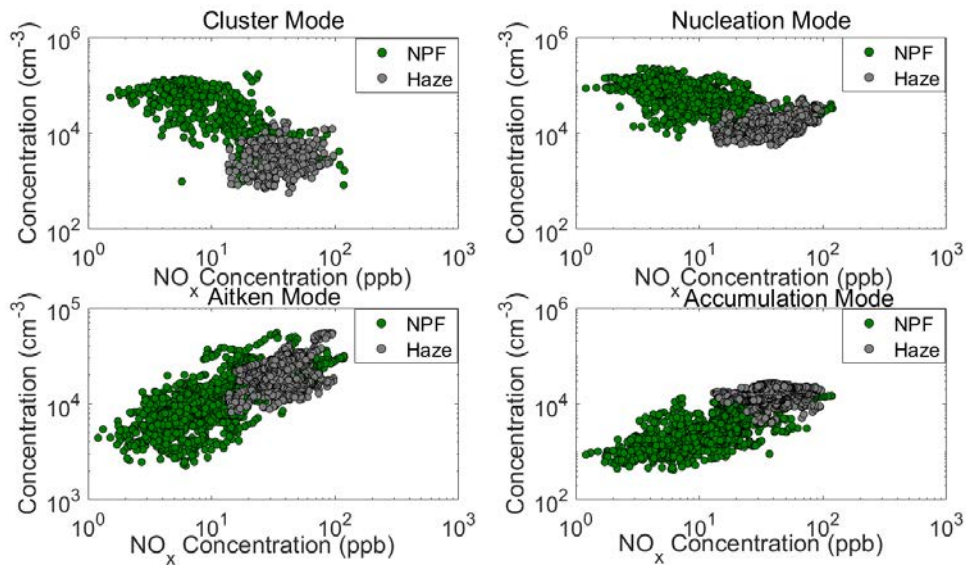


1244



a

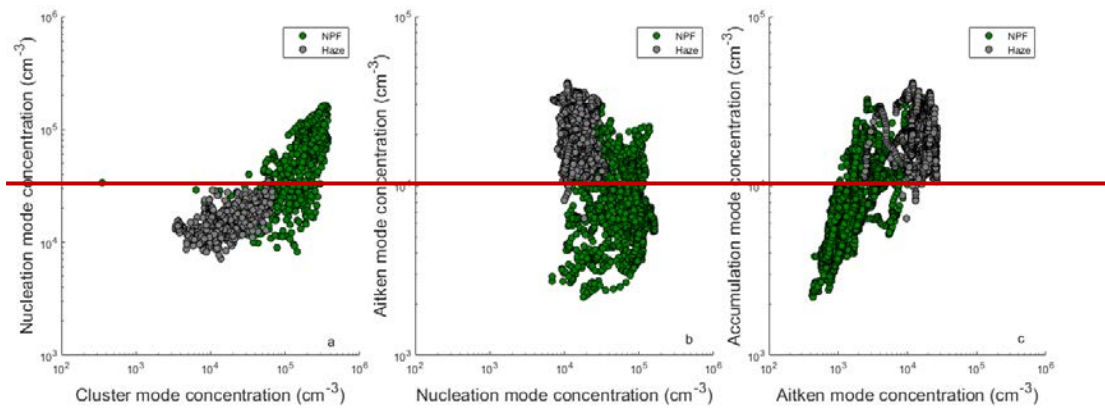
1245



1246 Figure 89. Relation between the NO_x concentration and particle number concentration
1247 in each mode. The time resolution of the data points arewas 1 hour.

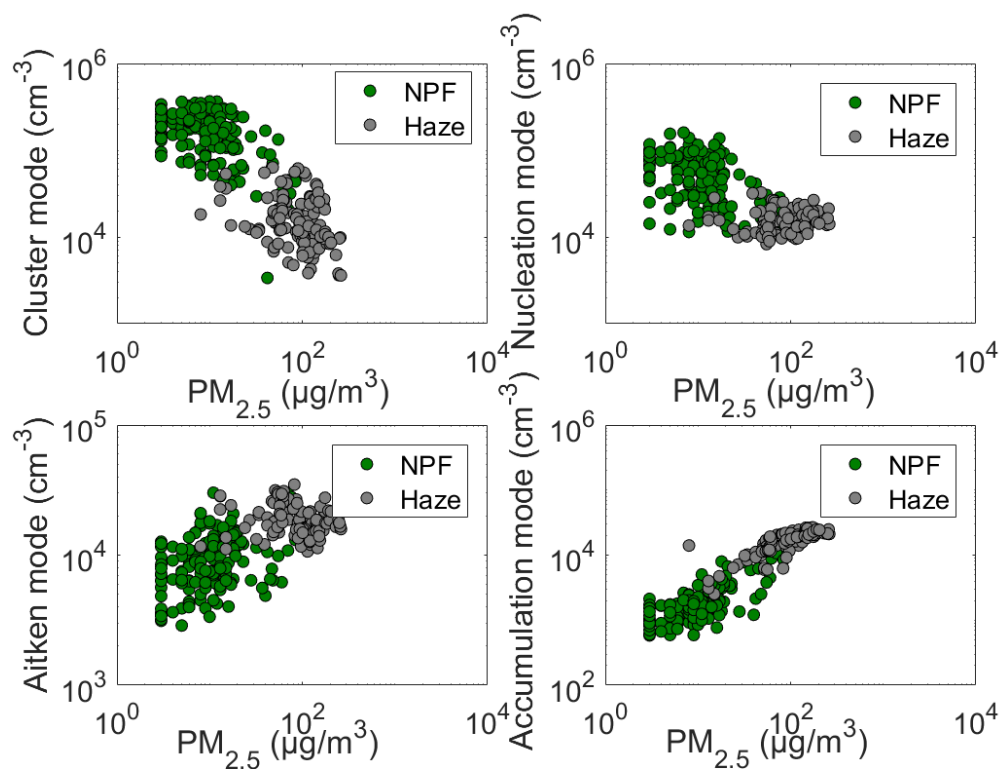
1248

1249



1250

1251

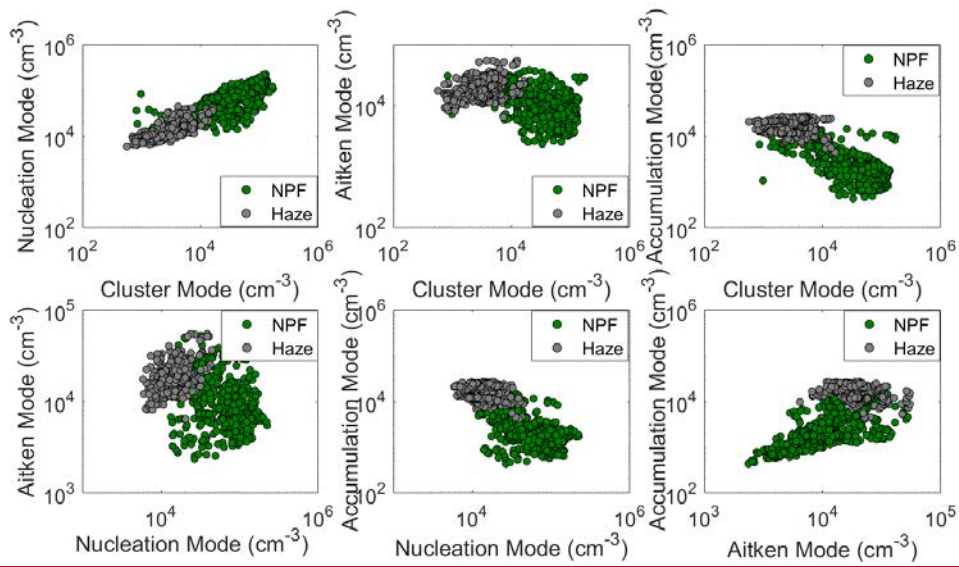


1252

1253 Figure 9. Correlations 10. Correlation between PM_{2.5} concentration and particle number
 1254 concentration in neighboring modes. each mode on the NPF event days (green dots) and
 1255 haze days (grey dots) separately. The time resolution of the data points are was 1 hour.-

1256

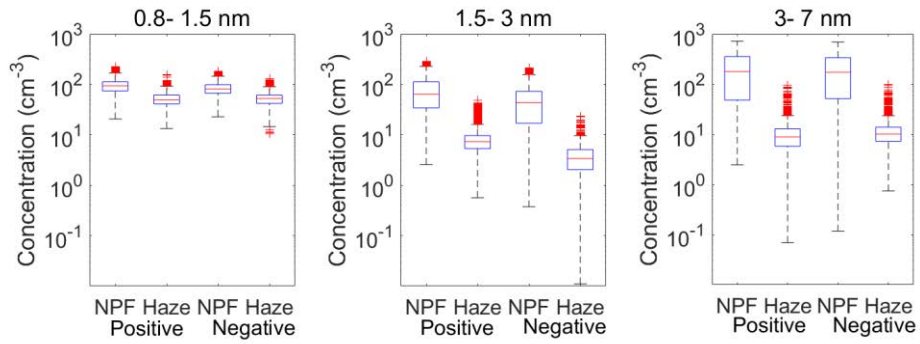
1257



1258

1259 Figure 11. Correlation between every mode each other on NPF event days (green
1260 dots) and haze days (grey dots). The time resolution of data in the plots of correlation
1261 between cluster mode and other modes was 12 min and the time resolution of other
1262 data points was 5 min.

1263

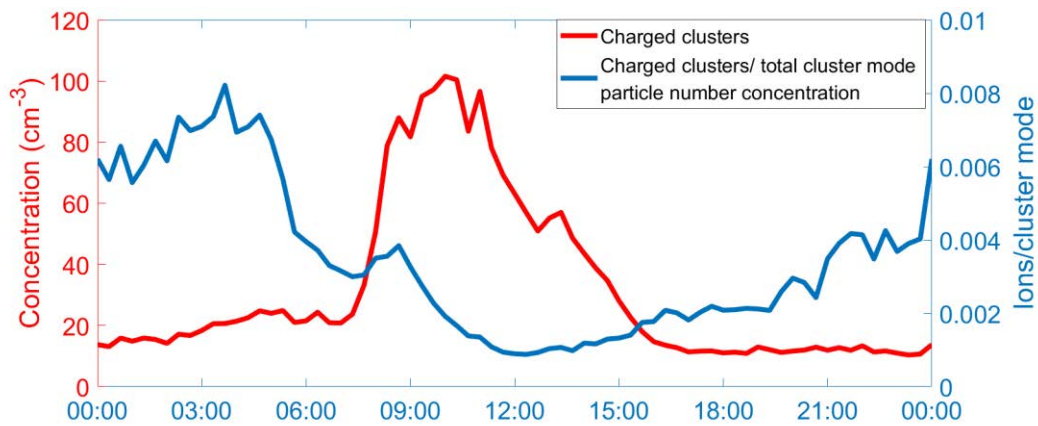


1264

1265 Figure 12. Positive and negative ion number concentrations in the size bins of 0.8-
 1266 1.5nm, 1.5-3 nm and 3-7 nm on NPF event days and haze days separately. The whiskers
 1267 include 99.3% of data of every group. Data out of $1.5 \times$ interquartile range are posited
 1268 outside the whiskers and considered as outliers. The lines in the boxes represent the
 1269 median value, the lower of the boxes represent 25% of the number concentration, and
 1270 the upper of the boxes represent 75% of the number concentration. Data marked with
 1271 red pluses represent outliers.

1272

1273

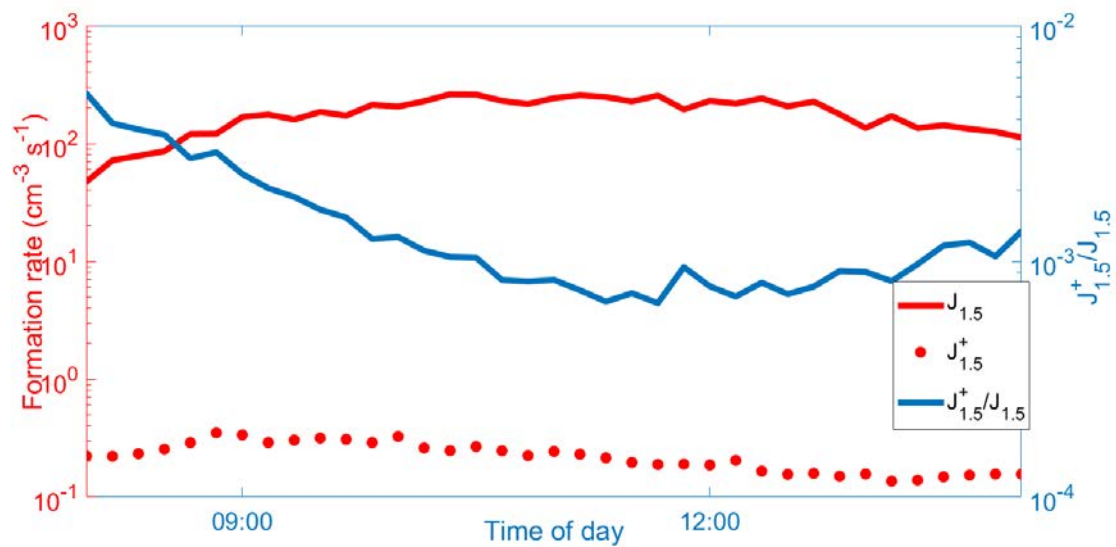


1274

1275 Figure 13. Diurnal pattern of charged clusters (1.5-3 nm) number concentration (red
 1276 line) and ratio of charged clusters to total cluster mode (1.5-3 nm) particle number
 1277 concentration on the NPF event days (blue line). The time resolution of the used data
 1278 was 12 min.

1279

1280

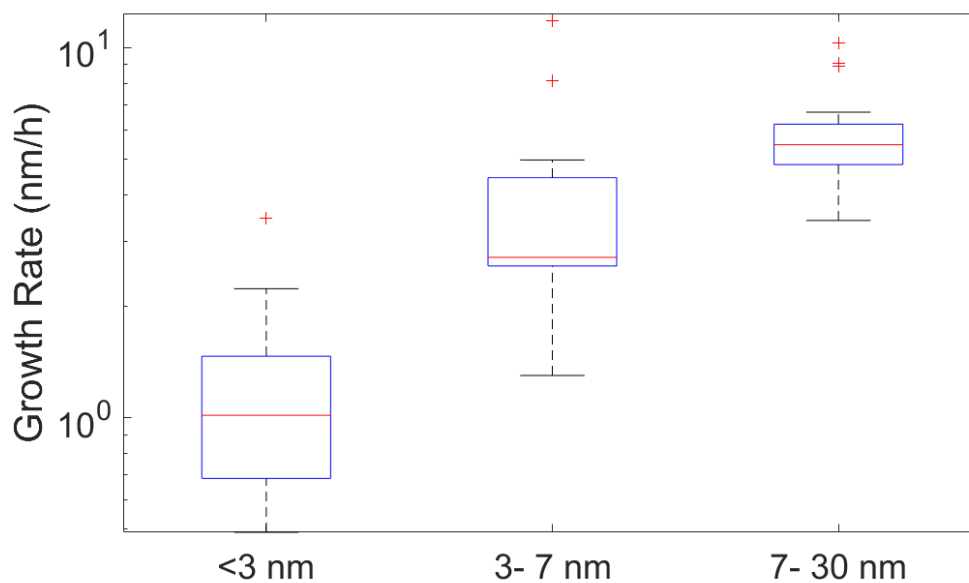


1281

1282 Figure 14. Diurnal pattern of formation rate of positive charged clusters of 1.5 nm (red
 1283 dots) and neutral clusters of 1.5 nm (red line) and the ratio between them (blue line) on
 1284 the NPF event days during the NPF time window we chose. The time resolution of the
 1285 used data was 12 min.

1286

1287



1288

1289 Figure 15. Growth rates of cluster mode and nucleation mode particles generated from
 1290 NPF events. The lines in the boxes represent the median value, the lower of the boxes
 1291 represent 25% of the growth rates and the upper of the boxes represent 75% of the
 1292 growth rates. Data marked with red pluses represent outliers.

1293